THE DESIGN AND SYNTHESIS OF METAL-FUNCTIONALIZED POLY(NORBORNENES) FOR POTENTIAL USE IN LIGHT-EMITTING DIODES

A Dissertation
Presented to
The Academic Faculty

by

Amy Meyers

In Partial Fulfillment
of the Requirements for the Degree
Doctor of Philosophy in the
School of Chemistry and Biochemistry

Georgia Institute of Technology
December 2004

THE DESIGN AND SYNTHESIS OF METAL-FUNCTIONALIZED POLY(NORBORNENES) FOR POTENTIAL USE IN LIGHT-EMITTING DIODES

Approved by:

Dr. Marcus Weck, Advisor
School of Chemistry and Biochemistry
Georgia Institute of Technology

Dr. Charles Liotta
School of Chemistry and Biochemistry
Georgia Institute of Technology

Dr. E. Kent Barefield
School of Chemistry and Biochemistry
Georgia Institute of Technology

Dr. Christopher Jones
School of Chemical and Biomolecular Engineering
Georgia Institute of Technology

Dr. David Collard
School of Chemistry and Biochemistry
Georgia Institute of Technology

Date Approved:

December 13, 2004

ACKNOWLEDGEMENT

I would like to start by first thanking my advisor, Marcus Weck, not for his support and management, but for his lack of guidance. He allowed me to decide the direction of the project and trusted that I would accomplish the work with minimal supervision. From this, I feel that I have become a confident and independent researcher. I would also like to acknowledge the Weck group for their continuous drive, making me work harder, and our conversations, not necessarily for the scientific value, but for the entertainment of them.

One of the keys to having a successful graduate career is having a support group to go to when you feel like the world (and science) is against you. I have a couple of people that I went to when I needed help. The first one I would like to thank is Mike McKittrick for our therapy lunches. While nothing was ever accomplished during these lunches, knowing that someone else was going through similar unbearable situations made me feel just a little bit better. The other person I would like to thank is Loretta Crowe, who assured me that it was okay to be obsessive compulsive. If only we could have annexed a lab and embezzled the funds to run our own research group.

Many other people and groups were involved in my success in graduate school, including the Collard group, the Jones group, the Lyon group, and the Tolbert group by allowing me to use their equipment. The Marder group, including J.D. Cho and Xiaowei Zhan, was very valuable in my research, not only for their equipment, but also for synthesizing some compounds for me that lead to a big breakthrough (i.e., working

devices) in my project. I would also like to acknowledge the Kippelen group for providing me the electroluminescence graph of my devices.

I was also fortunate to supervise an undergraduate, Clint South, during a summer research project. Even though the original project was not successful, I learned a lot by trying to instruct him and trying to get my ideas and thoughts into his head. I feel honored (and a bit disappointed that I did not scare him enough) that he decided to come back to Georgia Tech and to the Weck group to do his graduate work.

Finally I would like to thank my husband, Randall Wells, for supporting me the past four and a half years while I earned my doctorate. I know Atlanta was not his first choice in places to live and work, but I hope now that I will be able to support him in his future quests, even if that is retirement.

TABLE OF CONTENTS

LIST OF TABLES

LIST OF FIGURES

LIST OF FIGURES (continued)

LIST OF FIGURES (continued)

LIST OF FIGURES (continued)

LIST OF ABBREVIATIONS

OLED	Organic light-emitting diode
Alq_3	Aluminum tris(8-hydroxyquinoline)
LCD	Liquid crystal display
PDA	Personal digital assistant
DVD	Digital video disk
ETL	Electron-transport layer
HTL	Hole-transport layer
EML	Emission layer
$? E_e$	Energy barrier for electron injection
$? E_h$	Energy barrier for hole injection
Ea	Electron affinity
Ip	Ionization potential
F_{cat}	Work function of cathode
F_{an}	Work function of anode
ITO	Indium-tin-oxide
HOMO	Highest occupied molecular orbital
LUMO	Lowest unoccupied molecular orbital
E^*	Excitation energy
fac	Facial

mer	Meridianal
Gaq_3	Gallium tris(8-hydroxyquinoline)
Inq_3	Indium tris(8-hydroxyquinoline)
Snq_3	Tin tris(8-hydroxyquinoline)
Mgq_2	Magnesium bis(8-hydroxyquinoline)
Znq_2	Zinc bis(8-hydroxyquinoline)
ROMP	Ring-opening metathesis polymerization
PDI	Polydispersity index
M_n	Number average molecular weight
M_w	Weight average molecular weight
DSC	Differential scanning calorimetry
TGA	Thermogravimetric analysis
F	Photoluminescence quantum yields
TPD	*N,N'*-bis(*m*-tolyl-*N,N'*-diphenyl-1,1'-biphenyl-4,4'-diamine
TPF	2,7-bis(phenyl-*m'*-tolylamino)-9,9-dimethylfluorene
Ph_5SiCp	Pentaphenylsilacyclopentadiene

SUMMARY

The use of polymers in electro-optical devices, especially organic light-emitting diodes (OLEDs), has become very popular in recent years, due to their ease of processability. The major drawback of using polymers in these systems is their time-consuming synthesis when trying to improve upon their physical properties. For example, each time a new color or better conducting properties are desired, a new monomer must be synthesized. To circumvent these problems, the system described in this work is designed to connect the well-known chromophore aluminum tris(8-hydroxyquinoline) (Alq_3) to a norbornene monomer unit, followed by the polymerization using ring-opening metathesis polymerization (ROMP), thus allowing for the processability of a polymer while maintaining the fluorescent properties of the metalloquinolate.

The benefit of this system is that the monomers can be easily altered in order to tune color emission or to enhance the polymer properties. Some of the alterations include changing the metal center from aluminum to zinc in order to improve electron injection, adding substituents to the 8-hydroxyquinoline ligand in order to tune the emission color, and copolymerizing the Alq_3-monomer with other norbornene monomers containing either a hole- or an electron-transport material side-chain to improve conductivity. These alterations lead to improved device performance and, more importantly, to a new method of designing polymeric systems for use in electronic devices.

CHAPTER 1

INTRODUCTION TO ORGANIC LIGHT-EMITTING DIODES

Background Information

In recent years, the flat-panel display industry has grown tremendously due mostly to the success of liquid-crystal displays (LCD). However during this period, the technology of organic light-emitting diodes (OLEDs) has advanced so that it now can compete directly with LCD for high-information content display applications. OLEDs have many advantages over LCD including a wide-viewing angle (>170^{o}), faster data display, lightweight, flexibility, and power efficiency.[1] The biggest market for OLEDs is the small, portable electronic devices such as mobile phones, personal digital assistants (PDAs), digital cameras, digital video disk players (DVD), and automotive applications. The proposed market will be about $700 million per year in 2005, with companies such as Samsung, NEC Mobile Displays, Pioneer, and Philips Electronics having devices containing OLEDs on the market today.[2]

The generation of light by electrical excitation of organic material was first observed in the 1960s, when several hundred volts were applied across a single anthracene crystal.[3] Later in the 1980s, the first two-layer thin film organic device was fabricated by Kodak in which each layer was capable of only monopolar charge transport.[4] The radiative recombination in the charge-trapped region produced green

light with a quantum efficiency of one percent.[4] Today, efficiencies as high as 20% have been achieved.[5]

Basic Principles of OLEDs

The basic structure of an OLED is shown in Figure 1.1. The basic principles of an OLED include the injection of electrons from one electrode and injection of holes from the other electrode. The electrons move through the electron-transport layer (ETL), while the holes move through the hole-transport layer (HTL), until the capture of the oppositely charged carriers or recombination, followed by the radiative decay of the excited electron-hole state or exciton. The color of the light emitted during this process is determined by the band gap of the exciton.

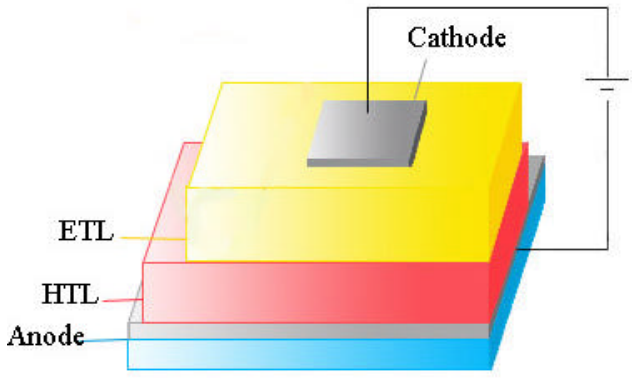

Figure 1.1 Diagram of an OLED.

In order to obtain high efficiencies and a long lifetime, a device must contain the following features: low injection barriers at the interface between the metal electrodes and organic material, allowing for as many charges as possible into the system; a balance of electron and hole density and mobility, so that, for example, the majority of the holes do not reach the cathode before they are captured by an electron, decreasing the efficiency of the system; a recombination zone away from the metal cathode, again so that the holes are not annihilated by the cathode before recombination; and a high thermal stability of all of the organic material so that they can sustain fabrication conditions.[6-10]

Properties of Cathode and Anode

In order to obtain a balanced injection, where the rate of injection of positive charges is equal to the rate of injection of negative charges, a low work function metal, such as calcium, magnesium, or aluminum as well as alloys containing these metals, is employed as the cathode. The low work function is necessary to decrease the energy barrier for the electron injection (? Ee) into the organic material, as shown in Figure 1.2.[6] The organic material that will act as the electron-transport layer should then have an electron affinity (Ea) close to the work function of the cathode (Fcat).[6] If a close match between the electron affinity and the work function of the cathode cannot be found, then inserting a metal-insulating layer, such as lithium fluoride, between the metal cathode and the electron-transport material can provide an intermediate level between the cathode and the LUMO of the electron-transport material.[11] The work function of the anode (Fan), usually indium-tin-oxide (ITO) should closely match the ionization potential (Ip) of the

hole-transport material and should contain a low energy barrier for hole injection (?Eh).[6] Other properties of anodes currently being used in OLEDs include good transmittance in the visible and near infrared region, low electrical resistivity, and easy processability.[12]

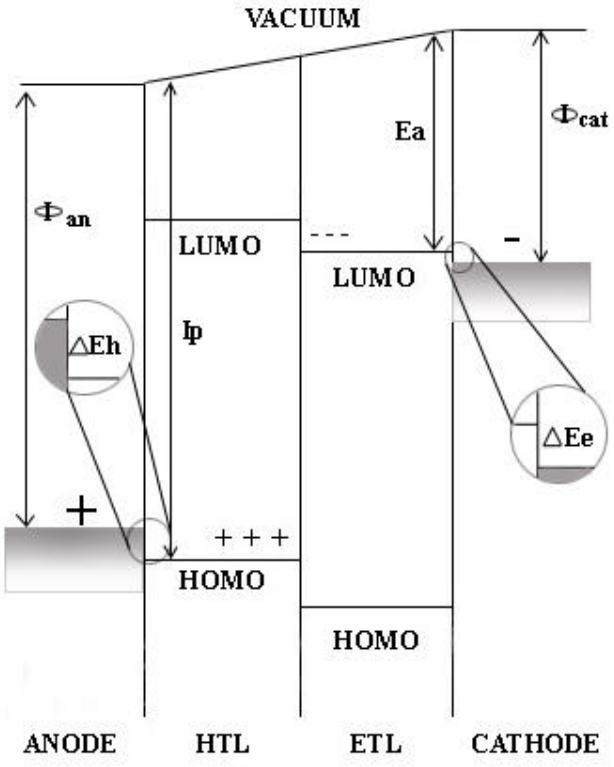

Figure 1.2 Schematic energy-level diagram for a four-layer device containing an anode, hole-transport layer (HTL), electron-transport layer (ETL), and a cathode.

Properties of Electron-Transport and Hole-Transport Materials

Electron-transport materials usually consist of ? -electron deficient heterocycles containing imine nitrogen atoms in an aromatic ring.[13] Some examples are shown in Figure 1.3. Heterocyclic moieties with high reduction potentials reduce the interface barriers between the organic material and the cathode.[13] They also have high ionization potential or low HOMO, which blocks holes from traveling through the material, and large electron affinities or low LUMO, which assists in the injection of electrons.[13] The oxadiazoles and triazoles, which both have high thermal stability, are generally used as hole-blocking layers between the emitting layer and the cathode in a multilayer device.[14,15] Both quinoxalines and quinolines are electroluminescent materials, allowing

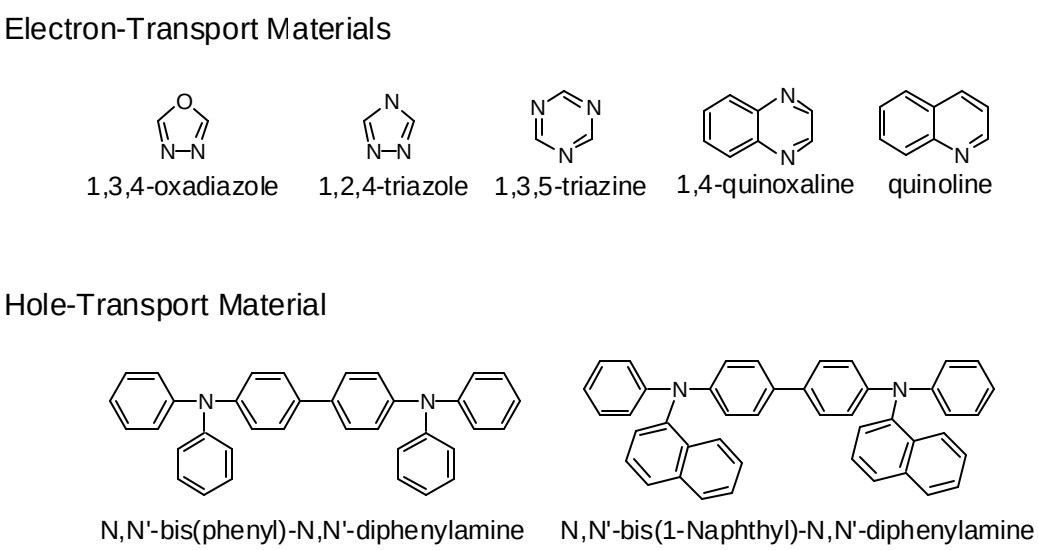

Figure 1.3 Structures of Electron- and Hole-Transport Materials.

these compounds to be used as the electron-transport and emitting layers in devices.[16,17] The biggest drawback with all of these heterocycles is their processability. These small molecules must be vacuum deposited, while their polymer analogs have limited solubility, making them difficult to process.[13]

Compared to the electron-transport materials, the hole-transport materials such as triarylamines, also shown in Figure 1.3, have small ionization potentials or high HOMO and small electron affinities or high LUMO which assist in hole injection and in electron blocking, respectively.[13] The properties of these compounds, such as the glass transition temperature and the ionization potential, can be improved by the addition of electron-withdrawing groups to the phenyl ring or by replacing the biphenyl moiety with a fluorene derivative.[18,19] In contrast to the polymeric electron-transport materials, the polymer analogs of the hole-transport materials are readily soluble.[20,21]

An optional emission layer (EML) can be used in OLEDs, which would be the location of recombination and the radiative decay. The electronic excitation energy (E*) or band gap energy of the HTL and the ETL should be higher than that of the EML.[13] Efficient OLED can be fabricated by following theses conditions:[13]

$$Ip\ (ITO) = Ip(HTL) \sim Ip(EML) \sim Ip\ (ETL) \qquad (1)$$

$$Ea(HTL) \sim Ea\ (EML) \sim Ea(ETL) = Ip(cathode) \qquad (2)$$

$$E^*(HTL) > E^*(EML) < E^*(ETL) \qquad (3)$$

Pathway of Radiative Decay

Charge carrier recombination is a bimolecular reaction between an electron and a positive charge. Electrons enter the system at the cathode and migrate towards the anode. During the migration, the electron can encounter a positive charge and recombine to form an excited state or the electron can transverse through the entire sample and discharge at the anode.[10] One requirement for recombination is low mobility of one of the charges. This will create a high local charge density which will ensure the other charge will pass within a collision capture radius.[1] The neutral bound excited state of an electron and a hole, called an exciton, is formed from two spin ½ charges. Assuming that the recombination process is spin-independent, excitons are formed in a 3:1 ratio of triplet to singlet state, where only 25% of all recombination form a singlet state.[10] Fluorescence is the spin-allowed radiative decay of excitons from the singlet state.[1] Triplet excitons do not produce light except when triplet-triplet annihilation occurs, which is known as phosphorescence.[1]

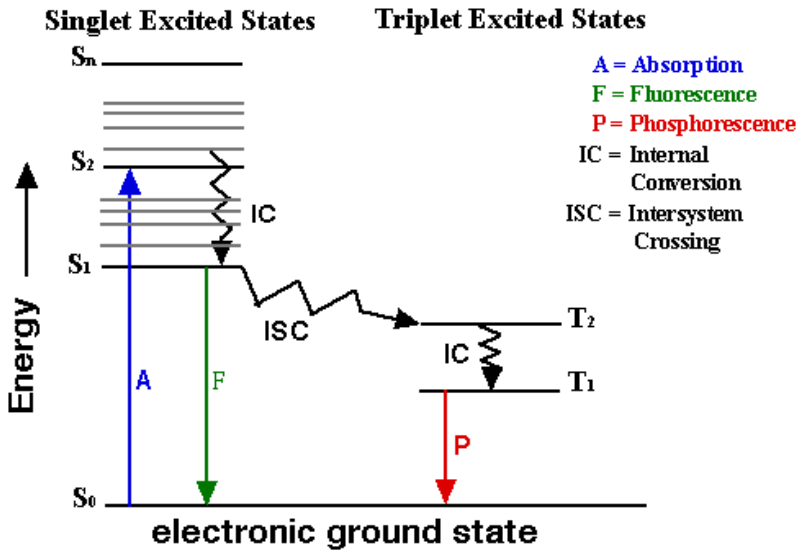

Figure 1.4 Jablonski diagram showing pathway of absorption, fluorescence, and phosphorescence.

While phosphorescent devices are highly desirable, fluorescence is the emission process used in the majority of the devices fabricated, thereby quantum efficiencies of 25% are the highest achievable efficiency for these devices. The main source for non-radiative decay or loss of efficiency in solid state materials is the quenching of the excited state due to either impurities or energy transfer.[10] Diluting the active chromophore in an inert binder (such as an electrically-inert polymer) will cause energy transfer to decrease, but brightness will also decrease due to the lower injection rate.[10]

Using Polymers in OLEDs

Besides their roles as inert binders, polymers have been used in OLEDs as electroluminescent materials since the late 1980s, when emission was observed in poly(1,4-phenylene vinylene).[22] The major advantage of using polymers over small organic molecules is that polymers can be solution processed. The simplicity of solution processing equates to a low manufacturing cost, which can lead to techniques known as roll-to-roll processing and ink-jet printing.[6] Roll-to-roll processing is a technique in which a polymer solution is sprayed onto a large flexible substrate which already contains the anode. After deposition of the cathode, the substrate can then be cut into smaller sections depending on the final application of the OLED. Ink-jet printing is a high-resolution patterning of red, green, and blue light-emitting polymers using the same technology found in an ink-jet printer. Based on a drop diameter of 20 μm and a 100 nm thick layer, ink-jet printing can use polymer solutions with concentrations as low as 1%.[6]

Examples of Electron-Transport Polymers

Many polymers have been designed and synthesized for application in OLEDs, but one of the most popular polymer for use in OLEDs is poly(*p*-phenylene vinylene) (PPV) and its derivatives as shown in Figure 1.5.[1, 2, 22-30] A readily soluble version of PPV can be made by the addition of alkyl chains (poly[2,3-bis(2-ethylhexyloxy-1,4-phenylene vinylene)] (BEH-PPV), however this results in the disruption of planarity of the polymer, decreasing the efficiency and brightness of the device.[23] Schmidt and co-

workers were able to achieve brightness as high as 146 cd/m^2 (equivalent to an LCD monitor) at 9.5 V by blending a 2,5-dialkoxysubstituted poly(*p*-phenylene ethynylene) (EHO-OPPE) derivative with a polymeric triphenyldiamine.[25] One of the brightest device was prepared by using a distyrylbenzene derivative (Distyrylbenzene-block-sexi(ethylene oxide) (DSB-block-SEO)), shown in Figure 1.5, reaching a brightness of 2000 cd/m^2 at 19 V.[31] Besides brightness, another desirable quality is color tunability. By copolymerizing 2.5-didodecyloxy-*p*-phenylenebutadiynylene with a fluorene derivative and a thiophene derivative (PPPBs), as shown in Figure 1.5, the emission color can be tuned from blue to red.[32] A variety of colors were also seen using poly(thiophene) derivative, with efficiencies ranging between 0.1-1%.[33]

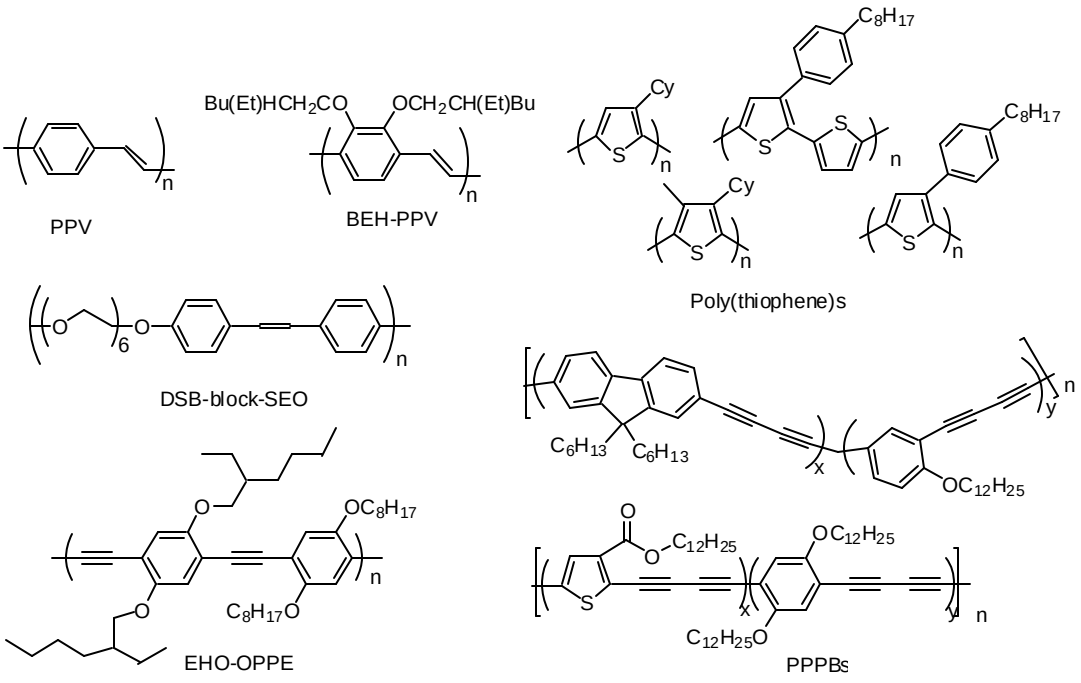

Figure 1.5 Structures of electron-transport polymers.

Examples of Hole-Transporting Polymers

Research on hole-transport polymers, some of which are shown in Figure 1.6, have also led to improved efficiencies.[15, 34-37] By copolymerizing both the hole- and electron-transporting derivatives of fluorenes, Morteani *et al*., have shown devices with a brightness of 100 cd/m^2 at 2.1 V that range in color from blue to red.[35] By using poly(N-vinylcarbazole) (PVK) as the hole-transporting layer, Kido and co-workers reached a brightness of 3400 cd/m^2 at 14 V.[15] However, Jen and co-workers have obtained brightness as high as 59,000 cd/m^2 with their perfluorocyclobutane-based arylamine hole-transporting materials (PFCBs).[37]

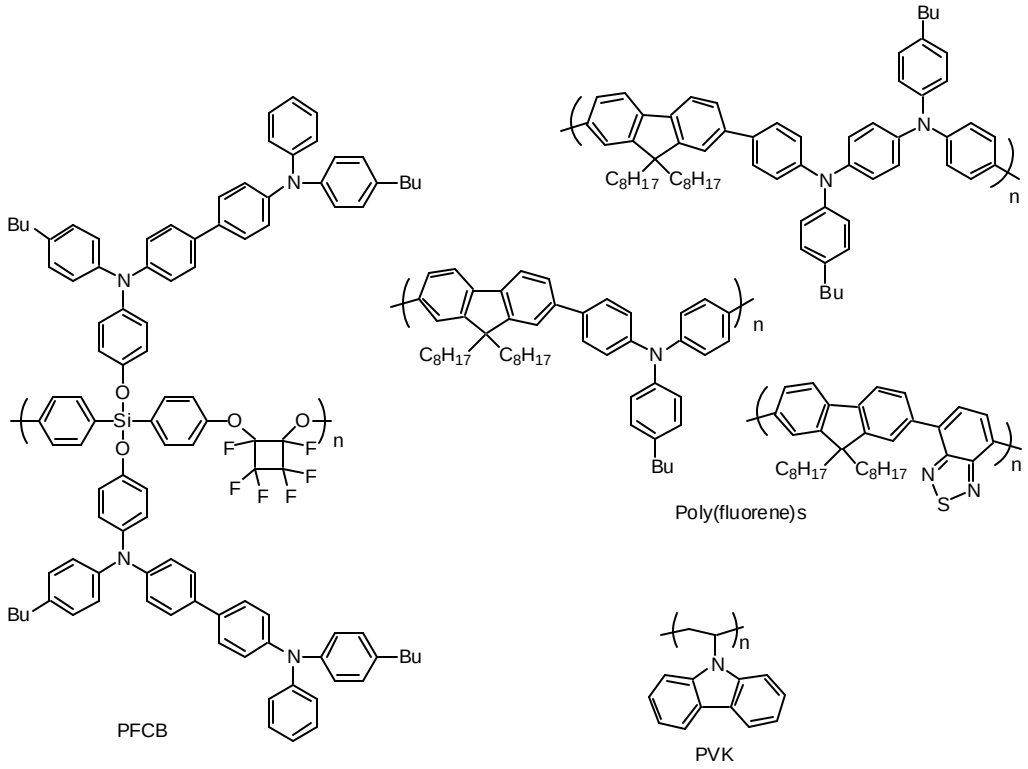

Figure 1.6 Structures of hole-transport polymers.

Even though much improvement of these polymeric systems has been seen over the past twenty years, the optimization of polymers can be very tedious. Polymers do have the advantage over small organic molecules of being solution processable, they are at a disadvantage when it comes to optimization. Small organic molecules can easily be modified in order to tune the properties of the OLED, whereas the monomers of the electroluminescent polymers must first be re-synthesized, then polymerized, and finally the polymers are re-tested in order to optimize the device.[6] A more efficient method would be to attach the small organic molecules onto a polymeric backbone, thereby maintaining the ease of optimization associated with the small molecule while gaining the processability of a polymer.

The focus of this thesis is the design of a polymer containing a functionalized side-chain for potential applications in OLEDs. The side-chains are capable of charge transport and light emission, while the polymer backbone functions only as the support linking the side-chains together. The emission properties of the polymer are easily tuned through small changes to the side-chain without the need of re-synthesizing or re-polymerizing the monomer. The functional side-chain was chosen to be a well-known small organic molecule, so that an easy comparison can be made between the small molecule and the polymeric system. The next chapter will introduce the electron-transport material that was attached to the polymer backbone.

References

1. Friend, R. H.; Gymer, R. W.; Holmes, A. B.; Burroughes, J. H.; Marks, R. N.; Taliani, C.; Bradley, D. D. C.; Santos, D. A. D.; Bredas, J. L.; Logdlund, M.; Salaneck, W. R. *Nature* **1999**, *397*, 121-128.

2. Sheats, J. R.; Antoniadis, H.; Hueschen, M.; Leonard, W.; Miller, J.; Moon, R.; Roitman, D.; Stocking, A. *Science* **1996**, *273*, 884-888.

3. Pope, M. *J. Chem. Phys.* **1963**, *38*, 2042-2043.

4. Tang, C. W.; VanSlyke, S. A. *Appl. Phys. Lett.* **1987**, *51*, 913-915.

5. Adachi, C.; Baldo, M. A.; Thompson, M. E.; Forrest, S. R. *J. Appl. Phys.* **2001**, *90*, 5048-5051.

6. Greiner, A. *Polym. Adv. Technol.* **1998**, *9*, 371-389.

7. Malinsky, J. E.; Jabbour, G. E.; Shaheen, S. E.; Anderson, J. D.; Richter, A. G.; Armstrong, N. R.; Kippelen, B.; Dutta, P.; Peyghambarian, N.; Marks, T. J. *Adv. Mater.* **1999**, *11*, 227-231.

8. Jabbour, G. E.; Kawabe, Y.; Shaheen, S. E.; Wang, J. F.; Morrell, M. M.; Kippelen, B.; Peyghambarian, N. *Appl. Phys. Lett.* **1997**, *71*, 1762-1764.

9. Ho, P. K. H.; Granstrom, M.; Friend, R. H.; Greenham, N. C. *Adv. Mater.* **1998**, *10*, 769-774.

10. Bassler, H. *Polym. Adv. Technol.* **1998**, *9*, 402-418.

11. Stoßel, M.; Staudigel, J.; Steuber, F.; Blassing, J.; Simmerer, J.; Winnacker, A.; Neuner, H.; Metzdorf, D.; Johannes, H.-H.; Kowalsky, W. *Synth. Met.* **2000**, *111-112*, 19-24.

12. Cui, J.; Wang, A.; Edleman, N. L.; Ni, J.; Lee, P.; Armstrong, N. R.; Marks, T. J. *Adv. Mater.* **2001**, *13*, 1476-1480.

13. Thelakkat, M.; Schmidt, H. *Polym. Adv. Technol.* **1998**, *9*, 429-442.

14. Tsutsui, T.; Aminaka, E.; Tokuhisa, H. *Synth. Met.* **1997**, *85*, 1201-1204.

15. Kido, J.; Hongawa, K.; Okuyama, K.; Nagai, K. *Appl. Phys. Lett.* **1994**, *64*, 815-817.

16. O'Brien, D. F.; Weaver, M. S.; Lidzey, D. G.; Bradley, D. D. C. *Appl. Phys. Lett.* **1996**, *69*, 881-883.

17. Kanabara, T.; Inoue, T.; Sugiyama, K.; Yamamoto, T. *Synth. Met.* **1995**, *71*, 2207-2208.

18. Hreha, R. D.; George, C. P.; Haldi, A.; Domercq, B.; Malagoli, M.; Barlow, S.; Bredas, J.-L.; Kippelen, B.; Marder, S. R. *Adv. Funct. Mater.* **2003**, *13*, 967-973.

19. Maldonado, J.-L.; Bishop, M.; Fuentes-Hernandez, C.; Caron, P.; Domercq, B.; Zhang, Y.-D.; Barlow, S.; Thayumanavan, S.; Malagoli, M.; Bredas, J.-L.; Marder, S. R.; Kippelen, B. *Chem. Mater.* **2003**, *15*, 994-999.

20. Domercq, B.; Hreha, R. D.; Zhang, Y.-D.; Larribeau, N.; Haddock, J. N.; Schultz, C.; Marder, S. R.; Kippelen, B. *Chem. Mater.* **2003**, *15*, 1491-1496.

21. Hreha, R. D.; Haldi, A.; Domercq, B.; Barlow, S.; Kippelen, B.; Marder, S. R. *Tetrahedron* **2004**, *60*, 7169-7176.

22. Burroughes, J. H.; Bradley, D. D. C.; Brown, A. R.; Marks, R. N.; MacKay, K.; Friend, R. H.; Burn, P. L.; Holmes, A. B. *Nature* **1990**, *347*, 539-541.

23. Martin, R. E.; Geneste, F.; Riehn, R.; Chuah, B. S.; Cacialli, F.; Holmes, A. B.; Friend, R. H. *Synth. Met.* **2001**, *119*, 43-44.

24. Zheng, C.; Braun, D.; Heeger, A. J. *J. Appl. Phys.* **1993**, *73*, 5177-5180.

25. Schmitz, C.; Posch, P.; Thelakkat, M.; Schmidt, H.-W.; Montali, A.; Feldman, K.; Smith, P.; Weder, C. *Adv. Funct. Mater.* **2001**, *11*, 41-46.

26. Cacialli, F.; Friend, R. H.; Moratti, S. C.; Holmes, A. B. *Synth. Met.* **1994**, *67*, 157-160.

27. Burn, P. L.; Holmes, A. B.; Kraft, A.; Bradley, D. D. C.; Brown, A. R.; Friend, R. H. *J. Chem. Soc.* **1992**, 32-34.

28. Baigent, D. R.; Greenham, N. C.; Gruner, J.; Marks, R. N.; Friend, R. H.; Moratti, S. C.; Holmes, A. B. *Synth. Met.* **1994**, *67*, 3-10.

29. Brown, A. R.; Bradley, D. D. C.; Burroughes, J. H.; Friend, R. H.; Greenham, N. C.; Burn, P. L.; Holmes, A. B.; Kraft, A. *Appl. Phys. Lett.* **1992**, *61*, 2793-2795.

30. Sheats, J. R. *Science* **1997**, *277*, 191-192.

31. Cacialli, F.; Friend, R. H.; Feast, W. J.; Lovenich, P. W. *Chem. Comm.* **2001**, 1778-1779.

32. Kinoshita, I.; Kijima, M.; Yoshikawa, K.; Mishima, Y.; Sasaki, N. *Synth. Met.* **2003**, *137*, 1059-1060.

33. Berggren, M.; Inganas, O.; Gustafsson, G.; Rasmusson, J.; Andersson, M. R.; Hjertberg, T.; Wennerstrom, O. *Nature* **1994**, *372*, 444-446.

34. Gong, X.; Moses, D.; Heeger, A. J.; Liu, S.; Jen, A. K.-Y. *Appl. Phys. Lett.* **2003**, *83*, 183-185.

35. Morteani, A.; Dhoot, A. S.; Kim, J.-S.; Silva, C.; Greenham, N. C.; Murphy, C.; Moons, E.; Cina, S.; Burroughes, J. H.; Friend, R. H. *Adv. Mater.* **2003**, *15*, 1708-1712.

36. Kido, J.; Kimura, M.; Nagai, K. *Science* **1995**, *267*, 1332-1334.

37. Jiang, X.; Liu, S.; Liu, M. S.; Herguth, P.; Jen, A. K.-Y.; Fong, H.; Sarikaya, M. *Adv. Funct. Mater.* **2002**, *12*, 745-751.

CHAPTER 2

INTRODUCTION TO ALUMINUM TRIS(8-HYDROXYQUINOLINE)

Background Information

In the early 1950's, 8-hydroxyquinoline was used extensively in the fluorimetric determination of aluminum in a variety of substances such as beer, paper, and steel.[1,2] Although the quinolate ligand chelates many metals, such as nickel, copper, lead, and iron, very few of the metalloquinolate compounds fluoresce.[3] In fact, it was found that only the group 3 metals of aluminum, gallium, and indium, zinc, and magnesium form fluorescent metalloquinolates, even in the presence of other chelating metals.[3] However, it was not until the late 1980s that the compound aluminum tris(8-hydroxyquinoline) (Alq_3) played a major role in the development of OLEDs. In 1987, Tang and VanSlyke fabricated a two-layer organic thin film device, which under a forward bias, emitted green light.[4] The two layers, each capable of monopolar transport, were comprised of Alq_3 and an aromatic diamine, as shown in Figure 2.1, where the diamine layer conducted the holes and the Alq_3 layer both transported electrons and emitted light.[4] They showed that emission from their device was visible (100 cd/m^2) at 5.5 V and was capable of brightness up to 1000 cd/m^2 at 10 V, with an external quantum efficiency of 1%.[4] Since this report, the research and development of Alq_3 as the electron-transport and emitting layer in OLEDs has exploded.[4-19]

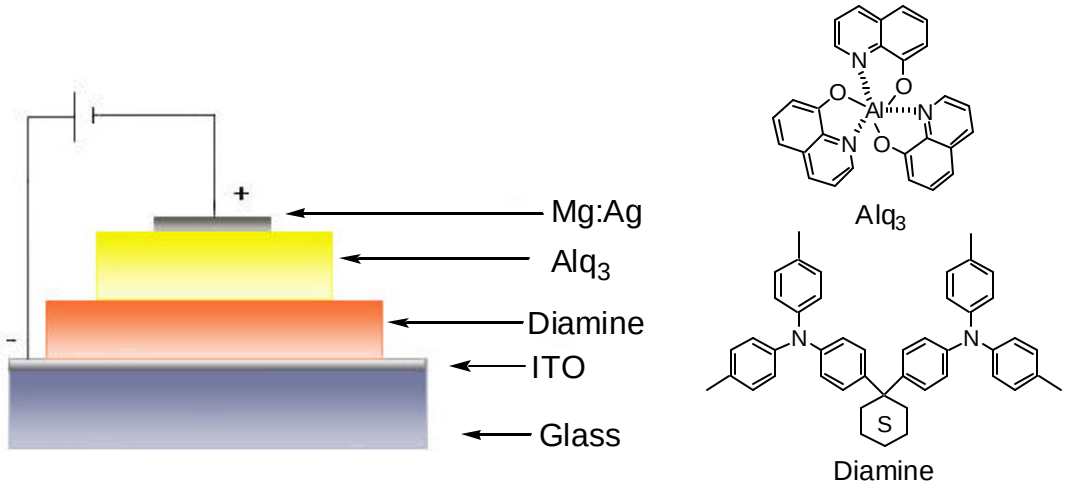

Figure 2.1 Diagram of Tang and VanSlyke's OLED and the structures of the compounds they used.

Today, the electrochemistry, the charge transport, the molecular orbitals, and the molecular packing of Alq_3 have all been reported in the literature.[6,8-10,15,18,20-25] The remainder of this chapter will provide the reader with a summary of those findings.

Probing the Site of Recombination

Soon after their initial report using Alq_3 in OLED, Tang and VanSlyke released another finding using Alq_3 with a dopant, which allowed for tuning of the emission color as well as improving the efficiency of the device.[19] However, it was not until 1998 that a

study was performed looking into the electrochemistry of Alq_3 and how dopants, such as quinacridones as shown in Figure 2.2, can be used to improve the efficiencies of Alq_3 devices.[6]

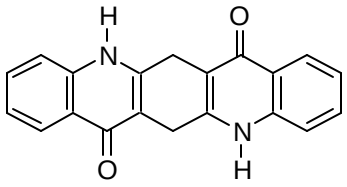

Quinacridone

Figure 2.2 Structure of quinacridone.

The study probed the interface region between the HTL and the EML, the location where the radical states recombine, in order to asses the exact role of Alq_3 in the presence of a quinacridone dopant (DIQA).[6] The hole-transport material that was used in the study was 4,4'-bis-(*m*-tolylphenylamino)biphenyl (TPD), an aromatic diamine similar to the one used by Tang and Van Slyke.[4,6,19] The findings of the electrochemical study can be summarized by the following equations:

$$Alq_3 + e^- \rightleftharpoons Alq_3^{-\cdot} \quad (1)$$

$$TPD \rightleftharpoons TPD^{+\cdot} + e^- \quad (2)$$

$$TPD^{+\cdot} + Alq_3 \rightleftharpoons Alq_3^{+\cdot} + TPD \quad (3)$$

$$Alq_3^{+\cdot} + Alq_3^{-\cdot} \rightleftharpoons Alq_3{}^{s*} + Alq_3 \quad (4)$$

$$Alq_3^{-\cdot} + TPD^{+\cdot} \rightleftharpoons Alq_3{}^{s*} + TPD \quad (5)$$

$Alq_3{}^{s*}$ is the singlet emission state of Alq_3, which is formed from the cross reactions between the cation radical state of TPD and the anion radical state of Alq_3.[6] In the presence of a dopant, the following equations hold true:

$$DIQA^{-\cdot} + DIQA^{+\cdot} \rightleftharpoons DIQA^{s*} + DIQA \quad (6)$$

$$DIQA^{-\cdot} + TPD^{+\cdot} \rightleftharpoons DIQA^{s*} + TPD \quad (7)$$

$$Alq_3^{-\cdot} + DIQA^{+\cdot} \rightleftharpoons DIQA^{s*} + Alq_3 \quad (8)$$

The quinacridone dopants act as charge traps for both the $Alq_3^{-\cdot}$ and the $TPD^{+\cdot}$ states, forming the emissive $DIQA^{s*}$.[6] Because the dopant can trap the charges from both the Alq_3 anion and the TPD cation, the optimally placement for the dopant should be very near the HTL-EML interface, which is where Tang and VanSlyke obtained their highest efficiencies.[6,19]

Understanding the Excited State

Without the presences of a dopant, Alq_3 will most likely be the emissive species in an OLED. As mentioned above, Alq_3 forms an excited emissive state when the negatively charged $Alq_3^{-\cdot}$ recombines with a positively charged $Alq_3^{+\cdot}$. The charges on the anion state are thought to transport by either a hopping of electrons between the LUMO states, or through a narrow conduction band.[20] However, in either case, it is the high density distribution of traps just below the energy of the LUMO which limits the current.[20] The low electron mobility observed at low voltages is due to the charge capture in these traps.[20] By increasing the bias, the number of injected electrons increases the number of filled traps, thereby increasing the mobility until all of the traps are filled.[20] One of the main reasons for the large number of traps in Alq_3 is due to the structural disorder of the compound during excitation.[20] The three lowest energy transitions are all π-π^* transitions localized on the quinoline ligands, where partial charge is transfer from the phenoxide side, where the HOMOs of the compound are found, to the pyridyl side, where the LUMOs are located, as shown in Figure 2.3.[24] The phenoxide side of the ligand, containing the highest-energy filled state, is the most readily oxidized and is the likely site for trapped holes, while the pyridyl side is the likely site for reduction and trapped electrons.[20]

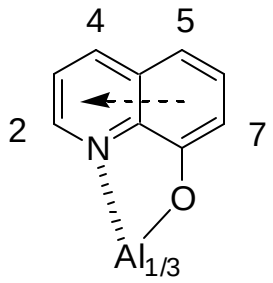

Figure 2.3 Schematic drawing of Alq_3, showing charge transfer from phenoxide side to pyridyl side of quinolate ligand.

In order to confirm the location of the trapped charges, the excited state structure of the compound was probed.[20] The electroluminescence of Alq_3 is 0.4 eV from the absorption of the compound (the difference between the ground state and the excited state), indicating a Franck-Condon shift, where a large conformational energy change occurs upon optical excitation.[20] The structural shift was calculated to take place on one of the quinolate ligands, by considering the difference in the total electron density between the excited and ground states for each ligand.[24] Further calculations were performed on Alq_3 with an extra "injected" electron.[20] The extra electron was found to reside on the pyridyl side of the quinolate ligand, therefore the optimized structure for the anion form of Alq_3 shows that the Al-O bond lengths remain the same and the Al-N bond lengths shift depending on which ligand contains the extra electron, as shown in Figure 2.4.[20] The increased negative charge on the quinolate ligand with the extra electron leads to a stronger interaction with the aluminum cation, resulting in a shorter bond, and the compound is said to be structurally relaxed.[20] These random conformational changes

lead to a continuous distribution of trap energies, which can be thought of as an extension of the Alq_3 LUMO, which is consistent with experimental results.[20]

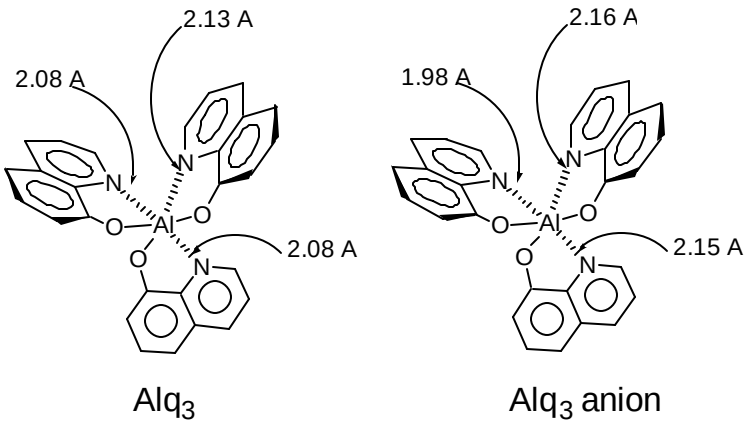

Figure 2.4 Bond length changes in Alq_3 due to presence of an extra electron.

A detailed study of the molecular orbitals of Alq_3 was performed in order to understand the HOMO-LUMO energy differences and how they give rise to the observed luminescent properties.[24] Alq_3 is comprised of an aluminum cation (+3) surrounded by three quinolate ligands in a pseudooctahedral coordination. Alq_3 has two geometric isomers, the facial (*fac*) and meridianal (*mer*), as shown in Figure 2.5. The *mer* isomer is the dominant form, being that the *fac* isomer is not detectable by NMR and was calculated to be 4 kcal/mol higher in energy than the other isomer.[24]

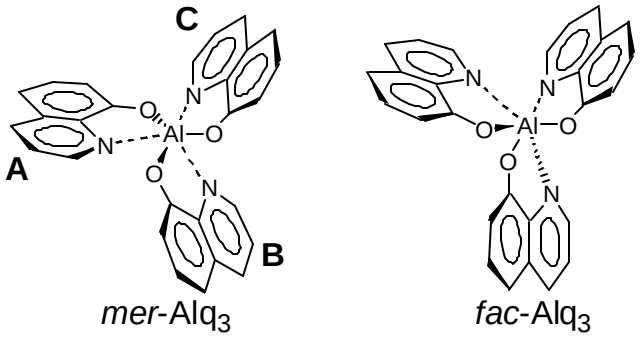

Figure 2.5 Meridianal and facial Alq_3.

The *fac* isomer contains a significantly higher dipole moment, which acts as a stabilizing factor in the aggregate phase, allowing the two isomers to coexist as an amorphous solid.[23] The HOMOs and LUMOs of Alq_3 preserve the electronic structure of the individual 8-hydroxyquinoline ligands with little contribution from the central aluminum atom.[24] The three HOMO orbitals of the *mer* ligand are split in energy, where the highest energy HOMO is localized on the A-ligand (see Figure 2.5). The HOMO for 8-hydroxyquinoline and the highest energy HOMO of Alq_3 are very similar, as are the LUMO for 8-hydroxyquinoline and the lowest energy LUMO of Alq_3.[24] Experimental results from the absorption and emission spectra of Alq_3, as well as Gaq_3, Inq_3, and Snq_3 also indicate that the HOMOs and LUMOs are localized on the individual ligands and are independent of the metal center.[24]

Altering the Emission Wavelength

When Tang and VanSlyke reported the application of Alq_3 in OLED, it opened the door for the possibility for many other metal chelates to be used in electronic devices.[4] Metal chelates are considered to be ideal materials for OLEDs because of their thermal stability, high fluorescence in the solid state, and their ability to transport electrons.[7] Other metals that form fluorescent material with quinolate ligands include zinc and beryllium. A device fabricated with beryllium bis(10-hydroxybenzo[h]quinoline) ($BeBq_2$) doped with rubrene (a fluorescent conducting material) showed electroluminescence at 562 nm with a lifetime of over 15,000 hours.[7] A greenish-white emitting device was fabricated with zinc-bis[2-(2-hydroxyphenyl)benzothiazolate) ($Zn(BTZ)_2$) that showed brightness over 10,000 cd/m^2 at only 8 V.[7]

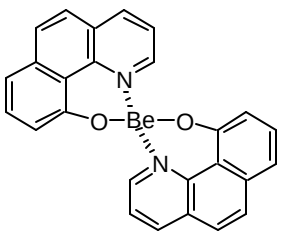

$BeBq_2$

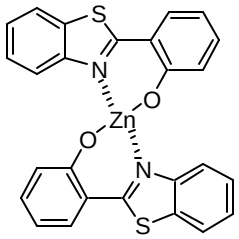

$Zn(BTZ)_2$

Figure 2.6 Structures of fluorescent beryllium and zinc compounds.

However, not all metals can be coordinated to the 8-hydroxyquinoline ligand and still be used as fluorescent materials. Paramagnetic metal ions, such as chromium and nickel, are essentially non-fluorescent due to the high rate of intersystem crossing.[7] Fluorescence is also reduced as the atomic number increases, again due to the increase rate of intersystem crossing, so that Inq_3 shows less fluorescence than Gaq_3, which is less fluorescent than Alq_3.[7] The emission wavelength can be tuned through the metal center, however. A more covalent character in the metal-ligand bond will be red-shifted compared to a more ionic one.[7] For example, Mgq_2 emits at 500 nm, while Znq_2 emits at 557 nm.

Another method of shifting the emission wavelength of metal chelates containing 8-hydroxyquinoline is by adding substituents to the quinoline ligand. As mentioned earlier (Figure 2.3), the filled orbitals (HOMO) are on the phenoxide side of the ligand, while the unfilled orbitals (LUMO) are on the pyridyl side, so adding an electron-withdrawing group on the phenoxide side of the ligand will lower the energy of the filled states resulting in a blue-shift in emission, while adding an electron-donating group on the pyridyl side will raise the vacant orbitals in energy also resulting in a blue-shift.[20] Another way to alter the $? ? ? *$ transition without distorting the shape of the ligand sphere is to introduce a heteroatom into the ring system.[7] Two such systems are shown in Figure 2.7, where the electron-withdrawing nature of nitrogen gives rise to a red-shift (+60 nm) in the quinoxaline compound, while the naphthyridine compound shows a blue-shifted emission (-80 nm).[7]

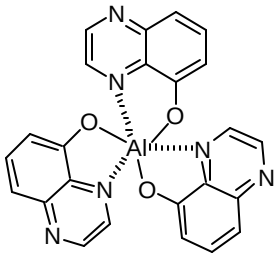

Aluminum tris(quinoxalinol)

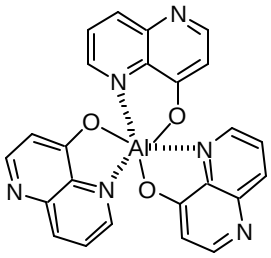

Aluminum tris(4-hydroxy-1,5-naphthyridne)

Figure 2.7 Structures of heteroatom aluminum quinolates.

Improving Efficiencies

The addition of methyl groups to the quinolate ligand was studied to determine if the efficiencies of Alq_3 compounds can be enhanced.[16] The quinolate ligand was methylated at the 3-, 4-, and 5-position as shown in Figure 2.8.[16]

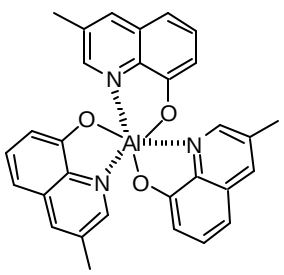

$Al(3Meq)_3$

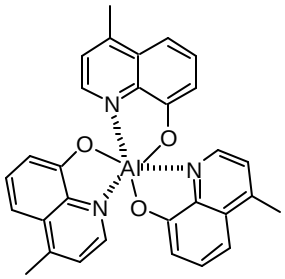

$Al(4Meq)_3$

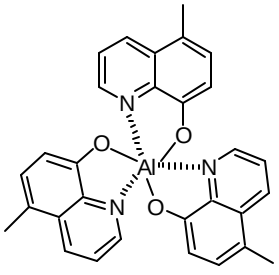

$Al(5Meq)_3$

Figure 2.8 Structures of the methylated aluminum quinolates.

Photoluminescence efficiencies are enhanced by the methylation at the C-3 and C-4 positions, while it is worsen by methylation at the C-5 position.[16] The methylations also increase the glass transition temperature, while decreasing the melting point due to the reduced intermolecular interactions.[16] This also leads to a decreased overlap of the *?*-electrons in the pyridyl rings where the LUMO orbitals are located, therefore increasing the injection of electrons, which drives the device operating voltages up.[16] The strong dipolar *?*-*?* stacking interactions of the overlapping pyridyl rings in Alq_3 leads to its good electron mobility versus hole mobility.[16] By methylating at the C-3 and C-4 positions, the pyridyl ring overlap decreases, which leads to a decrease in electroluminescence efficiencies.[16] However, methylation at the C-5 position does not prevent pyridyl overlap, but it does raise the HOMO, which may improve hole-injection efficiencies.[16]

Degradation of Alq_3

Despite the lower efficiencies, methylation or any other substitution does not lead to the degradation of Alq_3. Side reactions with impurities, such as oxygen and water, at elevated temperatures lead to the failure of Alq_3 in devices.[15] As shown in Figure 2.9, small amounts of water can catalyze the hydrolysis of Alq_3, generating 8-hydroxyquinoline, which then reacts with oxygen to form a brown, non-emissive polymer and water.[15] The absorption spectrum of this brown polymer shows a peak at 600 nm, indicating an n-*?* * transition found in quinones.[15] These results indicate that reaction

conditions, as well as device fabrication conditions, play a crucial role in the development and understanding of Alq_3 in OLED.

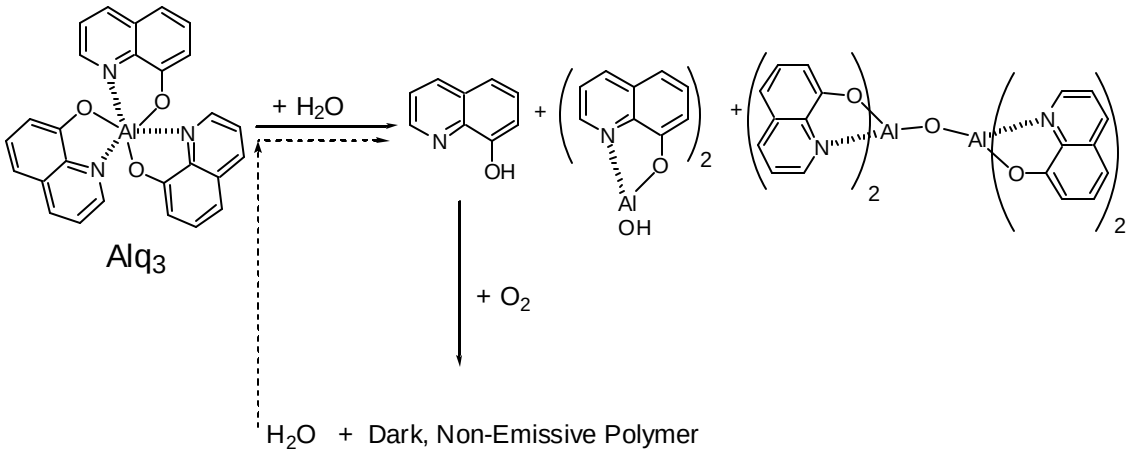

Figure 2.9 Proposed reaction scheme of the hydrolysis of Alq_3.

Why Alq_3 was Chosen

Since 1987, Alq_3 has been used extensively in organic light-emitting diodes as both the electron-transport and emissive layer.[4-7,9-19,22,26,27] Some of the reasons why Alq_3 has been used so frequently is because of its bright green emission, with photoluminescence efficiencies topping out around 30%, good electron mobility, and thermally stable up to 350 ^{o}C.[7] Another reason for utilizing Alq_3 is its tunability property. By simple changes in either the 8-hydroxquinoline ligand or the metal center

itself, both the emission color and efficiencies can be tuned.[5-7,9-14,16,28] The flexibility along with the extensive characterization is why Alq_3 was chosen as the focus of this research project.[4-7,9-14,16-20,22,27,28] One of the biggest drawbacks of working with Alq_3 is the difficulties encountered when processing the compound. In order to obtain a uniform thin film, the material must be vacuum deposited. To overcome this complex processing procedure yet maintain the luminescent properties of the compound, an Alq_3-functionalized polymer was targeted. The remaining chapters will discuss the designed, synthesis, and characterization of Alq_3-functionalized polymers, and how both the photoluminescent and electroluminescent properties of the polymers compared to those of the small molecule.

References

1. Wiberley, S. E.; Bassett, L. G. *Anal. Chem.* **1949**, *21*, 609-612.

2. Goon, E.; Petley, J. E.; McMullen, W. H.; Wiberley, S. E. *Anal. Chem.* **1953**, *25*, 608-610.

3. Freeman, D. C.; White, C. E. *J. Am. Chem. Soc.* **1956**, *78*, 2678-2682.

4. Tang, C. W.; VanSlyke, S. A. *Appl. Phys. Lett.* **1987**, *51*, 913-915.

5. Bryan, P. S.; Lovecchio, F. V.; VanSlyke, S. A. "Mixed ligand 8-quinolinolato aluminum chelate luminophors" **1992**, U.S. 5,141,671.

6. Anderson, J. D.; McDonald, E. M.; Lee, P. A.; Anderson, M. L.; Ritchie, E. L.; Hall, H. K.; Hopkins, T. A.; Mash, E. A.; Wang, J.; Padias, A. B.; Thayumanavan, S.; Barlow, S.; Marder, S. R.; Jabbour, G. E.; Shaheen, S.; Kippelen, B.; Peyghambarian, N.; Wightman, R. M.; Armstrong, N. R. *J. Am. Chem. Soc.* **1998**, *1998*, 9646-9655.

7. Chen, C. H.; Shi, J. *Coord. Chem. Rev.* **1998**, *171*, 161-174.

8. Coelle, M.; Gmeiner, J.; Milius, W.; Hillebrecht, H.; Brutting, W. *Adv. Funct. Mater.* **2003**, *13*, 108-112.

9. Ghedini, M.; La Deda, M.; Aiello, I.; Grisolia, A. *Inorganica Chim. Acta* **2004**, *357*, 33-40.

10. Hopkins, T. A.; Meerholz, K.; Shaheen, S.; Anderson, M. L.; Schmidt, A.; Kippelen, B.; Padias, A. B.; H.K. Hall, J.; Peyghambarian, N.; Armstrong, N. R. *Chem. Mater.* **1996**, *8*, 344-351.

11. Jang, H.; Do, L.-M.; Kim, Y.; Zyung, T.; Do, Y. *Synth. Met.* **2001**, *121*, 1667-1668.

12. Lu, J.; Hill, A. R.; Meng, Y.; Hay, A. S.; Tao, Y.; D'iorio, M.; Maindron, T.; Dodelet, J.-P. *J. Polym. Sci.: Part A: Polym. Chem.* **2000**, *38*, 2887-2892.

13. Meyers, A.; Weck, M. *Macromolecules* **2003**, *36*, 1766-1768.

14. Meyers, A.; Weck, M. *Chem. Mater.* **2004**, *16*, 1183-1188.

15. Papadimitrakopoulos, F.; Zhang, X.-M.; Thomsen, D. L.; Higginson, K. A. *Chem. Mater.* **1996**, *8*, 1363-1365.

16. Sapochak, L. S.; Padmaperuma, A.; Washton, N.; Endrino, F.; Schmett, G. T.; Marshall, J.; Fogarty, D.; Burrows, P. E.; Forrest, S. R. *J. Am. Chem. Soc.* **2001**, *123*, 6300-6307.

17. Sheats, J. R.; Antoniadis, H.; Hueschen, M.; Leonard, W.; Miller, J.; Moon, R.; Roitman, D.; Stocking, A. *Science* **1996**, *273*, 884-888.

18. Stoßel, M.; Staudigel, J.; Steuber, F.; Blassing, J.; Simmerer, J.; Winnacker, A.; Neuner, H.; Metzdorf, D.; Johannes, H.-H.; Kowalsky, W. *Synth. Met.* **2000**, *111-112*, 19-24.

19. Tang, C. W.; VanSlyke, S. A.; Chen, C. H. *J. Appl. Phys.* **1989**, *65*, 3610-3616.

20. Burrows, P. E.; Shen, Z.; Bulovic, V.; McCarty, M.; Forrest, S. R.; Cronin, J. A.; Thompson, M. E. *J. Appl. Phys.* **1996**, *79*, 7991-8006.

21. Brinkmann, M.; Gadret, G.; Muccini, M.; Taliani, C.; Masciocchi, N.; Sirani, A. *J. Am. Chem. Soc.* **2000**, *122*, 5147-5157.

22. Braun, M.; Gmeiner, J.; Tzolov, M.; Coelle, M.; Meyer, F. D.; Milius, W.; Hillebrecht, H.; Wendland, O.; von Schutz, J. U.; Brutting, W. *J. Chem. Phys.* **2001**, *114*, 9625-9632.

23. Curioni, A.; Boero, M.; Andreoni, W. *Chem. Phys. Lett.* **1998**, *294*, 263-271.

24. Halls, M. D.; Schlegel, H. B. *Chem. Mater.* **2001**, *13*, 2632-2640.

25. Kishore, V. V. N. R.; Aziz, A.; Narasimhan, K. L.; Periasamy, N.; Meenakshi, P. S.; Wategaonkar, S. *Synth. Met.* **2002**, *126*, 199-205.

26. Bassler, H. *Polym. Adv. Technol.* **1998**, *9*, 402-418.

27. Sheats, J. R. *Science* **1997**, *277*, 191-192.

28. Sapochak, L.; Benincasa, F. E.; Schofield, R. S.; Baker, J. L.; Riccio, K. K. C.; Fogarty, D.; Kohlmann, H.; Ferris, K. F.; Burrows, P. E. *J. Am. Chem. Soc.* **2002**, *124*, 6119-6125.

CHAPTER 3

DESIGN AND SYNTHESIS OF ALQ_3-FUNCTIONALIZED POLYMERS

As mentioned in the previous chapter, aluminum tris(8-hydroxyquinoline) (Alq_3) is one of the most stable and fluorescent solid-state materials, making it the emission and electron-transport layer of choice in organic light-emitting diodes (OLEDs).[1-5] One limitation associated with Alq_3 is its poor processability. The current trend in the fabrication of OLEDs is solution-processing; however, Alq_3 must be vacuum-deposited.[6,7] To overcome this limitation, polymers containing Alq_3 pendant groups can combine the fluorescent properties of Alq_3 while maintaining the processability of a polymer, allowing for the low-cost manufacturing techniques such as solution-processing and possibly ink-jet printing.[7] This chapter will propose the design of such a polymer-supported Alq_3, and introduce the initial synthesis and characterization of the Alq_3-functionalized polymers.

While most research activities of Alq_3 have been focused on manipulating the optical properties, the problem with the processability of Alq_3 has not been solved. One possible solution that has been utilized to enhance processability is the introduction of Alq_3-doped polymers, where the Alq_3 complex is embedded within a polymer matrix.[8,9] However, phase separation can occur, leading to poor optical properties in these systems.[10] To circumvent the phase separation problems, Alq_3 can be covalently attached to the polymer backbone. However, the only reported Alq_3-functionalized

polymer at the start of this research was a condensation polymer that was functionalized with Alq_3 in a post-polymerization step.[10] As a result of this post-polymerization step, the probability of having a fully functionalized polymer without cross-linking is a major concern. In contrast, the design strategy outlined in this chapter is based on a fully functionalized monomer that is polymerized after the attachment of the Alq_3 side-chain, potentially eliminating any cross-linking. Additionally, the polymer structure is controlled and altered by using co-monomers in order to tune the polymeric properties.

The monomer is designed with two structural motifs: (1) a polymerizable unit that allows for a high degree of control during the polymerization and (2) a functionalized 8-hydroxyquinoline ligand capable of being attached *via* an alkyl spacer to the polymerizable unit. Norbornene was chosen as the polymerizable unit. It can be polymerized using ring-opening metathesis polymerization (ROMP), a process where the carbon-carbon double bond of an olefin, such as norbornene, is broken and reformed in the presence of an organometallic catalyst, as shown in Figure 3.1. The thermodynamic stability of the olefin will determine how far to the right the equilibrium will fall. The more sterically strained the cyclic olefin, the more energy is released during the polymerization, driving the equilibrium towards the formation of polymers.[11-17] Besides norbornenes, some examples of other cyclic olefins that can be polymerized using ROMP include cyclooctenes, cyclopentenes, cyclobutenes, and oxanorbornenedicarbimides.[13]

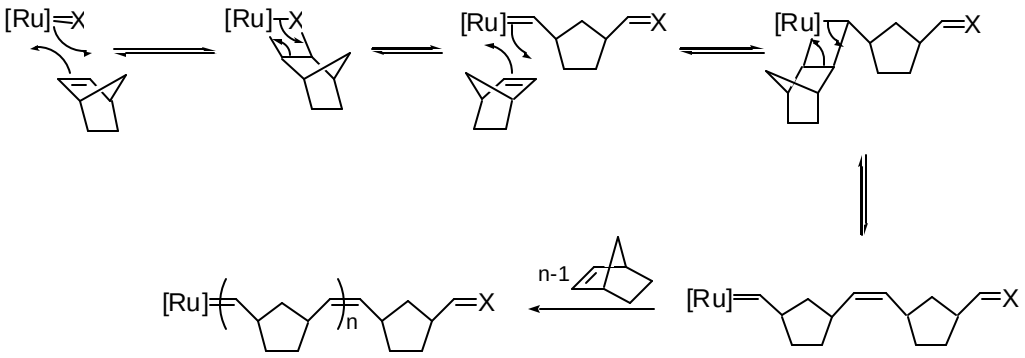

Figure 3.1 Mechanism of ring-opening metathesis polymerization with norbornene, where [Ru]=X is a ruthenium alkylidene, such as those shown in Figure 3.2.

Many catalysts are available to catalyze the ROMP of cyclic compounds. These catalysts are based on transition metals such as titanium, tungsten, molybdenum, and ruthenium.[18] Due to the tolerance towards most functional groups and the ease of handling in the presence of oxygen, water, and impurities, the Grubbs' ruthenium catalysts were chosen as the catalysts for the polymerizations in this work.[11-17] Some of the Grubbs' ruthenium catalysts, shown in Figure 3.2, exhibit high metathesis activity with fast initiation, controlled propagation, and virtually no chain-termination or chain-transfer, thus allowing for the formation of block copolymers or polymers with low polydispersities (PDI).[13-15,18,19]

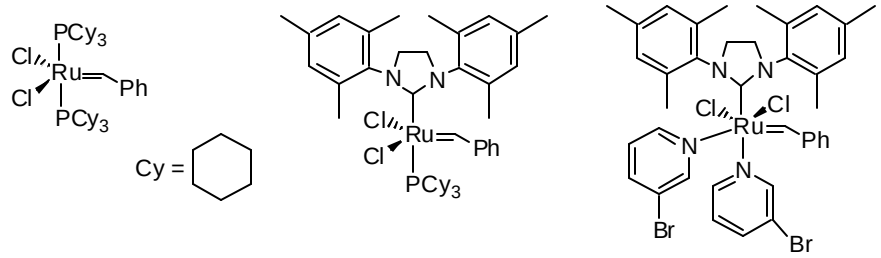

Figure 3.2 Structures of three of Grubb's ruthenium catalysts.

Results and Discussion

Synthesis. The synthesis of the monomer (Figure 3.3) began with the functionalization of the norbornene **1**, formed using a Diels-Alder reaction between allyl bromide and cyclopentadiene. Attachment of a bromoalkyl chain using Grignard chemistry followed by the conversion of the bromide to the nitrile and subsequent reduction of the nitrile resulted in the precursor **4** in an overall yield of 51%. Compound **4** was then coupled to 6, followed by the reduction of the resulting imine to yield monomer **8**.[20]

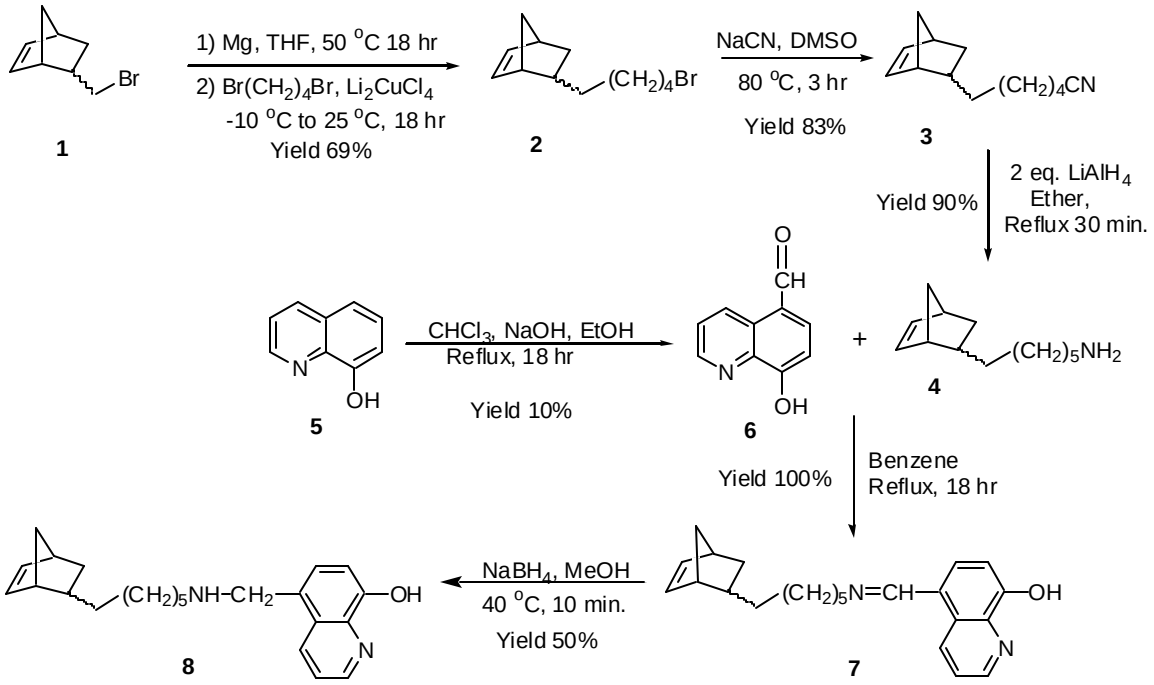

Figure 3.3 Synthetic scheme for Monomer **8**.

The formation of the Alq_3-functionalized monomer **9** was achieved by adding monomer **8** to10 equivalents of triethylaluminum followed by 20 equivalents of 8-hydroxyquinoline (Figure 3.4). This resulted in the formation of **1** equiv of **9** and 9 equiv of non-functionalized Alq_3. This procedure was developed to ensure full metallation of each monomer without coordination of two monomer units onto the same aluminum center, thereby preventing any cross-linking during the polymerization.[21]

Polymerizations. The 9:1 mixture (Alq_3:**9**) was used directly in the polymerizations, which were carried out in chloroform at room temperature using the ruthenium catalyst **11**. A 50:1 monomer-to-catalyst ratio was fully polymerized within 12 hours. After

complete polymerization, the excess Alq_3 was removed from the polymer through extensive washings with methanol and methylene chloride, yielding a polymer without any impurities.

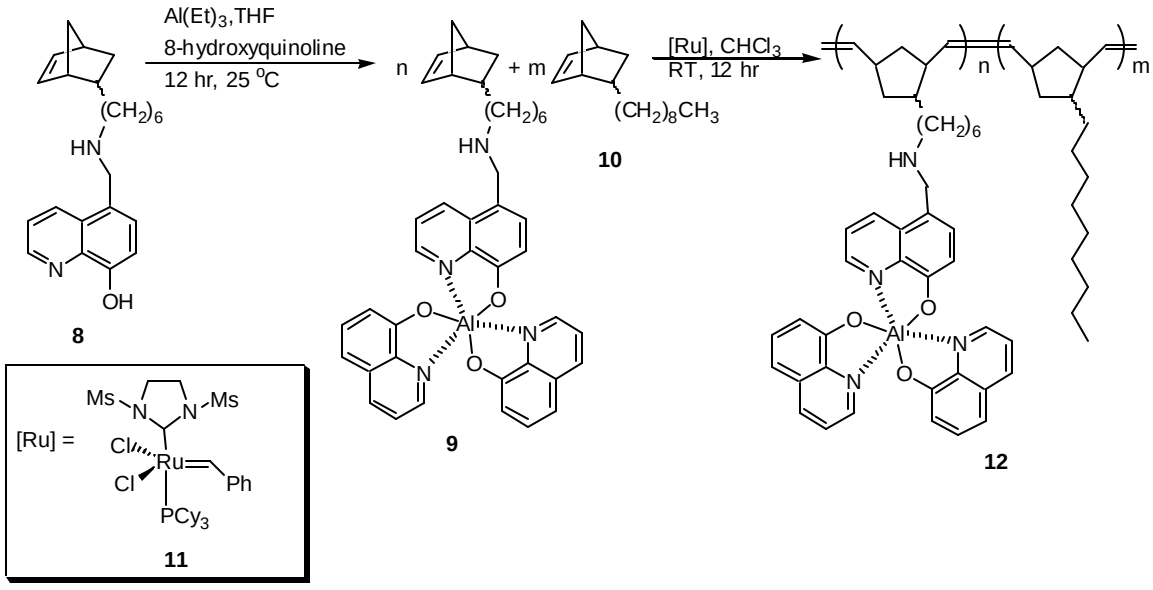

Figure 3.4 Formation of Alq_3-Monomer and copolymerization with nonylnorbornene.

Solubility of the polymer proved to be limited. However, solubility could be increased by copolymerizing **9** with 5-nonylnorbornene **10**, a non-functionalized monomer, which was synthesized in a similar manner as **2**. The optimal ratio of functional monomer to spacer monomer **(9:10)** (i.e., the highest percentage of **9** while retaining full and controlled solubility) was investigated through the synthesis of a series

of copolymers (Table 3.1). All copolymers with a **9:10** ratio of at least 1:4 could be fully solubilized in a 0.1% (v/v) chloroform/trifluoroacetic acid mixture. All resolubilized copolymers were characterized using gel permeation chromatography and showed polydispersities between 1.5 and 1.8, as shown in Table 3.1. Differential scanning calorimetry did not show a glass-transition temperature or a melting temperature, while thermogravimetric analysis showed the onset of polymer decomposition at 250 °C.

Table 3.1 Photoluminescence data for **8**, Alq_3, and a series of copolymers and copolymer characterization data.

Sample	*UV/Vis conc. (mg/mL)*	*UV/Vis* l_{max} *(nm)*	*Fluor. conc. (mg/mL)*	*Fluor.* l_{max} *(nm) [Intensity]*	*Mn*	*Mw*	*PDI*
Monomer **8**	0.02	319	---	---	---	---	---
Alq_3	0.1	316, 372	0.09	509	---	---	---
1:4 ***(9:10)*** Polymer	0.5	313, 370	0.05	512 [2.6×10^6]	68000	104000	1.53
1:5 ***(9:10)*** Polymer	0.5	313, 371	0.05	509 [2.3×10^6]	55000	94000	1.71
1:10 ***(9:10)*** Polymer	0.5	313, 373	0.05	506 [1.7×10^6]	57000	100000	1.74

Solution Photoluminescence Studies. Essential for the success of the polymer-supported Alq_3 strategy is that the copolymers retain the optical properties of Alq_3 and show no interference of the polymer backbone with the emission properties. Therefore, the photoluminescence of the copolymers and monomer **8** were investigated and compared to Alq_3 (Figures 3.5 and 3.6).[22] The UV/Visible absorption spectrum of monomer **8** shows a λ_{max} at 319 nm, corresponding to the low-energy singlet transition of the hydroxyquinoline group.[23] The absorption spectrum of Alq_3 as described in the literature and experimentally determined shows maxima at 372 nm and at 316 nm.[24] The absorption spectra of all copolymers show identical maxima as that of Alq_3, indicating that the same transitions taking place in the copolymers as the ones known for Alq_3.

The emission spectra of Alq_3 and the copolymers were collected from 400-700 nm with an excitation wavelength of 380 nm. As shown in Figure 3.6, all copolymers fluoresce at the same wavelength as Alq_3 in solution, demonstrating that the emission properties of Alq_3 are retained. As expected, the ratio of Alq_3-monomer to the non-functionalized monomer did affect the intensity of the emission. The intensity shows a linear relationship with the percentage of Alq_3 present in the copolymer, as indicated by the data provided in Table 3.1. These studies clearly show that the optical properties of Alq_3 are preserved in the polymer and not affected by the polymer backbone while in solution. Preliminary experiments of the spin coated copolymers resulted in thin films that show fluorescence emission similar to that of Alq_3 in the solid state. An in-depth study of the solid-state behavior of the copolymers is discussed in Chapter 4.

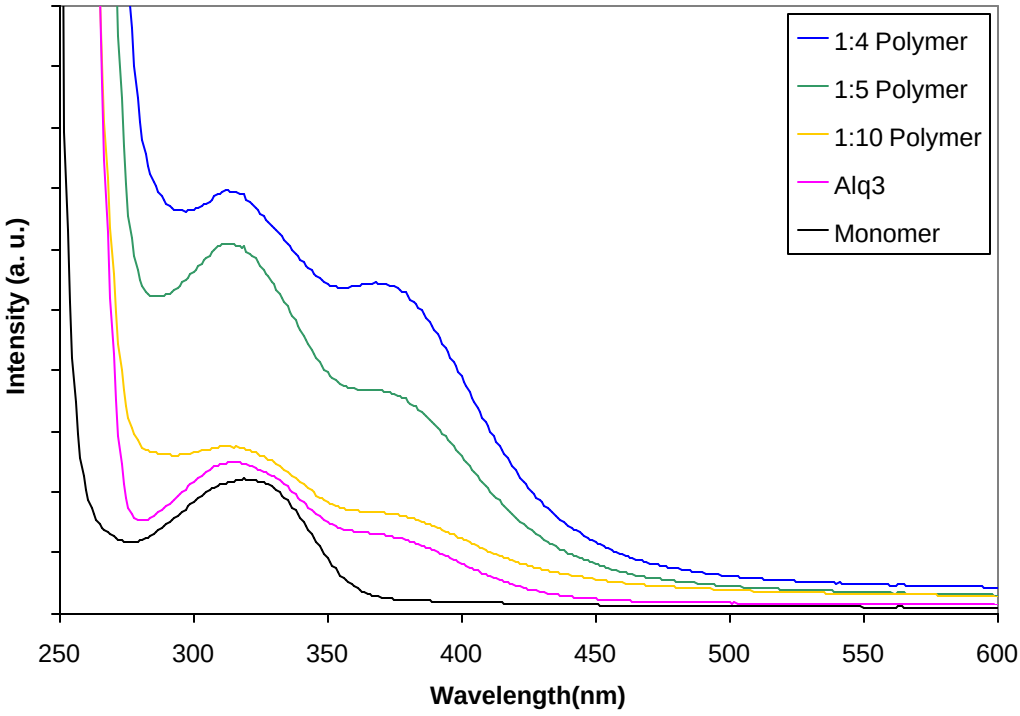

Figure 3.5 UV/Visible absorption spectra for Alq_3, Alq_3-Monomer and Alq_3-Polymers in $CHCl_3$.

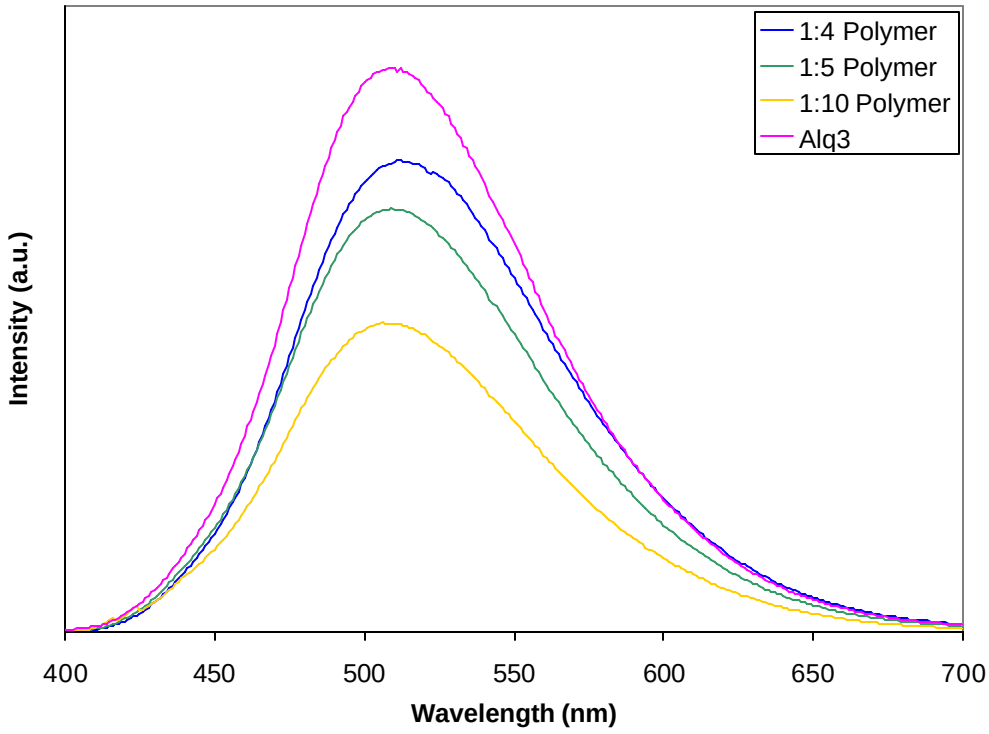

Figure 3.6 Photoluminescence spectra of Alq_3 and Alq_3-polymers in $CHCl_3$ excited at 380 nm.

Conclusions

This chapter describes the first successful synthesis of an Alq_3-containing monomer and its polymerization *via* ROMP. By covalently attaching 8-hydroxyquinoline to a norbornene monomer, a fully functionalized Alq_3-monomer can be formed by the addition of an aluminum source and excess 8-hydroxyquinoline. The monomer can then be polymerization, using ROMP conditions, resulting in a fully functionalized Alq_3-polymer. The insolubility of the Alq_3-homopolymer was alleviated by copolymerization of the Alq_3-monomer with nonylnorbornene. Most importantly, all

copolymers retained the absorption and emission properties of that of Alq_3 in solution, indicating that the polymer backbone does not interfere with the luminescence properties of the pendant Alq_3 groups. The next chapter will described the detail study of processing the Alq_3-copolymers into thin films and tuning the emission properties of the copolymers both in solution and in the solid-state.

Experimental

General: All chemicals were purchased from Acros Organics or Aldrich and used without further purification. Flash column chromatography was carried out on silica gel 60, 230-400 mesh (Sorbent Tech). ^{1}H (^{13}C) NMR spectra were recorded at 300 (75) MHz on a Varian Mercury 300 spectrometer. Mass spectra were obtained on a Micromass Quattro LC spectrometer and a VG-70se spectrometer. Elemental analyses were performed on a Perkin-Elmer CHNS/O Analyzer Series II 2400. Differential scanning calorimetry (DSC) was preformed under nitrogen using a Perkin-Elmer DSC 7 equipped with an Intracooler II device. The temperature program provided heating and cooling cycles between 0 and 300 °C at 20 °C/min. Gel permeation chromatography (GPC) analyses were carried out using a Waters 1525 binary pump coupled to a Waters 410 refractive index detector. The GPC was calibrated using polystyrene standards on an American Polymer Standards 10μ particle size, linear mixed bed packing columns set with CH_2Cl_2 as an eluent. UV/Visible spectra were obtained on a Perkin-Elmer Lambda 19 UV/VIS/NIR Spectrometer. The fluorescence spectra were obtained on a Spex

Fluorolog Spectrofluorimeter. Compounds **1-3** and **6** were synthesized from literature procedures.[20,25,26]

6-Bicyclo[2.2.1]hept-5-en-2-yl-hexylamine (4): A solution of the nitrile **3** (1.052 g, 0.005 mol) in diethyl ether was added drop wise to a $LiAlH_4$ suspension (0.43 g, 0.011 mol in 40 mL diethyl ether) at 0 °C. The mixture was allowed to warm to room temperature over a period of an hour, refluxed for 30 minutes, and then cooled back to room temperature. Water was added to neutralize any excess $LiAlH_4$. The ether layer was washed with water, 20% NaOH, brine, and dried over Na_2SO_4. The ether was removed to give a pale yellow liquid, which needed no further purification (0.726 g 67%). ^{1}H NMR (300 MHz, $CDCl_3$) δ 6.07 (1H endo, dd, *J* = 2.74, 5.49); 6.03-5.97 (2H exo, m); 5.87 (1H endo, *J* = 2.74, 5.49); 2.70 (2H, s); 2.65 (2H, t, *J* = 7.14); 1.94-1.74 (2H, m); 1.43-0.99 (12H, m); 0.46-0.40 (1H, m). ^{13}C NMR (75 MHz, $CDCl_3$) δ 137.1; 132.6; 49.8; 45.6; 42.7; 42.4; 38.9; 34.9; 33.9; 32.6; 29.9; 28.8; 27.1. HRMS (EI): calcd. for $C_{13}H_{23}N_1$ $[M]^+$ 193.1832, found 193.1852.

5-[(6-Bicyclo[2.2.1]hept-5-en-2-yl-hexylimino)-methyl]-quinolin-8-ol (7): Amine **4** (0.726 g, 0.00376 mol) and 5-formyl-8-hydroxyquinoline 6 (0.650 g, 0.00376 mol) were dissolved in 40 mL of benzene and refluxed for 18 hours. After cooling, the solvent was removed under reduced pressure to yield the product as an orange solid (1.308 g, 100%). ^{1}H NMR (300 MHz, $CDCl_3$) δ 9.75 (1H, dd *J* = 8.79, 1.64); 8.81 (1H, dd, *J* = 1.64, 4.39); 8.59 (1H, s); 7.69 (1H, d, *J* = 8.24); 7.56 (1H, dd, *J* = 4.39, 8.79); 7.19 (1H, d, *J* = 7.69); 6.10 (1H endo, dd, *J* = 2.74, 5.49); 6.06-5.99 (2H exo, m); 5.91 (1H endo,

dd, *J* =2.74, 5.94); 3.67 (2H, t, *J* = 7.14); 2.74 (2H, s); 1.99-1.69 (4H, m); 1.42-1.01 (12H, m); 0.50-0.44 (1H, m). ^{13}C NMR (75 MHz, $CDCl_3$) δ 160.8; 154.2; 148.1; 138.4; 137.0; 135.3; 133.0; 132.6; 127.0; 123.3; 123.2; 109.2; 62.9; 49.7; 45.6; 42.7; 38.9; 34.9; 32.6; 31.4; 29.9; 28.8; 27.6. HRMS (EI): calcd for $C_{23}H_{28}N_2O_1$ $[M]^+$ 348.2201, found 348.2186.

5-[(6-Bicyclo[2.2.1]hept-5-en-2-yl-hexylamino)-methyl]-quinolin-8-ol (8): Imine **7** was dissolved in 50 mL of dry methanol and 1 equivalent of $NaBH_4$ (0.136 g, 0.0036 mol) was added in small increments. After the addition was complete, the solution was allowed to stir for 10 minutes at room temperature. The solution was diluted with water and extracted three times with 20 mL of methylene chloride. The combined organic layers were washed with water, $NaHCO_3$, brine, and dried over Na_2SO_4. The solvent was removed under reduced pressure to yield a brown liquid. Purification by column chromatography (silica gel, 4:1 hexanes/ethyl acetate, then pure ethyl acetate, then 5% methanol in ethyl acetate) gave the product as a pale yellow solid (0.658 g, 50%). ^{1}H NMR (300 MHz, $CDCl_3$) δ 8.75 (1H, dd, *J* = 1.09, 4.39); 8.51 (1H, dd, *J* = 1.09, 8.24); 7.46 (1H, dd, *J* = 4.39, 8.24); 7.38 (1H, d, *J* = 7.69); 7.08 (1H, d, *J* = 7.69); 6.11 (1H endo, dd, *J* = 2.74, 5.49); 6.06-5.99 (2H exo, m); 5.90 (1H endo, dd, *J* = 2.74, 5.49); 4.10 (1H, s); 2.73 (2H, s); 2.71 (2H, t, *J* = 7.14); 1.99-1.02 (12H, m); 0.49-0.43 (1H, m). ^{13}C NMR (75 MHz, $CDCl_3$) δ 151.8; 147.6; 137.0; 136.3; 133.4; 132.6; 128.0; 127.4; 126.8; 121.8; 109.2; 51.2; 50.0; 49.7; 45.5; 42.7; 38.9; 34.9; 32.6; 30.2; 29.9; 28.8; 27.5. Anal. Calcd. for $C_{23}H_{30}N_2O$: C, 78.88; H, 8.63; N, 8.00. Found C: 78.79, H: 8.72, N: 8.00.

5-Nonyl-bicyclo[2.2.1]hept-2-ene (12): An oven-dried 3-neck round bottom flask was charged with magnesium turnings (0.809 g, 0.033 mol) and 40 mL of dry THF. 5-Bromomethylnorbornene (6.001 g, 0.032 mol) was added drop wise at room temperature. The mixture was then heated to 50 °C for 18 hours. In a separate flask, 10 mL of dry THF, Li_2CuCl_4 (5 mL, 0.0005 mol), and 1-bromooctane (6 mL, 0.035 mol) were combined and placed in a -10 °C ice bath. The Grignard reagent, which was transferred via cannula into an addition funnel, was added drop wise to the cooled solution. After the addition was complete, the solution was warmed to room temperature and stirred for 18 hours. The solution was diluted with ether, washed with NH_4Cl, brine, and dried over Na_2SO_4. The solvent was removed and the product was distilled at 76 °C at 0.4 mbar to yield a clear, colorless liquid (4.88 g, 69%). ^{1}H NMR (300 MHz, $CDCl_3$) δ 6.12 (1H endo, dd, J = 2.74, 5.49); 6.09-5.99 (2H exo, m); 5.93 (1H endo, dd, J = 2.74, 5.49); 2.75 (1H, s); 1.98-1.78 (2H, m); 1.40-1.07 (18H, m); 0.89 (3H, t, J = 6.05); 0.52-0.45 (1H, m). ^{13}C NMR (75 MHz, CDCl3) δ 137.0; 132.6; 49.7; 45.6; 42.7; 38.9; 35.0; 32.6; 32.1; 30.1; 29.9; 29.8; 29.5; 28.9; 22.9; 14.3.

Spin-casting procedure: The co-polymers were dissolved in chloroform at a concentration of approximately 30 mg/mL. Using a Specialty Coating Systems P-6000 spin-coater, the solution was dropped onto a glass slide, spinning at 1200 rpm.

References

1. Tang, C. W.; VanSlyke, S. A. *Appl. Phys. Lett.* **1987**, *51*, 913-915.

2. Tang, C. W.; VanSlyke, S. A.; Chen, C. H. *J. Appl. Phys.* **1989**, *65*, 3610-3616.

3. O'Brien, D. F.; Baldo, M. A.; Thompson, M. E.; Forrest, S. R. *Appl. Phys. Lett.* **1999**, *74*, 442-444.

4. Kido, J.; Hongawa, K.; Okuyama, K.; Nagai, K. *Appl. Phys. Lett.* **1994**, *64*, 815-817.

5. Jang, H.; Do, L.-M.; Kim, Y.; Zyung, T.; Do, Y. *Synth. Met.* **2001**, *121*, 1667-1668.

6. Friend, R. H.; Gymer, R. W.; Holmes, A. B.; Burroughes, J. H.; Marks, R. N.; Taliani, C.; Bradley, D. D. C.; Santos, D. A. D.; Bredas, J. L.; Logdlund, M.; Salaneck, W. R. *Nature* **1999**, *397*, 121-128.

7. Chen, C. H.; Shi, J. *Coord. Chem. Rev.* **1998**, *171*, 161-174.

8. Affinito, J. D.; Martin, P. M.; Graff, G. L.; Burrows, P. E.; Gross, M. E.; Sapochak, L. "Method of making molecularly doped composite polymer materials" **2002**, U. S. Patent 6,228436.

9. Antoniadis, H.; Roitman, D.; Miller, J. "Organic electroluminescent device" **1998**, U. S. Patent 5, 719467.

10. Lu, J.; Hill, A. R.; Meng, Y.; Hay, A. S.; Tao, Y.; D'iorio, M.; Maindron, T.; Dodelet, J.-P. *J. Polym. Sci.: Part A: Polym. Chem.* **2000**, *38*, 2887-2892.

11. Fürstner, A. *Angew. Chem. Int. Ed. Engl.* **2000**, *39*, 3012-3043.

12. Piotti, M. E. *Curr. Opin. Solid State Mater. Sci.* **1999**, *4*, 539-547.

13. Bielawski, C. W.; Grubbs, R. H. *Angew. Chem. Int. Ed.* **2000**, *39*, 2903-2906.

14. Sanford, M. S.; Ulman, M.; Grubbs, R. H. *J. Am. Chem. Soc.* **2001**, *123*, 749-750.

15. Schwab, P.; France, M. B.; Ziller, J. W.; Grubbs, R. H. *Angew. Chem. Int. Ed. Engl.* **1995**, *34*, 2039-2041.

16. Ivin, K. J. *Olefin Metathesis* Academic Press: London, **1996**.

17. Ivin, K. J.; Mol, J. C. *Olefin Metathesis and Metathesis Polymerization* Academic Press: New York, **1997**.

18. Buchmeiser, M. R. *Chem. Rev.* **2000**, *100*, 1565-1604.

19. Love, J. A.; Morgan, J. P.; Trnka, T. M.; Grubbs, R. H. *Angew. Chem.* **2002**, *114*, 4207-4209.

20. Clemo, G. R.; Howe, R. *J. Chem. Soc.* **1955**, 3552-3553.

21. The statistical probability of having two monomer units attached to the same aluminum center is 0.1%. Currently, we do not have the means for measuring this amount of cross-linking to determine if any is present.

22. Commercial Alq_3 was treated with the same chloroform/trifluoroacetic acid mixture as the copolymers. No changes in the optical properties before and after this treatment were detected.

23. Ravi Kishore, V. V. N.; Aziz, A.; Narasimhan, K. L.; Periasamy, N.; Meenakshi, P. S.; Wategaonkar, S. *Synth. Met.* **2002**, *126*, 199-205.

24. Halls, M. D.; Schlegel, H. B. *Chem. Mater.* **2001**, *13*, 2632-2640.

25. Giraudi, G.; Baggiani, C.; Giovannoli, C.; Marletto, C.; Vanni, A. *Anal. Chim. Acta* **1999**, *378*, 225-233.

26. Stubbs, L. P.; Weck, M. *Chem. Eur. J.* **2003**, *9*, 992-999.

CHAPTER 4

SOLUTION AND SOLID-STATE CHARACTERIZATION OF ALQ_3-FUNCTIONALIZED POLYMERS

In the previous chapter, the synthesis of Alq_3 side-chain functionalized norbornene polymers that combined the outstanding optical properties of Alq_3 with basic polymer properties was reported. The polymer system included the following design motifs: a) a norbornene monomer, b) an eight-atom spacer, and c) an Alq_3 moiety. The Alq_3-containing monomer was copolymerized with a spacer monomer in order to tune solubility. In this chapter, the potential of the polymeric Alq_3 system is evaluated in regards to the solid-state fluorescence properties and modifications on the Alq_3 side-chain. The ligand sphere around the aluminum center on the polymer is functionalized with electron-donating and withdrawing groups thereby allowing the emission of the polymer to be tuned from blue to yellow (430-549 nm). The resulting polymer is then spin-coated onto surfaces, overcoming fabrication problems associated with pure Alq_3. The Alq_3-copolymers, both in solution and in the solid-state, show outstanding emission properties clearly indicating that the polymer backbones do not interfere with the optical properties of the pendant Alq_3 side-chains. The optical properties of the copolymers, both in solution and in the solid-state, are reported to be independent of the polymer backbone and are comparable to their small molecule counterpart, demonstrating the potential of a polymer-supported Alq_3 OLED.

Results and Discussion

Synthesis. The synthesis of the modified polymers is shown in Figure 4.1. Metallation of monomer **1** was carried out by the addition of **1** to a solution of triethylaluminum, resulting in the formation of the metallated monomer **2**. The addition of two equivalents of the modified 8-hydroxyquinoline ligands **X** to monomer **2** – modified ligands are shown in Figure 4.2 – resulted in the formation of monomer **3** in quantitative yields. Polymerizations were carried out by combining **3** and **4** in chloroform and adding catalyst **5**. As mentioned in the previous chapter, copolymerization with nonylnorbornene was needed to render all polymers soluble in common organic solvents.[1] A ratio of $AlqX_2$-monomer to nonylnorbornene of 1:20 was used in all fluorescence studies unless otherwise noted.[2]

The polymers were characterized by NMR, gel-permeation chromatography (GPC), differential scanning calorimetry (DSC), and thermogravimetric analysis (TGA), with the results summarized in Table 4.1. The polymerizations were followed in situ by NMR and were considered complete when no monomer olefin signals were detected. The molecular weights of the polymers, determined by GPC, range from 7,000 to 55,000, with polydispersities (PDI) between 1.26 and 2.74. All polymers showed a decomposition temperature around 250 ^{o}C, and no glass transition or any other endotherms were detected.

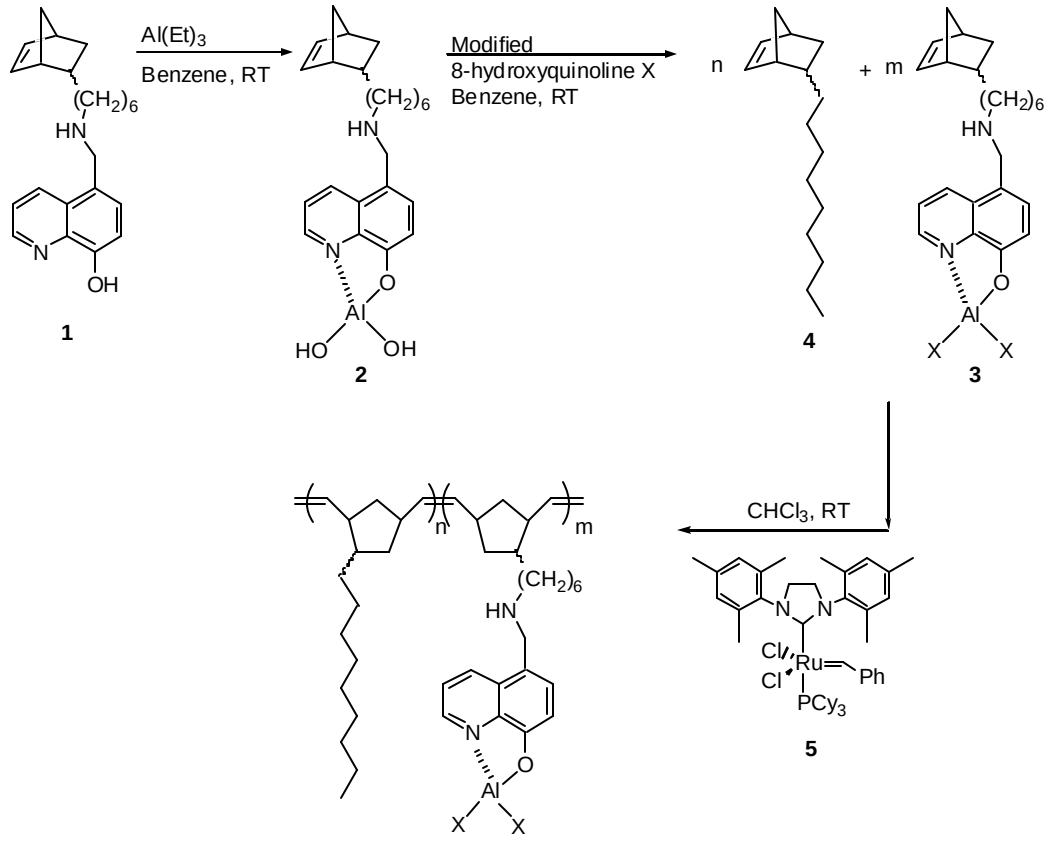

Figure 4.1 Formation of Alq_3-functionalized polymers.

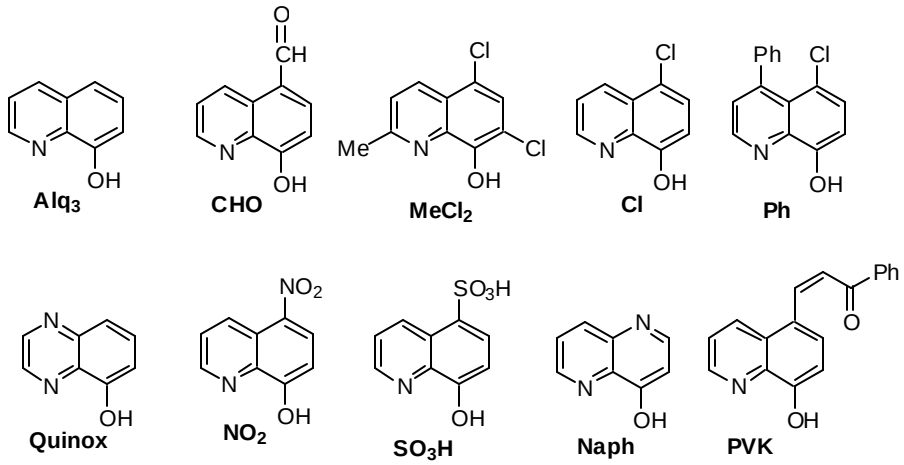

Figure 4.2 Structure and names of modified Alq_3-ligands.

Table 4.1 The monomer ratios, modified ligands, and molecular weight properties of all of the investigated polymers.

Polymer[1]	m/n ratio	X	Mn	Mw	PDI
$Alq_3$110	1:10	Alq_3	11000	16300	1.47
$Alq_3$120	1:20	Alq_3	7600	11600	1.53
$Alq_3$150	1:50	Alq_3	24000	58400	2.43
$Alq_3$500mer[2]	1:20	Alq_3	10400	18600	1.77
$Alq_3$1000mer[2]	1:20	Alq_3	19400	35400	1.82
Bu	1:20	Bu	6600	16100	2.46
CHO110	1:10	CHO	14200	29200	2.06
CHO120	1:20	CHO	24200	52600	2.16
CHO150	1:50	CHO	19000	42600	2.24
Cl	1:20	Cl	17500	43000	2.45
$MeCl_2$	1:20	$MeCl_2$	15000	28700	1.92
Naph120	1:20	Naph	21100	35100	1.67
NO_2	1:20	NO_2	11000	17000	1.56
Ph	1:20	Ph	17300	38300	2.21
PVK110	1:10	PVK	14500	27500	1.89
PVK120	1:20	PVK	10200	20800	2.04
PVK150	1:50	PVK	20000	55000	2.74
Quinox	1:20	Quinox	15600	31200	1.99
SO_3H	1:20	SO_3H	4700	7700	1.63

1. Polymers are named after the functionalized ligand **X** and the ratio of **3:4**. If a number is not present, then the polymer was composed of a 1:20 ratio.

2. 500mer and 1000mer refer to the number of repeat units in the polymer.

Solution Fluorescence Studies. The solution emission results are summarized in Figure 4.3 and Table 4.2. The emission of the unmodified Alq_3-polymer (**Alq_3**) emits at the same wavelength as pure Alq_3 (523 nm). Similar to modified-Alq_3, the polymers containing functionalized Alq_3 side-chains show either a blue- or red-shifted emission, depending on the functionalization. As an example, Figure 4.4 shows the emission of both modified and unmodified Alq_3-polymers in solution while being irradiated with UV light.

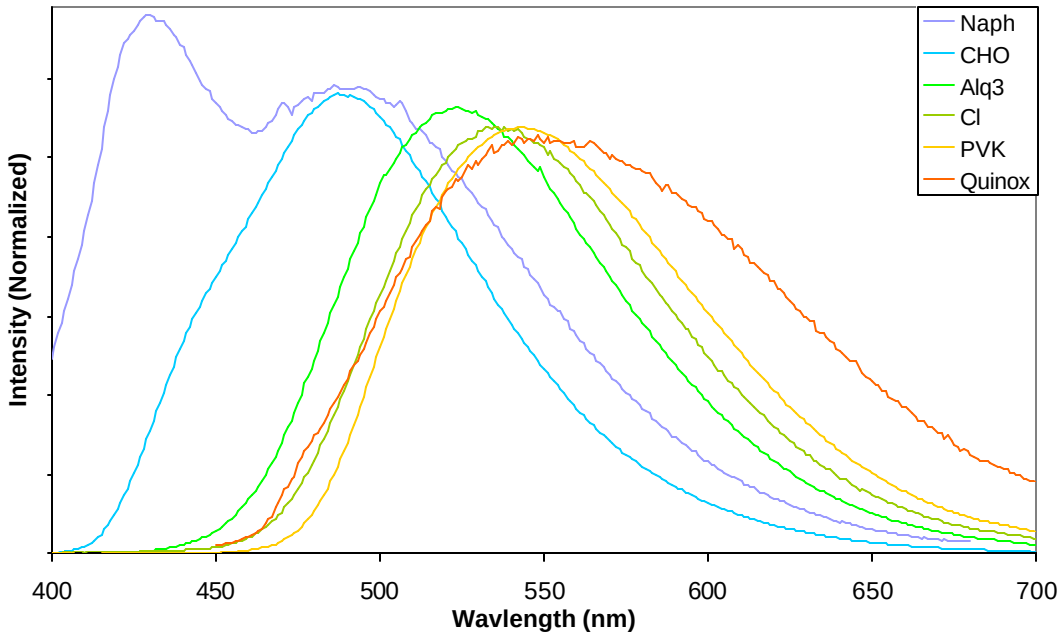

Figure 4.3 Photoluminescence spectra of selected $AlqX_2$-functionalized polymers in $CHCl_3$.

Table 4.2. Excitation and emission wavelength for the polymers in solution and the solid-state.

Polymer [1]	Excitation ? (nm)	Solution Emission $?_{max}$ (nm)	Solid-State Emission $?_{max}$ (nm)
Alq_3	380	523	511
Bu	380	522	515
CHO	380	488	510
Cl	380	537	520
$MeCl_2$	380	510	505
Naph	330	430, 490	437, 498
NO_2	380	510	n/a
Ph	380	524	n/a
PVK	380	543	537
Quinox	400	570	n/a
SO_3H	380	508	495
Alq500mer[2]	380	523	510
Alq1000mer[2]	380	522	512
Alq1000mer[2]	380	522	512

1. Polymers are named after the functionalized ligand **X**. All polymers are composed of a 1:20 ratio of **3:4**.

2. 500mer and 1000mer refer to the number of repeat units in the polymer.

While most of the modified 8-hydroxyquinoline ligands induce shifts in the emission spectra, the most noticeable shifts result from polymers functionalized with either the 4-hydroxy-1,5-naphthyridine (**Naph**) or the quinoxalinol (**Quinox**) ligands. The naphthyridine ligand induces a strong blue-shifted of about 90 nm, while the quinoxalinol ligand induces a red-shifted of about 50 nm. Other dramatic shifts occurred after functionalization with the aldehyde-functionalized ligand (**CHO**) (-32 nm) and the phenyl-vinyl-ketone-functionalized ligand (**PVK**) (+21 nm). Less dramatic shifts were seen for the polymers based on dichloromethyl- (**$MeCl_2$**), chloride- (**Cl**), and sulfonic acid- (**SO_3H**) functionalized hydroxyquinolines. The phenyl-functionalized (**Ph**) polymer did not shift the emission wavelength, probably because the donating ability of the phenyl group was offset by the withdrawing ability of the chloride group. The nitro-polymer (**NO_2**) did show a 20 nm blue-shift, but the intensity of this emission was very low in comparison to all other polymers. As reported for their small molecule counterparts, all shifts can be rationalized by considering the electron-donating and electron-withdrawing ability of the substituents on the modified ligands.

Figure 4.4 The Cl-, Alq_3-, SO_3H-, and CHO-functionalized polymers in chloroform irradiated with UV light.

Interestingly, the emission spectrum of the **Naph**-polymer shows two maxima, one at 430 nm and the other one at 490 nm. The two maxima can be attributed to the two different ligands around the aluminum center: two naphthyridine ligands and one hydroxyquinoline ligand. It is known that the emission from the Alq_3 molecule is due to the one 8-hydroxyquinoline ligand which is in-plane with the aluminum center.[3] It has been reported that the aluminum tris(naphthyridine) complex emits at 430 nm.[4] Therefore, the maximum at 430 nm is the result of the naphthyridine ligand being in the proper position to contribute to the fluorescence of the polymer, while the emission peak at 490 nm is the result of the hydroxyquinoline ligand. The electronics of the hydroxyquinoline ligand are affected by the naphthyridine ligand, resulting in a blue-shift from the usual 520 nm. This idea was tested by preparing the small molecule counterpart containing two naphthyridine ligands and one hydroxyquinoline ligand around an aluminum center. The emission spectrum of this compound was identical to that of the

polymer. This two ligand effect can also be seen in the **CHO**-polymer, with a small shoulder occurring at 450 nm.

From the solution emission studies, it is clear that the polymer backbone does not interfere with the optical properties of the Alq_3 side-chain. Furthermore, the solution studies clearly demonstrate that the emission can be tuned through simple ligand modifications.

Thin-Film Characterization. The thin films were fabricated by spin coating techniques and were characterized using optical microscopy, ellipsometry, and fluorescence spectroscopy. The thicknesses of the films range from 200 nm to 600 nm depending on the concentration of the polymer solution. The uniformity of the films was observed using an inverted microscope while irradiating the films with UV light. As shown in Figure 4.5, all of the films showed very smooth surfaces with good uniformity and very little defects.

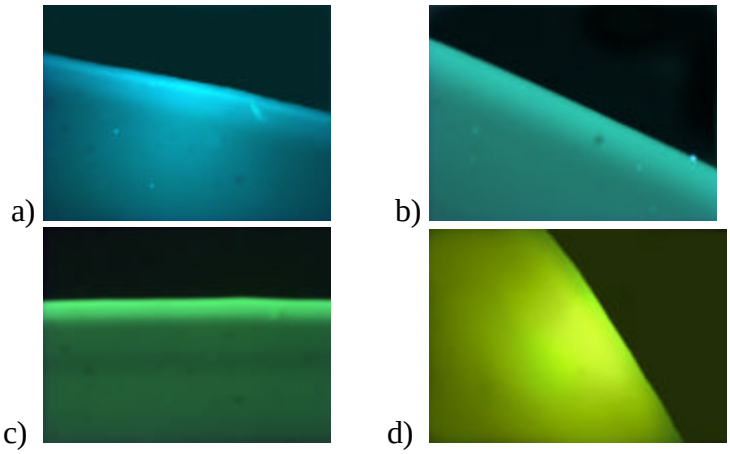

Figure 4.5 Images of thin films of a) 1:50 CHO-polymer, b) 1:10 CHO-polymer, c) 1:10 Alq_3-polymer, d) 1:20 PVK-polymer. Images, taken with a RS Photometrics camera using an Olympus inverted microscope and a viewing area of 1 cm, are irradiated with UV light.

Solid-State Fluorescence Studies. Good solid-state properties are essential for the potential use of the polymer-Alq_3 system. Therefore, the optical properties of all functionalized polymers were investigated in the solid-state. All polymers were excited at 380 nm (except for the **Naph**- and **Quinox**-polymers, which were excited at 330 nm and 400 nm, respectively) and their emission data are shown in Table 4.2. Figure 4.6 shows the normalized fluorescence spectra of selected polymers as thin films on quartz. All spectra show shifts in the emission compared to the unmodified Alq_3-polymer. However, in all cases the shifts were not as pronounced as described above in solution. Furthermore, the **Nitro**-, **Quinox**-, and **Phenyl**-polymers showed no emission at all. A previous report on aluminum tris(quinoxalinol) indicated that the solid-state emission of this compound is extremely weak, so it is not surprising that the **Quinox**-polymer does

not emit in the solid-state.[5] It is also well-known that the nitro-group quenches fluorescence in the solid-state, but no reports on phenyl-groups quenching fluorescence in Alq_3 systems have been reported.[6] Nevertheless, the shifts do clearly demonstrate that tuning the emission color is possible and that the polymer backbone does not inhibit fluorescence even in the solid-state.

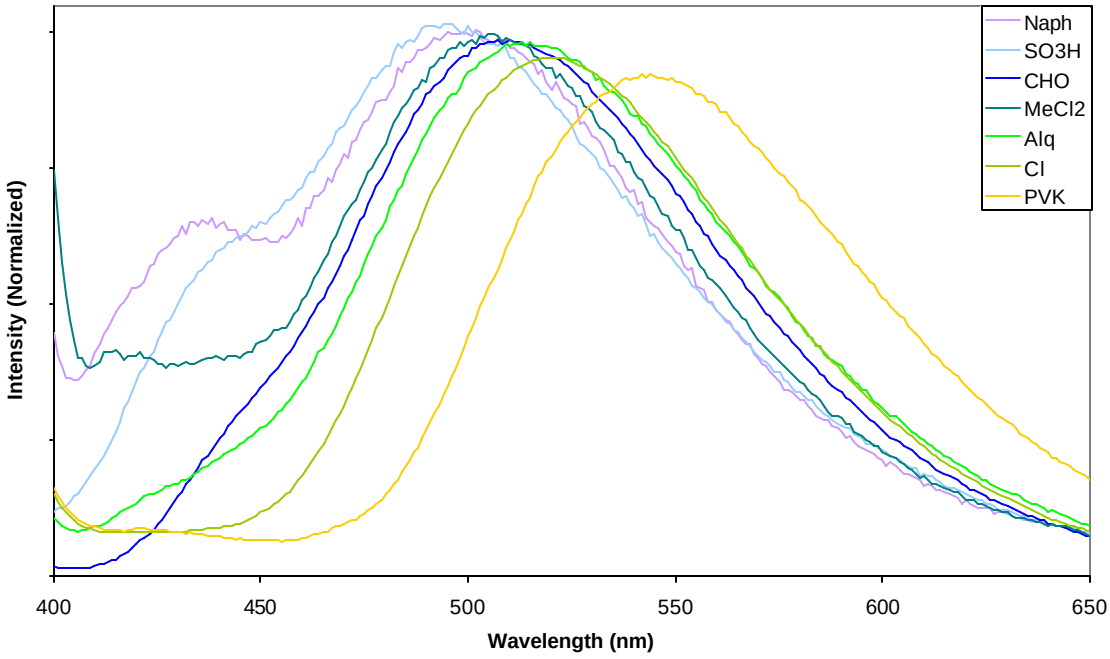

Figure 4.6 Solid-state photoluminescence spectra of selected modified polymers on quartz.

In order to investigate the influence of chromophore density on the emission, the ratio of the $AlqX_2$-monomer and nonylnorbornene was varied. The results of this study are shown in Figures 4.7-4.9 and are summarized in Table 4.4. Figure 4.7 shows the solid-state fluorescence spectra of the **Alq_3**-polymer with functionalized Alq_3-monomer (**3**) to nonylnorbornene (**4**) ratios of 1:10, 1:20, and 1:50. The emission wavelength is blue-shifted with decreasing chromophore density. Similar results can also be seen in Figure 4.8 for the **CHO**-polymer and Figure 4.9 for the **PVK**-polymer. While the shifts are different for each polymer, the trend is the same in all cases. However, this chromophore dilution effect is limited. A 1:100 ratio of **3:4** of the **CHO**-polymer showed identical emission peaks as that of the 1:50 **CHO**-polymer. This indicates that the emission wavelength is dependant on the packing of the $AlqX_2$-complex, agreeing with previously published results indicating that the shorter the inter-ligand contacts, the more red-shifted the emission.[7]

Table 4.3 Solution and solid-state emission wavelength for the polymers of varying chromophore ratios.

Polymer[1]	Excitation ? (nm)	Solution Emission $?_{max}$ (nm)	Solid-State Emission $?_{max}$ (nm)
$Alq_3$110	380	522	522
$Alq_3$120	380	523	511
$Alq_3$150	380	522	502
CHO110	380	486	522
CHO120	380	488	510
CHO150	380	487	494
PVK110	380	543	549
PVK120	380	543	537
PVK150	380	544	530

1. Polymers are named after the functionalized ligand **X** and the ratio of **3:4**.

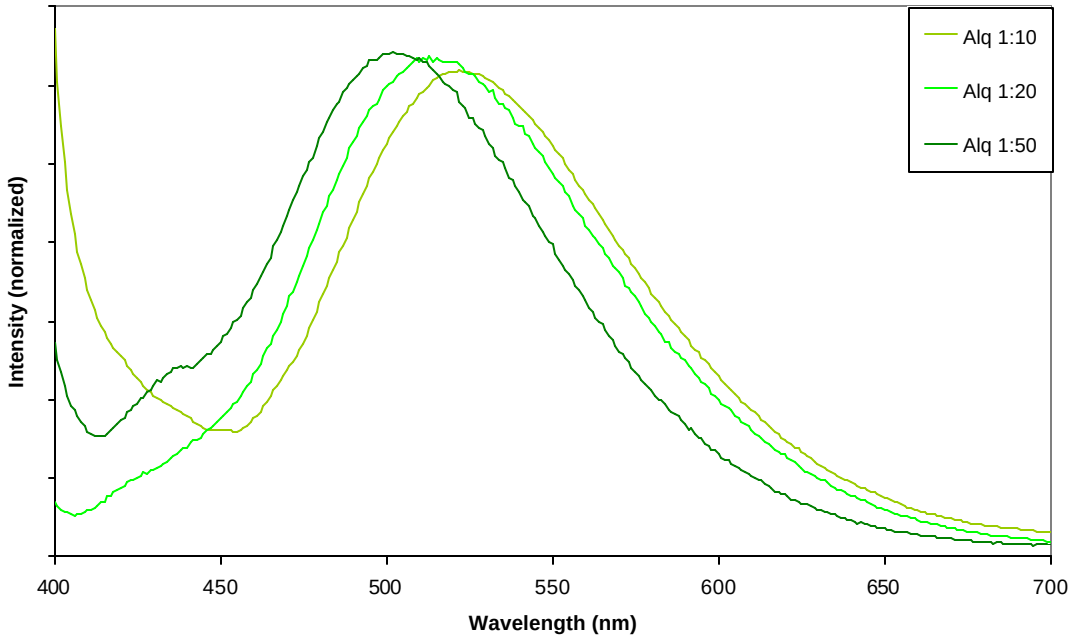

Figure 4.7 Solid-state photoluminescence spectra of three different co-monomer ratios of the Alq_3-polymer.

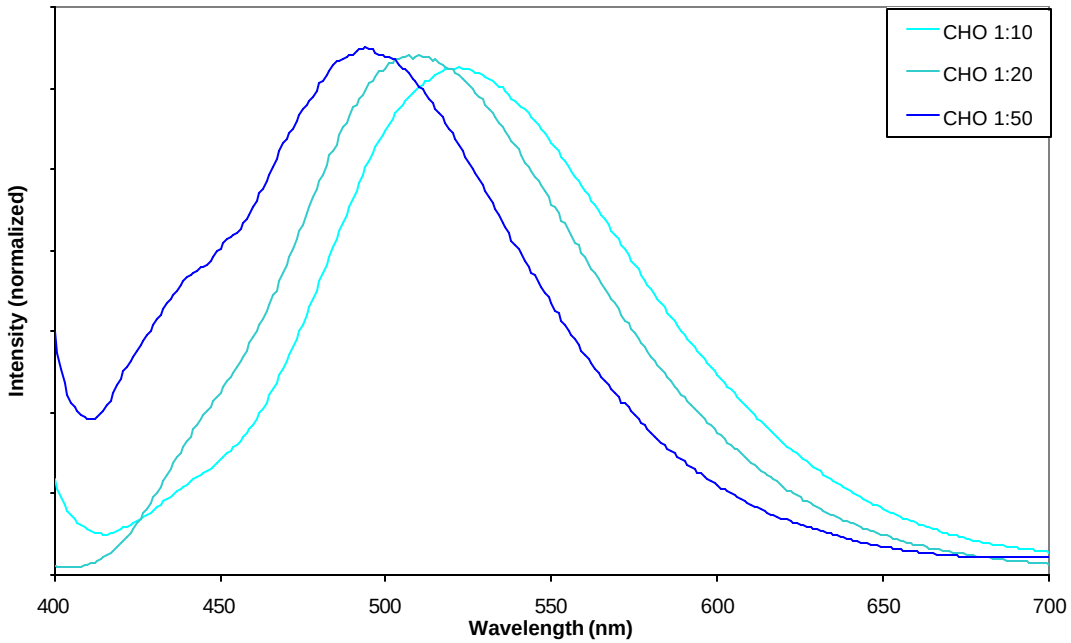

Figure 4.8 Solid-state photoluminescence spectra of three different co-monomer ratios of the CHO-polymer.

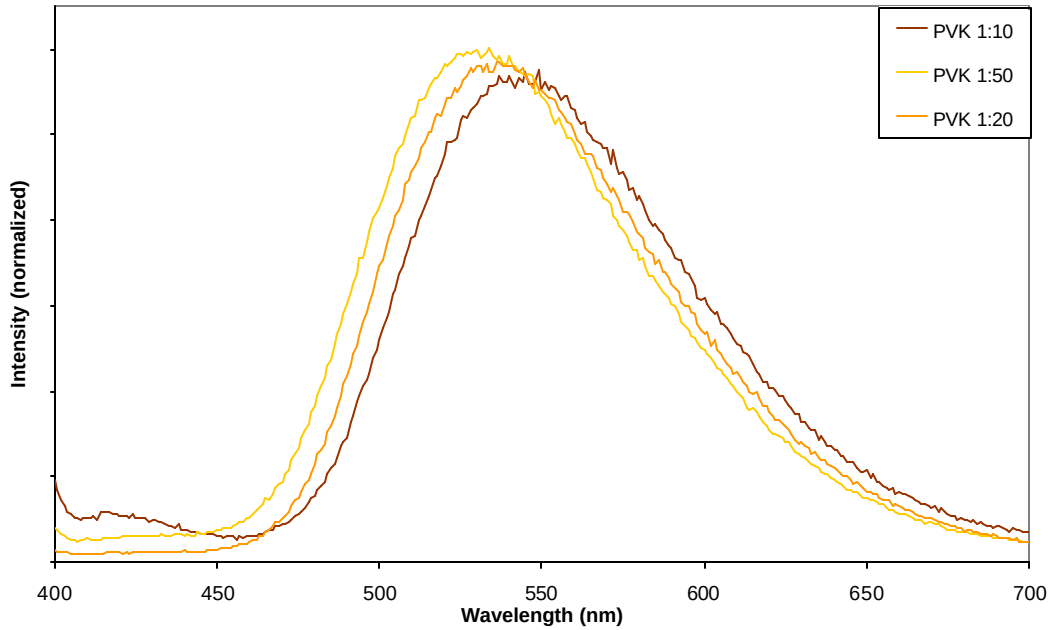

Figure 4.9 Solid-state photoluminescence spectra of three different co-monomer ratios of the PVK-polymer.

The effect of molecular weight on the optical properties was also investigated. As shown in Table 2, it was found that the changes in molecular weight have very little effect on the emission of the polymer, both in solution and the solid-state.

Conclusions

The Alq_3-polymers not only exhibit excellent agreement with the known-emitting molecule Alq_3, but the emission wavelength of the polymers can be altered by simple substitutions on the hydroxyquinoline ligand. Using ligands that are known to shift the photoluminescence, the emission of the functionalized polymers can be tuned in solution as well as in the solid-state from ranging from 490 nm up to 550 nm. The intensity of the

solid-state emission can be altered by adjusting the concentration of the polymer solution before spin-casting, while the emission wavelength can be shifted up to 30 nm by changing the chromophore density. This study clearly demonstrates that Alq_3-functionalized polymers are a viable option for potential use as electron-transport and emission layers in OLED. The next chapter will look into changing the metal center, to examine the effect different metals have on the emission wavelength.

Experimental

General: All chemicals were purchased from Acros Organics or Aldrich and used without further purification. Flash column chromatography was carried out on silica gel 60, 230-400 mesh (Sorbent Tech.). NMR spectra were recorded on a Varian Mercury 300 spectrometer. Differential scanning calorimetry (DSC) was preformed under nitrogen using a Perkin-Elmer DSC 7 equipped with an Intracooler II device. The temperature program provided heating and cooling cycles between -30 and 150 °C at 10 °C/min. Thermogravimetric analysis (TGA) measurements were performed using Nietzsche TG 209 from 30 to 800 °C at 20 °C/min. Gel permeation chromatography (GPC) analyses were carried out using a Waters 1525 binary pump coupled to a Waters 410 refractive index detector. The GPC was calibrated using polystyrene standards on an American Polymer Standards 10 µm particle size, linear mixed bed packing columns set with CH_2Cl_2 as an eluent. UV/Visible spectra were obtained on a Perkin-Elmer Lambda 19 UV/VIS/NIR Spectrometer. The fluorescence spectra were obtained on a Spex Fluorolog Spectrofluorimeter. Ellipsometry measurements were taken on a J. A. Woollam Co. Inc. Spectroscopic Ellipsometer, M-2000VI.

Monomers **1** and **4** and the modified 8-hydroxyquinoline ligands **Naph, Quinox, Ph, CHO,** and **PVK** were prepared from literature procedures.[1,8-11] The remaining modified 8-hydroxyquinoline ligands are commercially available.

Synthesis of 5-[6-Bicyclo[2.2.1]hept-5-en-2-yl-hexylamino)-methyl]-8-quinolinato-(dihydroxy)-aluminum (2). Monomer **1** (0.025 g, 0.07 mmol) was dissolved in 5 mL benzene, and added drop wise to a solution of triethylaluminum (0.04 mL, 0.07 mmol) in 10 mL benzene. The reaction was stirred for 2 hours under argon, the precipitate was filtered off, and the solvent was removed to yield a yellow solid **2** (0.03 g, 96 % yield). ^{1}H NMR (300 MHz, $CDCl_3$) δ 8.86 (0.5H, dd, J_1 = 4.94, 17.58); 8.68 (0.5H, m); 7.72 (1H, dd, *J* = 3.29, 5.50); 7.54 (2H, m); 7.03 (1H, t, *J* = 8.24); 6.11 (1H endo, dd, *J* = 2.74, 5.49); 6.06-5.99 (2H exo, m); 5.90 (1H endo, dd, *J* = 2.74, 5.49); 4.10 (1H, s); 2.73 (2H, s); 2.71 (2H, t, *J* = 7.14); 1.99-1.02 (12H, m); 0.49-0.43 (1H, m). ^{13}C NMR (75 MHz, $CDCl_3$) δ 137.0; 132.8; 51.2; 50.0; 49.7; 45.5; 42.7; 38.9; 34.9; 32.6; 30.2; 29.9; 28.8; 27.5.

Synthesis of 5-[6-Bicyclo[2.2.1]hept-5-en-2-yl-hexylamino)-methyl]-8-quinolinato-(diligand X)-aluminum (3). Two equivalents of the modified 8-hydroxyquinoline ligands **X** were dissolved in benzene and added drop wise to one equivalent of monomer **2**, dissolved in 10 mL of benzene. The solution was allowed to stir under argon for two hours, followed by the removal of the solvent to yield a solid ranging in color from bright yellow to dark orange. The exceptions to this procedure are when **X** was 4-hydroxy-1,5-

naphthyridine or 8-hydroxyquinoline-5-sulfonic acid. These compounds were dissolved in DMSO, while monomer **2** was dissolved in THF.

5-[6-Bicyclo[2.2.1]hept-5-en-2-yl-hexylamino)-methyl]-8-quinolinato-(di-8-hydroxyquinoline)-aluminum (Alq_3). ^{1}H NMR (300 MHz, $CDCl_3$) d 8.77 (3H, m); 8.57 (1H, m); 8.16 (2H, m); 7.44 (2H, m); 7.32 (2H, m); 7.19 (3H, m); 7.01 (2H, m); 6.11 (1H endo, dd, *J* = 2.74, 5.49); 6.06-5.99 (2H exo, m); 5.90 (1H endo, dd, *J* = 2.74, 5.49); 4.10 (1H, s); 2.73 (2H, s); 2.71 (2H, t, *J* = 7.14); 1.99-1.02 (12H, m); 0.49-0.43 (1H, m). ^{13}C NMR (75 MHz, $CDCl_3$) δ 152.67; 148.00; 147.57; 138.82; 136.95; 133.28; 132.54; 128.82; 127.82; 121.78; 118.04; 110.82; 50.39; 49.83; 45.68; 42.83; 39.04; 35.06; 32.75; 30.16; 28.9227.17; 25.95.

5-[6-Bicyclo[2.2.1]hept-5-en-2-yl-hexylamino)-methyl]-8-quinolinato-(di-5-formyl-8-hydroxyquinoline)-aluminum (CHO). ^{1}H NMR (300 MHz, $CDCl_3$) d 10.01 (3H, m); 9.95 (2H, dd, *J* = 4.39, 8.79); 8.88 (3H, dd, *J* = 4.94, 19.28); 8.05 (3H, m); 7.76 (2H, dd, *J* = 4.39, 8.24); 7.49 (2H, m); 7.18 (3H, m); 6.11 (1H endo, dd, *J* = 2.74, 5.49); 6.06-5.99 (2H exo, m); 5.90 (1H endo, dd, *J* = 2.74, 5.49); 4.10 (1H, s); 2.73 (2H, s); 2.71 (2H, t, *J* = 7.14); 1.99-1.02 (12H, m); 0.49-0.43 (1H, m). ^{13}C NMR (75 MHz, $CDCl_3$) δ 191.56; 145.97; 145.48; 144.27; 143.90; 143.48; 143.06; 141.11; 140.26; 139.50; 137.0; 132.8; 125.42; 125.05; 124.50; 118.87; 113.01; 51.2; 50.0; 49.7; 45.5; 42.7; 38.9; 34.9; 32.6; 30.2; 29.9; 28.8; 27.5.

5-[6-Bicyclo[2.2.1]hept-5-en-2-yl-hexylamino)-methyl]-8-quinolinato-(di-5-chloro-8-hydroxyquinoline)-aluminum (Cl). ^{1}H NMR (300 MHz, $CDCl_3$) δ 8.88 (1H, dd, *J* = 3.85, 19.23); 8.66 (2H, m); 7.76 (8H, m); 7.04 (4H, m); 6.11 (1H endo, dd, *J* = 2.74, 5.49); 6.06-5.99 (2H exo, m); 5.90 (1H endo, dd, *J* = 2.74, 5.49); 4.10 (1H, s); 2.73 (2H, s); 2.71 (2H, t, *J* = 7.14); 1.99-1.02 (12H, m); 0.49-0.43 (1H, m). ^{13}C NMR (75 MHz, $CDCl_3$) δ 145.66; 145.25; 143.07; 137.62; 137.24; 122.73; 122.07; 113.79; 113.35; 112.77; 51.2; 50.0; 49.7; 45.5; 42.7; 38.9; 34.9; 32.6; 30.2; 29.9; 28.8; 27.5.

5-[6-Bicyclo[2.2.1]hept-5-en-2-yl-hexylamino)-methyl]-8-quinolinato-(di-5,7-dichloro-2-methyl-8-hydroxyquinoline)-aluminum ($MeCl_2$). ^{1}H NMR (300 MHz, $CDCl_3$) δ 8.72 (1H, d, *J* = 3.85); 8.65 (1H, d, *J* = 3.85); 8.56 (1H, d, *J* = 8.79); 8.42 (1H, d, *J* = 8.79); 7.32 (2H, m); 7.06 (1H, dd, *J* = 7.69, 18.29); 6.89 (4H, m); 6.11 (1H endo, dd, *J* = 2.74, 5.49); 6.06-5.99 (2H exo, m); 5.90 (1H endo, dd, *J* = 2.74, 5.49); 4.10 (1H, s); 2.73 (2H, s); 2.71 (2H, t, *J* = 7.14); 1.99-1.02 (12H, m); 0.49-0.43 (1H, m). ^{13}C NMR (75 MHz, $CDCl_3$) δ 158.72; 151.86; 147.49; 143.97; 138.14; 136.99; 136.28; 133.74; 132.56; 128.30; 127.75; 123.48; 121.72; 121.38; 120.41; 115.25; 109.24; 68.24; 67.48; 49.63; 45.68; 42.82; 42.16; 39.01; 35.03; 33.39; 32.72; 30.08; 29.90; 28.89; 28.68; 27.69; 25.99; 25.10.

5-[6-Bicyclo[2.2.1]hept-5-en-2-yl-hexylamino)-methyl]-8-quinolinato-(di-5-nitro-8-hydroxyquinoline)-aluminum (NO_2). ^{1}H NMR (300 MHz, $CDCl_3$) δ 9.67 (1H, m); 8.90 (2H, m); 8.45 (2H, m); 8.19 (5H, m); 7.82 (1H, m); 7.56 (2H, m); 7.08 (3H, m); 6.11 (1H endo, dd, *J* = 2.74, 5.49); 6.06-5.99 (2H exo, m); 5.90 (1H endo, dd, *J* = 2.74, 5.49); 4.10

(1H, s); 2.73 (2H, s); 2.71 (2H, t, *J* = 7.14); 1.99-1.02 (12H, m); 0.49-0.43 (1H, m). ^{13}C NMR (75 MHz, $CDCl_3$) δ 151.85; 148.10; 147.78; 146.55; 144.03; 139.50; 136.95; 134.35; 133.67;132.49; 130.55; 127.79; 126.15; 125.82; 124.05; 121.01; 112.07; 110.09; 109.12; 49.78; 45.53; 42.74; 41.07; 38.86; 34.94; 32.66; 32.57; 29.51; 28.57; 27.56; 25.91.

5-[6-Bicyclo[2.2.1]hept-5-en-2-yl-hexylamino)-methyl]-8-quinolinato-(di-4-phenyl-5-chloro-8-hydroxyquinoline)-aluminum (Ph). ^{1}H NMR (300 MHz, $CDCl_3$) δ 8.75 (2H, m); 8.70 (4H, m); 8.58 (4H, m); 7.61 (3H, m); 7.39 (9H, m); 7.15 (3H, m); 6.11 (1H endo, dd, *J* = 2.74, 5.49); 6.06-5.99 (2H exo, m); 5.90 (1H endo, dd, *J* = 2.74, 5.49); 4.10 (1H, s); 2.73 (2H, s); 2.71 (2H, t, *J* = 7.14); 1.99-1.02 (12H, m); 0.49-0.43 (1H, m). ^{13}C NMR (75 MHz, $CDCl_3$) δ 155.25; 151.57; 138.35; 138.05; 137.05; 134.09; 132.58; 130.06; 129.00; 127.51; 127.12; 125.15; 120.41; 120.11; 110.45; 62.83; 61.38; 53.94; 49.89; 45.71; 45.56; 42.86; 39.06; 32.76; 30.05; 28.96; 27.71; 26.09.

5-[6-Bicyclo[2.2.1]hept-5-en-2-yl-hexylamino)-methyl]-8-quinolinato-(di-5-phenyl-vinyl-ketone-8-hydroxyquinoline)-aluminum (PVK). ^{1}H NMR (300 MHz, $CDCl_3$) δ 8.86 (2H, m); 8.51 (3H, m); 8.19 (4H, m); 8.05 (6H, m); 7.68 (10H, m); 7.17 (2H, m); 7.09 (2H, m); 6.11 (1H endo, dd, *J* = 2.74, 5.49); 6.06-5.99 (2H exo, m); 5.90 (1H endo, dd, *J* = 2.74, 5.49); 4.10 (1H, s); 2.73 (2H, s); 2.71 (2H, t, *J* = 7.14); 1.99-1.02 (12H, m); 0.49-0.43 (1H, m). ^{13}C NMR (75 MHz, $CDCl_3$) δ 193.23; 191.96;185.73; 183.27; 182.15; 178.75; 177.41; 175.02; 173.41; 171.89; 170.16; 169.73; 167.05; 165.31; 155.06; 150.19; 148.97; 139.72; 138.96; 137.07; 136.32; 132.82; 131.21; 130.90; 128.55; 127.89;

122.99; 119.86; 117.70; 114.34; 113.49; 50.05; 49.83; 45.68; 45.53; 42.82; 39.02; 35.03; 33.36; 32.76; 30.69; 29.75; 29.39; 28.89; 27.58; 26.93; 24.10; 23.40.

5-[6-Bicyclo[2.2.1]hept-5-en-2-yl-hexylamino)-methyl]-8-quinolinato-(di-8-hydroxyquinoline-5-sulfonic acid)-aluminum (SO_3H). ^{1}H NMR (300 MHz, $CDCl_3$) δ 9.00 (2H, m); 8.59 (6H, m); 8.08 (2H, m); 7.39 (1H, m); 7.03 (4H, m); 6.11 (1H endo, dd, *J* = 2.74, 5.49); 6.06-5.99 (2H exo, m); 5.90 (1H endo, dd, *J* = 2.74, 5.49); 4.10 (1H, s); 2.73 (2H, s); 2.71 (2H, t, *J* = 7.14); 1.99-1.02 (12H, m); 0.49-0.43 (1H, m). ^{13}C NMR (75 MHz, $CDCl_3$) δ 173.28; 167.36; 163.85; 156.84; 154.31; 151.89; 147.85; 147.66; 143.27; 141.39; 140.90; 140.14; 138.74; 136.89; 136.13; 134.25; 132.51; 131.79; 129.52; 127.82; 125.72; 1222.41; 122.17; 120.86; 117.59; 110.07; 109.27; 58.86; 56.85; 53.88; 49.72; 47.98; 45.50; 42.65; 42.01; 41.37; 40.74; 39.09; 38.76; 34.75; 33.30; 32.57; 29.54; 28.75; 27.62.

5-[6-Bicyclo[2.2.1]hept-5-en-2-yl-hexylamino)-methyl]-8-quinolinato-(di-5-quinoxalinol)-aluminum (Quinox). ^{1}H NMR (300 MHz, $CDCl_3$) δ 8.87 (5H, m); 7.82 (2H, m); 7.56 (2H, m); 7.45 (2H, m); 7.25 (4H, m); 6.11 (1H endo, dd, *J* = 2.74, 5.49); 6.06-5.99 (2H exo, m); 5.90 (1H endo, dd, *J* = 2.74, 5.49); 4.10 (1H, s); 2.73 (2H, s); 2.71 (2H, t, *J* = 7.14); 1.99-1.02 (12H, m); 0.49-0.43 (1H, m). ^{13}C NMR (75 MHz, $CDCl_3$) δ 158.78; 146.51; 145.85; 144.96; 143.68; 138.65; 137.83; 137.05; 136.28; 135.28; 133.31; 132.58; 131.06; 128.94; 114.67; 114.35; 113.95; 111.85; 49.87; 45.68; 42.80; 39.03; 35.18; 32.75; 30.69; 29.80; 28.96; 27.72; 23.46.

5-[6-Bicyclo[2.2.1]hept-5-en-2-yl-hexylamino)-methyl]-8-quinolinato-(di-4-hydroxy-1,5-naphthrydine)-aluminum (Naph). ^{1}H NMR (300 MHz, $CDCl_3$) δ 9.07 (4H, m); 7.62 (3H, m); 7.36 (2H, m); 7.15 (4H, m); 7.03 (2H, m); 6.11 (1H endo, dd, *J* = 2.74, 5.49); 6.06-5.99 (2H exo, m); 5.90 (1H endo, dd, *J* = 2.74, 5.49); 4.10 (1H, s); 2.73 (2H, s); 2.71 (2H, t, *J* = 7.14); 1.99-1.02 (12H, m); 0.49-0.43 (1H, m). ^{13}C NMR (75 MHz, $CDCl_3$) δ 159.63; 146.45; 145.42; 144.25; 138.50; 138.14; 137.72; 137.02; 135.18; 133.07; 132.62; 129.54; 128.49; 114.35; 114.16; 49.84; 45.68; 42.80; 39.06; 35.06; 32.54; 30.32; 29.26; 28.05; 27.59; 23.54.

General polymerization procedure. Monomers **3** and **4** were dissolved in chloroform in the desired ratio, the ruthenium catalyst **5** was dissolved in chloroform, and both solutions were combined. The polymerizations were monitored by NMR and were complete within 12 hours. All polymers were purified by repeated precipitation into methanol. Again, the exceptions to this procedure are when **X** was 4-hydroxy-1,5-naphthyridine or the 8-hydroxyquinoline-5-sulfonic acid. In these cases, the $AlqX_2$-monomer **3** was dissolved in a 1:1 ratio of DMSO/chloroform.

Solution photoluminescence studies. Approximately 5 mg of each of the polymers was dissolved in 10 mL of chloroform. Dilutions were made as needed. UV/Visible and fluorescence measurements were taken in a 1.0 cm quartz cell.

Thin film fabrication and characterization. The concentrations of the polymers in solution were varied from 15-100 mg of polymer per mL of chloroform. One drop of

each solution was dropped onto a quartz slide spinning at 2000 rpm. The polymer solutions that showed the highest fluorescence intensity in the solid-state ranged from 30-50 mg/mL. The films made for the ellipsometry experiment were prepared in a similar manner using gold-coated glass slides (100 nm of Au) instead of quartz slides. The film thicknesses were measured by ellipsometry by collecting data every 5° from 65° to 75° and were fitted using a Cauchy film on gold model.

References

1. Meyers, A.; Weck, M. *Macromolecules* **2003**, *36*, 1766-1768.

2. The monomers and subsequent polymers contain one 8-hydroxyquinoline ligand attached to a norbornene unit and two functionalized ligands. The nomenclature of the polymers is as follows: (**X**)-polymer, where **X** is equal to the functionality on the modified 8-hydroxyquinoline ligand.

3. Halls, M. D.; Schlegel, H. B. *Chem. Mater.* **2001**, *13*, 2632-2640.

4. Chen, C. H.; Shi, J. *Coord. Chem. Rev.* **1998**, *171*, 161-174.

5. Shoustikov, A.; You, Y.; Burrows, P. E.; Thompson, M. E.; Forrest, S. R. *Synth. Met.* **1997**, *91*, 217-221.

6. Li, Y.; Vamvounis, G.; Holdcroft, S. *Macromolecules* **2002**, *35*, 6900-6906.

7. Brinkmann, M.; Gadret, G.; Muccini, M.; Taliani, C.; Masciocchi, N.; Sirani, A. *J. Am. Chem. Soc.* **2000**, *122*, 5147-5157.

8. Freeman, S. K.; Spoerri, P. E. *J. Org. Chem.* **1951**, *16*, 438-442.

9. Eck, T. D.; Wehry Jr., E. L.; Hercules, D. M. *J. Inorg. Nucl. Chem.* **1966**, *28*, 2439-2441.

10. Hojjatie, M.; Muralidhara, S.; Dietz, M. L.; Freiser, H. *Synth. Comm.* **1989**, *19*, 2273-2282.

11. Clemo, G. R.; Howe, R. *J. Chem. Soc.* **1955**, 3552-3553.

CHAPTER 5

DESIGN, SYNTHESIS, CHARACTERIZATION, AND FLUORESCENT STUDIES OF THE FIRST ZINC-QUINOLATE POLYMER

In the previous chapter, substituents were added to the 8-hydroxyquinoline ligand in order to either increase or decrease the energy difference between the HOMO and LUMO of Alq_3, which resulted in emission wavelengths ranging from 430 nm to 565 nm. As mentioned in Chapter 2, another method of altering the energy band gap and perhaps improving the electroluminescent properties of Alq_3 is to change the metal center. A number of groups have replaced the aluminum center with boron and studied both the photoluminescence and the electroluminescence of the boron quinolate.[1-4] When similar devices were fabricated using the boron quinolate and Alq_3, the emission wavelength of the boron-containing device was centered around 514 nm, similar to that of the Alq_3 device, but the efficiencies were much lower than the Alq_3 device.[1,2] Other group 3 metals that were used in place of aluminum included gallium, which emitted at 502 nm, and indium, which emitted at 545 nm, however the relative photoluminescent quantum yields (F) decreased dramatically compared to Alq_3 ($F_{Gaq_3} = 0.36$, $F_{Inq_3} = 0.76$, $F_{Alq_3} = 1.00$).[5] Lithium, beryllium, magnesium, and zinc have also been used with 8-hydroxyquinoline to form a fluorescent metalloquinolate complex, showing emission wavelengths from 495 nm for the lithium complex up to 568 nm for the zinc complex.[5-

[13,15] However, out of all of these metal centers, only the zinc-quinolate complex showed an improved performance over Alq_3 as the electron-transport and emitting layer in an OLED.[6,9,10,12,15]

The zinc-quinolate complex (Znq_2) can exist in two different forms, either as a dihydrate under normal atmospheric conditions or as a tetramer under anhydrous condition.[11,14-16] The dihydrate complex contains two water molecules axial to the zinc metal while the hydroxyquinoline ligands are in-plane.[12] The tetrameric Znq_2, shown in Figure 5.1, is comprised of four Znq_2 complexes bridged together through the oxygen atoms.[14] The complex is symmetrical around an inversion center, which is quite different from the Alq_3 compound that lacks symmetry.[12,14] The HOMO and LUMO of the Znq_2 complex, similar to Alq_3, are preserved on the 8-hydroxyquinoline ligands, in particular on the terminal ligands.[12] It is the terminal ligands that exhibit strong *?-?* stacking, both intramolecular and intermolecular between the pyridyl-side of the ligand with the phenoxide-side of a neighboring ligand.[12] This is different from the pyridyl-pyridyl stacking of Alq_3.[12,16] As mentioned in Chapter 2, the lowest energy electronic transition for Alq_3 is the *?-?** transition that involves partial charge transfer from the phenoxide-side of the hydroxyquinoline ligand to the pyridyl-side.[17] So the phenoxide-pyridyl overlap in Znq_2 provides a more efficient pathway for electron transport, which results in lower operating voltages and higher efficiencies.[6,9,10,12,15]

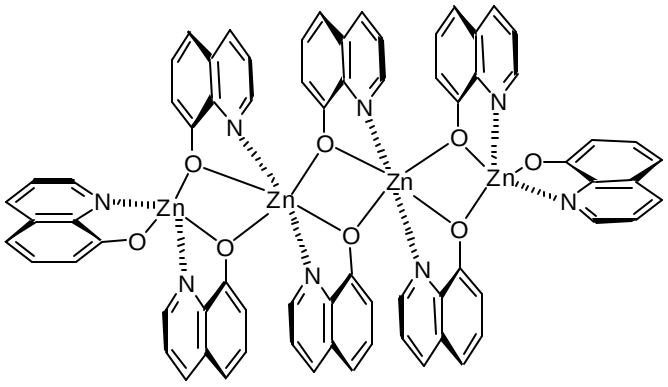

Figure 5.1 Structure of the tetrameric Znq_2.

Znq_2 can provide many benefits as an electron-transport and emitting material over Alq_3.[6,9,10,12,15] However, as in the case with Alq_3, the major drawback of Znq_2 is the need for vacuum deposition for thin film formation. The previous two chapters described a polymer-supported Alq_3 system that is able to overcome this processable limitation.[18,19] This chapter will describe the next generation of fluorescent material designed by combining the previously mentioned polymerization strategy with the outstanding photoluminescence and electroluminescence properties of Znq_2 in the preparation and characterization of the first Znq_2-functionalized polymers.

Results and Discussion

In order to directly compare the photoluminescent properties between the Alq_3-polymer and the Znq_2-polymer, the same monomer and polymerization techniques were employed for the preparation of the Znq_2-polymer, as shown in Figure 5.2. One

equivalent of monomer **1** was added to one equivalent of diethylzinc, insuring complete metallation without the addition of two monomers to one zinc atom as determined by elemental analysis. One equivalent of 8-hydroxyquinoline or one of the modified hydroxyquinoline ligands **X**, the structures and abbreviations are shown in Figure 5.1, was then added to the metallated monomer **2**, resulting in the formation of the zinc-monomer **3** in quantitative yields. The modified hydroxyquinoline ligands were used in a similar manner as in the previous chapter, to tune the emission wavelength of the Znq_2-polymers.[20]

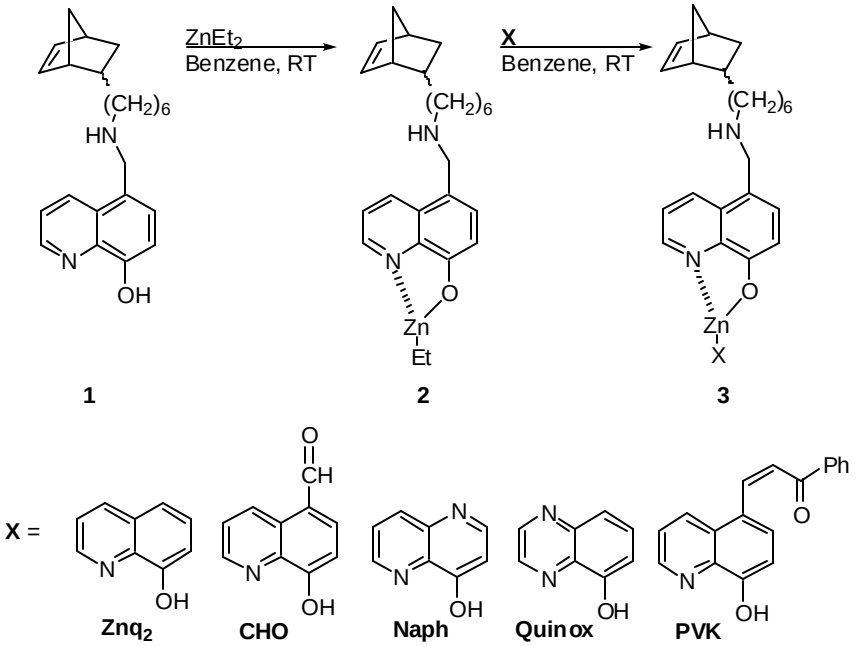

Figure 5.2 Formation of the ZnqX-monomers and the structures of the modified hydroxyquinoline ligands.

Polymerization of **3** was carried out using the ring-opening metathesis polymerization (ROMP) ruthenium catalyst **5** in chloroform at room temperature (shown in Figure 5.3) and was complete after 12 hours.[21] As outlined in chapter 3, the solubility of the polymeric material can be tailored by copolymerizing **3** with a spacer monomer, nonylnorbornene **4**, in ratios of 1:1, 1:5, 1:10, and 1:20 (**3**/**4**), resulting in copolymers that were readily soluble. For the optical properties characterization of the copolymers, the 1:20 ratios were used unless otherwise noted.

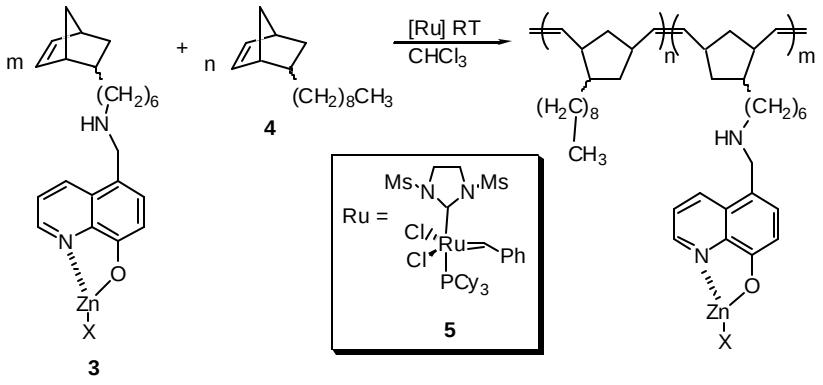

Figure 5.3 Polymerization scheme of ZnqX-copolymers.

All copolymers were characterized using NMR, gel-permeation chromatography (GPC), differential scanning calorimetry (DSC), and thermogravimetric analysis (TGA). The polymerizations were followed in situ by NMR and were considered complete when no monomer olefin signals were detected. The molecular weights of the copolymers

ranged from 8,000 to 40,000, with polydispersities between 1.5 and 2.5. All polymers showed a decomposition temperature around 250 °C, but no glass transition or any other endotherms were detected.

The UV/Vis and fluorescence spectra of the copolymers were recorded in dry chloroform and the results are summarized in Table 5.1. The photoluminescence spectra of all copolymers in chloroform are shown in Figure 5.4. All copolymers were excited at 380 nm, except for the **Naph** copolymer which was excited at 330 nm due to the strong absorption at this wavelength, which was not seen for the other polymers. As illustrated in Figure 5.4, the emission can be tuned in solution from blue (427 nm) to yellow (565 nm) through variations of the functionalized quinolines. These results clearly demonstrate that the fluorescence properties of the material can be tuned in solution and that the polymer backbone does not interfere with the optical properties of the Znq_2 moiety.

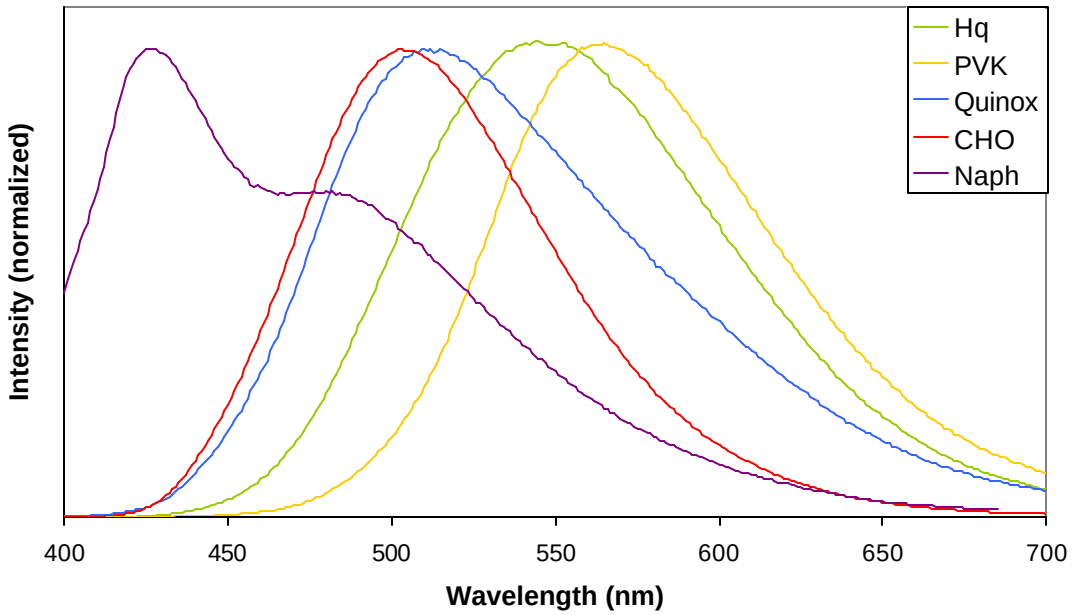

Figure 5.4 Photoluminescence spectra of ZnqX-polymers in $CHCl_3$.

The relative quantum yields of the copolymers were calculated based on Alq_3 as the standard and are summarized in Table 5.1. As suggested by other reports, Znq_2 has a higher quantum yield than Alq_3.[15] Surprisingly, the 1:1, 1:5, and 1:10 Znq_2-copolymers have even higher quantum yields then their small molecule counterpart. It is not until the concentration of the Znq_2-monomer drops below 10 mol% of the total copolymer composition that the quantum yields decrease below that of pure Znq_2. The increase in quantum yields going from Znq_2 to the 1:1 Znq_2-copolymer to the 1:5 Znq_2-copolymer indicates the possibility of some self-quenching occurring at higher Znq_2 concentrations. It is noteworthy that all 1:20 copolymers have approximately the same quantum yields,

except for the **CHO**-copolymer, which is significantly higher than that of Znq_2 suggesting an exceptional material for electroluminescence.

Essential for the use of these materials in electronic devices are their solid-state properties. To characterize the solid-state properties of all copolymers, thin films were spun on quartz slides, with thicknesses ranging between 200-400 nm as determined by ellipsometry. The fluorescence spectra were recorded at an excitation wavelength of 380 nm (**Naph** at 330 nm) and are shown in Figure 5.5, with the $?_{max}$ reported in Table 5.1. Similar to the solution studies, the emission colors of the films range from the blue to the yellow. The influence of the lumophore density on the solid-state properties was also investigated. The 1:1 copolymer emission is red-shifted in comparison to the emission of the 1:5 copolymer, which also shows a bathochromic shift compared to the 1:10 copolymer. This phenomenon has previously been described in relation to Alq_3, where the emission wavelength is dependant on the packing of the quinolate ligands.[22] The shorter the interligand contacts, the more red-shifted the emission.[22] This effect was also seen for the Alq_3-copolymers studied in the previous chapter. Regardless of the lumophore concentration and the quinoline ligand used, the emission of the thin films again indicates that the polymer backbone does not inhibit fluorescence, even in the solid-state.

Table 5.1 Photoluminescence data for Znq_2-polymers.

Name[a]	Absorption (nm) $?_{max}$	Solution Emission (nm) $?_{max}$	Solid-State Emission (nm) $?_{max}$	Relative Quantum Yields
Alq_3	381	525	519[b]	1.0
Znq_2	379	542	542[b]	1.3
1:1 Znq_2	378	544	548	1.8
1:5 Znq_2	375	543	520	3.9
1:10 Znq_2	375	545	512	2.0
1:20 Znq_2	378	546	505	0.30
CHO	381	503	487	2.2
PVK	373	565	545	0.33
Naph	325	427	445	0.37
Quinox	379	510	467	0.44

a. Polymers are names after the functionalized ligand **X**. All copolymers are composed of a 1:20 ratio of **3:4** unless otherwise noted.

b. Reported in reference 11.

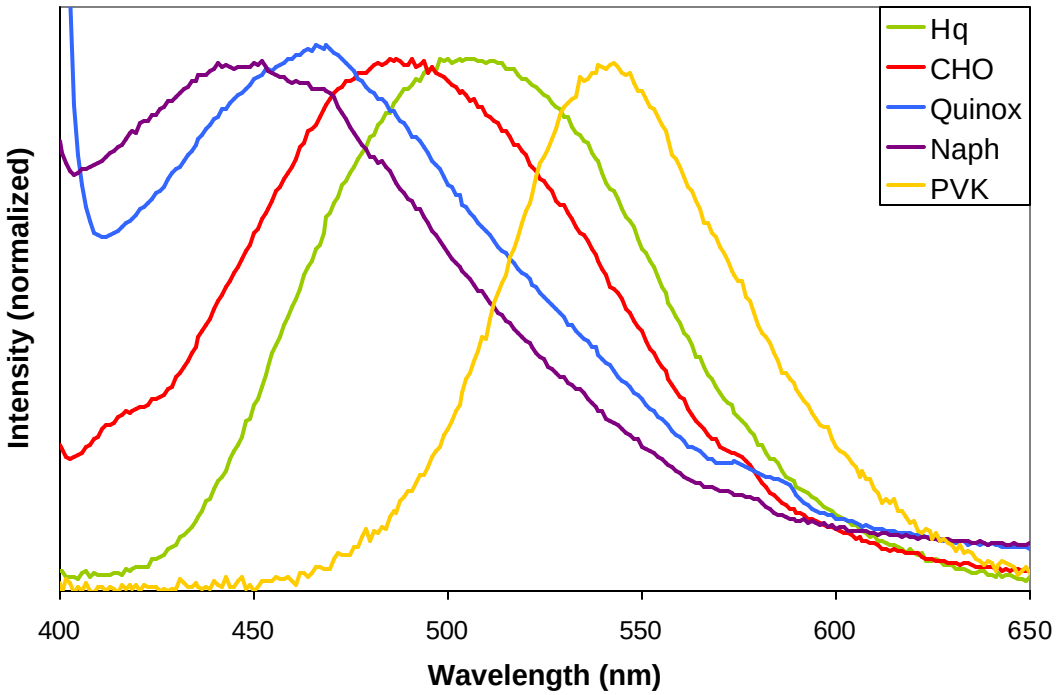

Figure 5.5 Solid-state photoluminescence spectra for ZnqX-polymers.

Table 5.2 lists the emission wavelength maxima for both the Znq_2- and Alq_3-copolymers. It appears that the Znq_2-copolymers emit at a higher wavelength compared to their Alq_3-copolymer counterparts in solution, with the exception of the **Naph** and **Quinox** copolymers. This red-shift can be attributed to the more covalent nature of the zinc-nitrogen bond compared to the aluminum-nitrogen bond.[23] However, in the solid-state, no clear trend can be observed between the two different metal centers. Another interesting observation is the emission of the **Quinox**-Zn-copolymer at 510 nm compared to the emission of the **Quinox**-Al-copolymer at 570 nm. It was reported that the quinoxalinol ligand would have a bathochromic shift compared to 8-hydroxyquinoline

due to the electron-withdrawing nature of the nitrogen in the ring, however it appears to have the opposite effect when zinc is used as the metal center compared to aluminum.[23] In the solid-state, the metal center has a dramatic impact on the emission. The zinc-**Quinox**-copolymer shows a blue-shifted emission in the solid-state compared to solution, while the emission of the aluminum-**Quinox**-copolymer is not detected in the solid-state. The solid-state emission of the aluminum-**Quinox** small molecule has previously been reported as being low, with an efficiency of 0.015 relative to Alq_3, due to the strong intermolecular interactions between the nitrogen atoms in the ring, which quenches the emission.[24] It is proposed that the pyridyl-phenoxide-overlap of the ligands of the zinc tetramer prevents the intermolecular interactions of the nitrogen atoms, therefore preventing the emission of the **Quinox**-ligand to be quenched. The other nitrogen-containing ligand, **Naph**, showed almost identical emission for both the zinc and aluminum complexes in solution, with only slight differences in the solid-state.

Table 5.2 Solution and Solid-state emission for the Znq_2- and Alq_3-copolymers.

Name[a]	Solution Emission (nm) $?_{max}$	Solid-State Emission (nm) $?_{max}$
1:20 Alq_3	523	511
1:20 Znq_2	546	505
Al-CHO	488	510
Zn-CHO	503	487
Al-PVK	543	537
Zn-PVK	565	545
Al-Naph	430	437
Zn-Naph	427	445
Al-Quinox	570	not detected
Zn-Quinox	510	467

a. Polymers are names after the metal center and functionalized ligand **X**. All copolymers are composed of a 1:20 ratio of functionalized monomer/nonylnorbornene.

Conclusion

The first Znq_2-based monomers were synthesized and copolymerized with a spacer monomer *via* ROMP. The resulting copolymers retained the photoluminescent properties of the metalloquinolates while gaining the added advantage of being solution processable. Similar to the Alq_3-copolymers discussed in the previous chapter, the

emission wavelength of the Znq_2-copolymers can be tuned from blue to yellow through simple modifications to the 8-hydroxyquinoline ligand. The copolymers demonstrated extremely high quantum yields in solution, far exceeding that of the extensively used Alq_3. While some differences in the emission wavelength were detected, the general trend of a bathochromic shift was observed for the zinc-copolymers compared to the aluminum-copolymers discussed in the previous chapter. While the electroluminescence was not measured and no conclusions can be made about the electron-transport properties of these copolymers, this study suggests that the Znq_2-copolymers are excellent candidates for potential use in organic electroluminescent devices.

Experimental

General: All chemicals were purchased from Acros Organics or Aldrich and used without further purification. Flash column chromatography was carried out on silica gel 60, 230-400 mesh (Sorbent Tech.). NMR spectra were recorded on a Varian Mercury 300 spectrometer. Gel permeation chromatography (GPC) analyses were carried out using a Waters 1525 binary pump coupled to a Waters 410 refractive index detector. The GPC was calibrated using polystyrene standards on an American Polymer Standards 10 μm particle size, linear mixed bed packing columns set with CH_2Cl_2 as an eluent. UV/Visible spectra were obtained on a Perkin-Elmer Lambda 19 UV/VIS/NIR Spectrometer. The fluorescence spectra were obtained on a Spex Fluorolog Spectrofluorimeter. Ellipsometry measurements were taken on a J. A. Woollam Co. Inc. Spectroscopic Ellipsometer, M-2000VI. Monomers **1** and **4** and the modified 8-

hydroxyquinoline ligands **Naph, Quinox, CHO**, and **PVK**, as well as Alq_3 and Znq_2 were prepared from literature procedures.[11,18,19,25-27]

Synthesis of 5-[6-Bicyclo[2.2.1]hept-5-en-2-yl-hexylamino)-methyl]-8-quinolinato-(ligand X)-zinc (3). Monomer **1** (0.025 g, 0.07 mmol) was dissolved in 5 mL dry benzene and added drop wise to a solution of diethylzinc (0.04 mL, 0.07 mmol) in 10 mL dry benzene. The reaction was stirred for two hours under argon. The resulting precipitate was filtered off and the solvent was removed to yield a yellow solid **2** which was used without further purification (0.03 g, 96 % yield). One equivalent of the 8-hydroxyquinoline ligand **X** was dissolved in 10 mL dry benzene and added drop wise to one equivalent of the zinc-monomer, dissolved in 10 mL dry benzene. The solution was allowed to stir under argon for two hours, followed by the removal of the solvent to yield a solid ranging in color from bright yellow to dark orange in quantitative yields.

5-[6-Bicyclo[2.2.1]hept-5-en-2-yl-hexylamino)-methyl]-8-quinolinato-(8-hydroxyquinoline)-zinc (Znq_2). ^{1}H NMR (300 MHz, $CDCl_3$) d 8.73 (2H, m); 8.60 (1H, m); 8.12 (1H, m); 7.44 (2H, m); 7.32 (2H, m); 7.21 (2H, m); 7.04 (1H, m); 6.11 (1H endo, dd, *J* = 2.74, 5.49); 6.06-5.99 (2H exo, m); 5.90 (1H endo, dd, *J* = 2.74, 5.49); 4.10 (1H, s); 2.73 (2H, s); 2.71 (2H, t, *J* = 7.14); 1.99-1.02 (12H, m); 0.49-0.43 (1H, m). ^{13}C NMR (75 MHz, $CDCl_3$) δ 153.47; 147.90; 146.87; 139.12; 137.15; 132.88; 132.44; 128.62; 127.22; 121.78; 117.74; 111.32; 50.39; 49.83; 45.68; 42.83; 39.04; 35.06; 32.75; 30.16; 28.9227.17; 25.95.

5-[6-Bicyclo[2.2.1]hept-5-en-2-yl-hexylamino)-methyl]-8-quinolinato-(5-formyl-8-hydroxyquinoline)-zinc (CHO). ^{1}H NMR (300 MHz, $CDCl_3$) d 10.01 (1H, m); 8.78 (2H, dd, *J* = 4.94, 19.28); 8.07 (2H, m); 7.71 (2H, dd, *J* = 4.39, 8.24); 7.51 (2H, m); 7.16 (2H, m); 6.11 (1H endo, dd, *J* = 2.74, 5.49); 6.06-5.99 (2H exo, m); 5.90 (1H endo, dd, *J* = 2.74, 5.49); 4.10 (1H, s); 2.73 (2H, s); 2.71 (2H, t, *J* = 7.14); 1.99-1.02 (12H, m); 0.49-0.43 (1H, m). ^{13}C NMR (75 MHz, $CDCl_3$) δ 190.06; 145.87; 144.78; 144.07; 143.78; 143.28; 142.86; 140.91; 140.16; 138.60; 136.81; 131.68; 126.02; 125.35; 124.60; 118.27; 112.93; 51.24; 50.03; 49.77; 45.56; 42.72; 38.49; 34.95; 32.36; 30.82; 29.92; 28.84; 27.53.

5-[6-Bicyclo[2.2.1]hept-5-en-2-yl-hexylamino)-methyl]-8-quinolinato-(5-phenyl-vinyl-ketone-8-hydroxyquinoline)-zinc (PVK). ^{1}H NMR (300 MHz, $CDCl_3$) δ 8.76 (2H, m); 8.49 (1H, m); 8.17 (1H, m); 8.10 (1H, m); 7.75 (10H, m); 7.12 (1H, m); 7.03 (1H, m); 6.11 (1H endo, dd, *J* = 2.74, 5.49); 6.06-5.99 (2H exo, m); 5.90 (1H endo, dd, *J* = 2.74, 5.49); 4.10 (1H, s); 2.73 (2H, s); 2.71 (2H, t, *J* = 7.14); 1.99-1.02 (12H, m); 0.49-0.43 (1H, m). ^{13}C NMR (75 MHz, $CDCl_3$) δ 195.13; 191.36; 184.23; 183.57; 182.45; 177.65; 177.11; 174.92; 173.21; 171.39; 170.26; 168.43; 166.85; 164.31; 154.86; 150.49; 149.07; 139.02; 138.96; 137.57; 135.12; 132.62; 131.71; 131.20; 127.95; 126.29; 122.29; 118.76; 116.80; 114.34; 113.49; 50.05; 49.83; 45.68; 45.53; 42.82; 39.02; 35.03; 33.36; 32.76; 30.69; 29.75; 29.39; 28.89; 27.58; 26.93; 24.10; 23.40.

5-[6-Bicyclo[2.2.1]hept-5-en-2-yl-hexylamino)-methyl]-8-quinolinato-(5-quinoxalinol)-zinc (Quinox). ^{1}H NMR (300 MHz, $CDCl_3$) δ 8.97 (4H, m); 7.72 (1H, m);

7.66 (2H, m); 7.51 (2H, m); 7.26 (1H, m); 6.11 (1H endo, dd, *J* = 2.74, 5.49); 6.06-5.99 (2H exo, m); 5.90 (1H endo, dd, *J* = 2.74, 5.49); 4.10 (1H, s); 2.73 (2H, s); 2.71 (2H, t, *J* = 7.14); 1.99-1.02 (12H, m); 0.49-0.43 (1H, m). ^{13}C NMR (75 MHz, $CDCl_3$) δ 157.38; 147.61; 146.45; 145.36; 142.68; 137.65; 137.43; 137.05; 135.88; 135.08; 132.91; 132.38; 131.06; 129.04; 115.47; 114.65; 113.15; 112.35; 49.87; 45.68; 42.80; 39.03; 35.18; 32.75; 30.69; 29.80; 28.96; 27.72; 23.46.

5-[6-Bicyclo[2.2.1]hept-5-en-2-yl-hexylamino)-methyl]-8-quinolinato-(4-hydroxy-1,5-naphthrydine)-zinc (Naph). ^{1}H NMR (300 MHz, $CDCl_3$) δ 9.01 (2H, m); 7.76 (2H, m); 7.29 (1H, m); 7.10 (4H, m); 7.04 (1H, m); 6.11 (1H endo, dd, *J* = 2.74, 5.49); 6.06-5.99 (2H exo, m); 5.90 (1H endo, dd, *J* = 2.74, 5.49); 4.10 (1H, s); 2.73 (2H, s); 2.71 (2H, t, *J* = 7.14); 1.99-1.02 (12H, m); 0.49-0.43 (1H, m). ^{13}C NMR (75 MHz, $CDCl_3$) δ 158.63; 147.55; 144.92; 144.05; 139.20; 137.84; 137.52; 136.82; 135.38; 133.27; 131.72; 129.04; 128.29; 115.45; 113.26; 49.84; 45.68; 42.80; 39.06; 35.06; 32.54; 30.32; 29.26; 28.05; 27.59; 23.54.

General polymerization procedure. Monomers **3** and **4** were dissolved in dry chloroform in the desired ratio. Ruthenium catalyst **5** was dissolved in dry chloroform, and both solutions were combined. The polymerizations were monitored by NMR and were complete within 12 hours. All polymers were purified by repeated precipitation into dry methanol.

Relative quantum yields measurements. The relative quantum yields of the solutions were measured using a procedure published in reference.[28] All samples were dissolved in dry chloroform and the UV/Vis spectra were taken. The concentration of the samples were adjusted with dry chloroform until the absorbance measured 0.5 for each solution, then the samples were diluted by a factor of 10 with dry chloroform. The fluorescence spectra of the diluted samples were then taken, the area under the curve was recorded, and the relative quantum yields were calculated.

Thin film fabrication and characterization. The concentrations of the polymers in solution were varied from 15-100 mg of polymer per mL of dry chloroform. One drop of each solution was dropped onto a quartz slide spinning at 2000 rpm. The polymer solutions that showed the highest fluorescence intensity in the solid-state ranged from 30-50 mg/mL. The films made for the ellipsometry experiment were prepared in a similar manner using gold-coated glass slides (100 nm of Au) instead of quartz slides. The film thicknesses were measured by ellipsometry by collecting data every 5° from 65° to 75° and were fitted using a Cauchy film on gold model.

References

1. Anderson, S.; Weaver, M. S.; Hudson, A. J. *Synth. Met.* **2000**, *111-112*, 459-463.

2. Wu, Q.; Esteghamatian, M.; Hu, N.-X.; Popovic, Z.; Enright, G.; Tao, Y.; D'iorio, M.; Wang, S. *Chem. Mater.* **2000**, *12*, 79-83.

3. Qin, Y.; Cheng, G.; Achara, O.; Parab, K.; Jäkle, F. *Macromolecules* **2004**, *37*, 7123-7131.

4. Qin, Y.; Pagba, C.; Piotrowiak, P.; Jäkle, F. *J. Am. Chem. Soc.* **2004**, *126*, 7015-7018.

5. Ghedini, M.; La Deda, M.; Aiello, I.; Grisolia, A. *Synth. Met.* **2003**, *138*, 189-192.

6. Giro, G.; Cocchi, M.; Kalinowski, J.; Fattori, V.; Di Marco, P.; Dembech, P.; Seconi, G. *Adv. Mater. Opt. Electron.* **1999**, *9*, 189-194.

7. Hamada, Y.; Kanno, H.; Sano, T.; Fujii, H.; Nishio, Y.; Takahashi, H.; Usuki, T.; Shibata, K. *Appl. Phys. Lett.* **1998**, *72*, 1939-1941.

8. Hamada, Y.; Sano, T.; Fujii, H.; Nishio, Y. *Jpn. J. Appl. Phys* **1996**, *35*, L1339-L1341.

9. Hamada, Y.; Sano, T.; Fujita, M.; Fujii, T.; Nishio, Y.; Shibata, K. *Jpn. J. Appl. Phys.* **1993**, *32*, L514-L515.

10. Donzé, N.; Péchy, P.; Grätzel, M.; Schaer, M.; Zuppiroli, L. *Chem. Phys. Lett.* **1999**, *315*, 405-410.

11. Hopkins, T. A.; Meerholz, K.; Shaheen, S.; Anderson, M. L.; Schmidt, A.; Kippelen, B.; Padias, A. B.; H.K. Hall, J.; Peyghambarian, N.; Armstrong, N. R. *Chem. Mater.* **1996**, *8*, 344-351.

12. Sapochak, L.; Benincasa, F. E.; Schofield, R. S.; Baker, J. L.; Riccio, K. K. C.; Fogarty, D.; Kohlmann, H.; Ferris, K. F.; Burrows, P. E. *J. Am. Chem. Soc.* **2002**, *124*, 6119-6125.

13. Schmitz, C.; Schmidt, H.-W.; Thelakkat, M. *Chem. Mater.* **2000**, *12*, 3012-3019.

14. Kai, Y.; Morita, M.; Yasuoka, N.; Kasai, N. *Bull. Chem. Soc. Jpn.* **1985**, *58*, 1631-1635.

15. Ghedini, M.; La Deda, M.; Aiello, I.; Grisolia, A. *Inorganica Chim. Acta* **2004**, *357*, 33-40.

16. Sapochak, L. S.; Padmaperuma, A.; Washton, N.; Endrino, F.; Schmett, G. T.; Marshall, J.; Fogarty, D.; Burrows, P. E.; Forrest, S. R. *J. Am. Chem. Soc.* **2001**, *123*, 6300-6307.

17. Halls, M. D.; Schlegel, H. B. *Chem. Mater.* **2001**, *13*, 2632-2640.

18. Meyers, A.; Weck, M. *Macromolecules* **2003**, *36*, 1766-1768.

19. Meyers, A.; Weck, M. *Chem. Mater.* **2004**, *16*, 1183-1188.

20. The nomenclature of the polymers is as follows: **X**-polymer, where **X** is equal to functionality on the modified 8-hydroxyquinoline ligand, as shown in Figure 5.2.

21. Trnka, T. M.; Grubbs, R. H. *Acc. Chem. Res.* **2001**, *34*, 18-29.

22. Brinkmann, M.; Gadret, G.; Muccini, M.; Taliani, C.; Masciocchi, N.; Sirani, A. *J. Am. Chem. Soc.* **2000**, *122*, 5147-5157.

23. Chen, C. H.; Shi, J. *Coord. Chem. Rev.* **1998**, *171*, 161-174.

24. Shoustikov, A.; You, Y.; Burrows, P. E.; Thompson, M. E.; Forrest, S. R. *Synth. Met.* **1997**, *91*, 217-221.

25. Clemo, G. R.; Howe, R. *J. Chem. Soc.* **1955**, 3552-3553.

26. Freeman, S. K.; Spoerri, P. E. *J. Org. Chem.* **1951**, *16*, 438-442.

27. Eck, T. D.; Wehry Jr., E. L.; Hercules, D. M. *J. Inorg. Nucl. Chem.* **1966**, *28*, 2439-2441.

28. Fery-Forgues, S.; Lavabre, D. *J. Chem. Edu.* **1999**, *76*, 1260-1264.

CHAPTER 6

THE PHOTOLUMINESCENCE AND ELECTROLUMINESCENCE CHARACTERIZATION OF A HOLE- AND ELECTRON-TRANSPORTING COPOLYMER

As outlined in the introductory chapter, the current trend in fabricating OLEDs is solution-processing.[1,2] By using polymers instead of small organic molecules, devices can be made by spin-casting or ink-jet printing.[2] However, problems can arise when trying to fabricate multi-layer devices due to the dissolution of lower layers during the processing.[2] This problem can be overcome by casting two polymers from the same solution. Berggren and co-workers were able altered to incorporate a variety of electroluminescent and charge-transport groups into a single polymer layer by casting one solution containing poly(thiophene)s with electron-transport, hole-transport, and emission properties.[3] The self-organizing property of poly(thiophene)s allowed for the phase separation of the polymers into submicrometer-sized domains of hole-transporting and electron-transporting/emitting materials.[3] This blending of hole- and electron-transport polymers was also demonstrated using a poly(*p*-phenylene ethylynylene) derivative as the electron-transport and emitting material and poly(*N*,*N'*-diphenylbenzidine diphenylether) (polyTPD) as the hole-transport material.[4] Another example of blending two polymers containing either a hole- or an electron-transporting group was demonstrated when block copolymers of poly(fluorene) derivatives were used to fabricated devices that showed a high efficiency at low potentials.[5] One drawback to

blending two polymers is the limited control on color emission, due to the transfer of the exciton from the higher-band-gap polymer to the lower band-gap one.[3] This can be avoided by adding a large excess of the higher-band-gap polymer, resulting in only a fraction of the excitons formed by this polymer being lost to the lower-band-gap polymer.[3] However, this technique is highly dependent on the microstructure of the polymer blend, so being able to control the size and shape of the phase separation could circumvent this problem.[3]

Another drawback of the polymer blend concept is that two different polymers must be synthesized, characterized, and optimized in hopes that they are energetically compatible. A more efficient method would be to synthesize a polymer containing a known hole-transport material and a known electron-transport/emitting material that are compatible with each other. By covalently attaching the hole- and electron-transport material to one polymer, the movement of these materials is suppressed leading to less phase separation, so the need to control the size and shape of the microstructure becomes unnecessary.[6] Statistical copolymers using poly(N-vinylcarbazole) (a known hole-transport material) and an oxadiazole (a known electron-transport material) monomers were prepared, resulting in devices with efficiencies between 0.1-0.4 % with brightness as high as 160 cd/m^2 at 25 V.[6] The advantage of this system is that all of the monomers were polymerized by the same method (free radical polymerization), and a wide variety of compositions could be prepared, allowing for the tuning of the charge transport properties.[6]

In this work, the previous chapters showed the copolymerization of nonylnorbornene with the Alq_3-monomer in order to form a polymer that was solution-

processable. Fabrication of devices using these copolymers yielded no electroluminescence and very little current running through the device. It was suspected that the nonylnorbornene portion of the copolymer was acting as an insulating material and should not be used in conjunction with the Alq_3-monomer for electroluminescent devices.[7-9] This chapter, the results from the copolymerization of the Alq_3-monomer with a monomer containing a hole-transport material will be discussed. This technique leads to an increasing amount of conducting material in the copolymer, while retaining the ability to be solution-processed.

The hole-conducting monomer that was chosen is a derivative of a well-known hole-transporting material, TPD (*N*,*N'*-bis(*m*-tolyl-*N*,*N'*-diphenyl-1,1'-biphenyl-4,4'-diamine), shown in Figure 6.1.[10-18] TPD has been used since that later 1980s as a hole-transporting material in OLEDs.[10,19,20] Recent reports have shown the synthesis of attaching TPD to a norbornene molecule, and polymerization of the resulting monomers yielded a poly(norbornene) backbone with TPD side-chains.[16] This polymer was shown to have mobilities of 1.5×10^{-4} cm^2/Vs, and devices using the polymer as the hole-transporting layer had efficiencies around 0.75%.[14] Due to the difficulties in synthesizing the TPD-monomer, another hole-transporting material was attached to a norbornene molecules, TPF (2,7-bis(phenyl-*m'*-tolylamino)-9,9-dimethylfluorene), also shown in Figure 6.1.[15,16] The resulting TPF-polymer has a higher glass transition temperature compared to the TPD-polymer, but also has lower mobilities (1.1×10^{-4} cm^2/Vs) and devices made with the TPF-polymer as the hole-transporting layer instead of the TPD-polymer had lower efficiencies (0.66%).[15,16] However, the easier synthesis overcomes the loss of device performance.

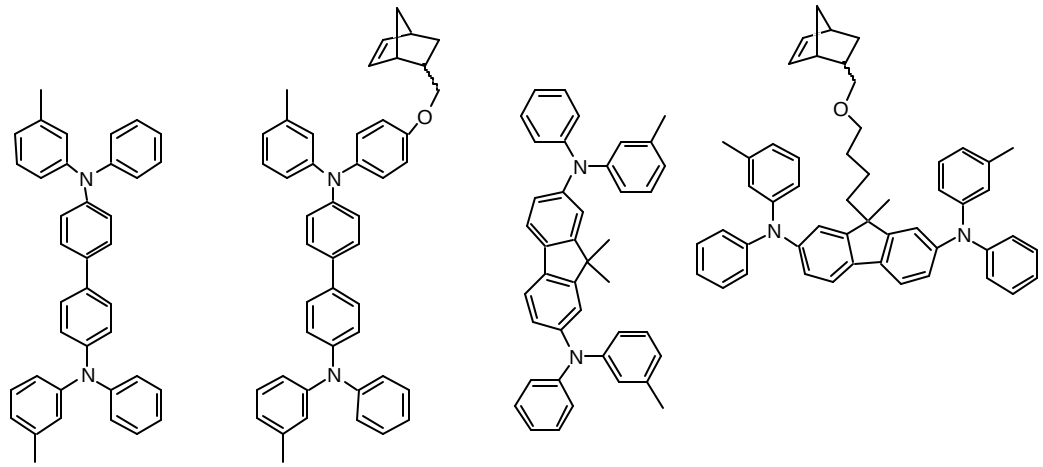

Figure 6.1 Structures of the hole-transporting compounds.

While fabricating a single-layer device is highly desirable, the formation of a multi-layer polymeric device is possible. A copolymer containing the TPD-side-chain and a cinnamate side-chain was synthesized and reported to form an insoluble cross-linked thin film when the casted polymer was exposed to UV light as discussed later in this chapter.[14,21-23] This not only allows for photopatterning of the hole-transport layer, but it also allows for another polymer solution to be casted on top of the cross-linked hole-transport layer.[14,21-23] A loss of performance is seen, however, in the cross-linked system compared to the un-cross-linked system (0.37% vs 0.76%).[14]

This chapter will focus on the synthesis and characterization of a copolymer containing both the hole- and electron-transporting groups of TPF and Alq_3, respectively. The copolymer will then be used in conjunction with a cross-linked TPD layer to form a multilayer polymeric LED. The results presented in this chapter show the initial progress

towards a multi-layer polymeric device by attaching well-known small molecules, capable of charge transport, to an inert polymeric backbone.

Results and Discussion

In the previous chapters, the Alq_3-monomer was synthesized, then polymerized. However after purification, the Alq_3-homopolymer, as well as most of the copolymers with nonylnorbornene, was insoluble. Based on fluorescence evidence, it appeared that the hydroxyquinoline ligands were rapidly exchanging with each other, forming a cross-linked network. To circumvent this problem, a new hydroxyquinoline-monomer was synthesized that can be polymerized and purified before the addition of the aluminum center and the remaining hydroxyquinoline ligands.

The new hydroxyquinoline-monomer was synthesized, as shown in Figure 6.2, by first preparing 5-chloromethyl-8-hydroxyquinoline hydrochloride **2**,[24] then reacting it with norbornene methanol **3** to yield the quinoline monomer **4** in an overall yield of 61%. The monomer was then polymerized using the 3rd generation Grubbs' catalyst in chloroform. After purification, the polymer was again dissolved in chloroform and a prepared sampled of Alq_3 was added to the polymer solution.[25] After stirring for 30 minutes, the polymer was precipitated into hexanes repeatedly. However, each precipitation yielded a polymer that was less soluble than the previous one, until the third precipitation yielded an insoluble polymer, suggesting that again the hydroxyquinoline ligands are exchanging with each other forming a cross-linked network.

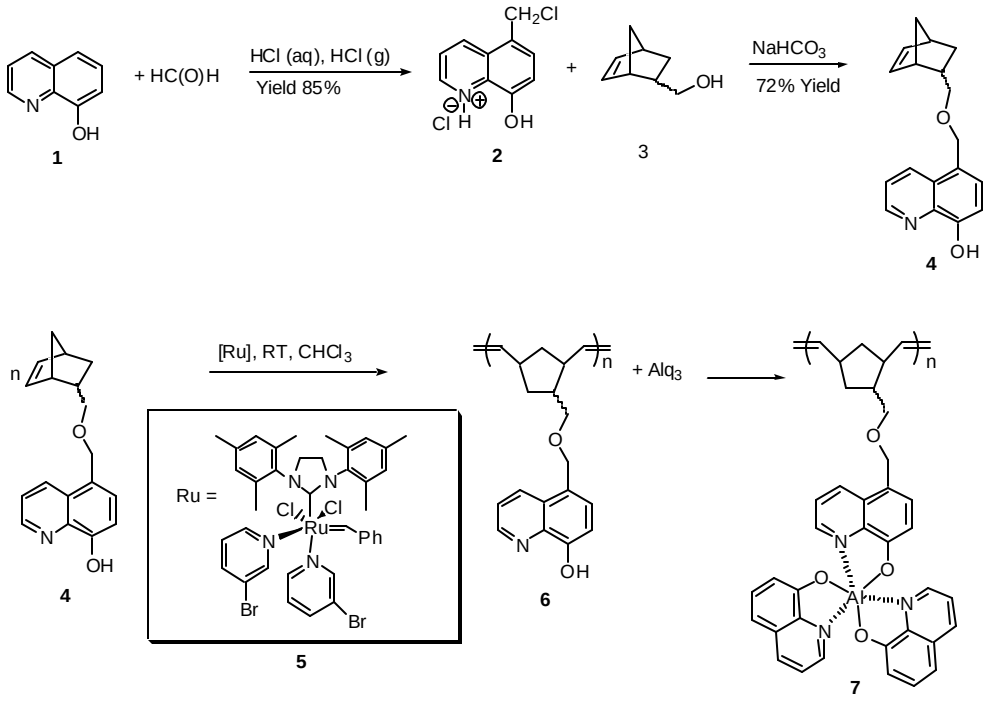

Figure 6.2 Synthetic scheme of quinoline-monomer, homopolymer, and formation of Alq_3-polymer.

In order to form a soluble polymer, a 1:1 molar ratio of the hydroxyquinoline monomer was copolymerized with the TPF-monomer **8**, which was previously synthesized.[16] The monomers were copolymerized with the ruthenium catalyst **5** to yield the copolymer TPF-co-Q **9**, as shown in Figure 6.3. After purification, the copolymer was dissolved in chloroform, and freshly prepared Alq_3 was added to the solution. Upon repeated precipitation of the copolymer into hexanes, a pure TPF-co-Alq_3 copolymer **10** was isolated. The copolymers were characterized by NMR, GPC, DSC, UV/Vis, and fluorescence spectroscopy, with the results being summarized in Table 6.1. From the

table, it is clear that the Alq_3 side-chain plays a major role in the thermal properties of the polymer. The TPF-co-Q copolymer shows a glass transition temperature at 102 °C, while the TPF-co-Alq_3 copolymer does not show a glass transition temperature at all. However, both copolymers decompose at approximately the same temperature 250-260 °C (which is approximately the same temperature as the copolymers discussed in the previous chapters), indicating that it is the norbornene backbone that decomposes before the TPF or Alq_3 side-chains.

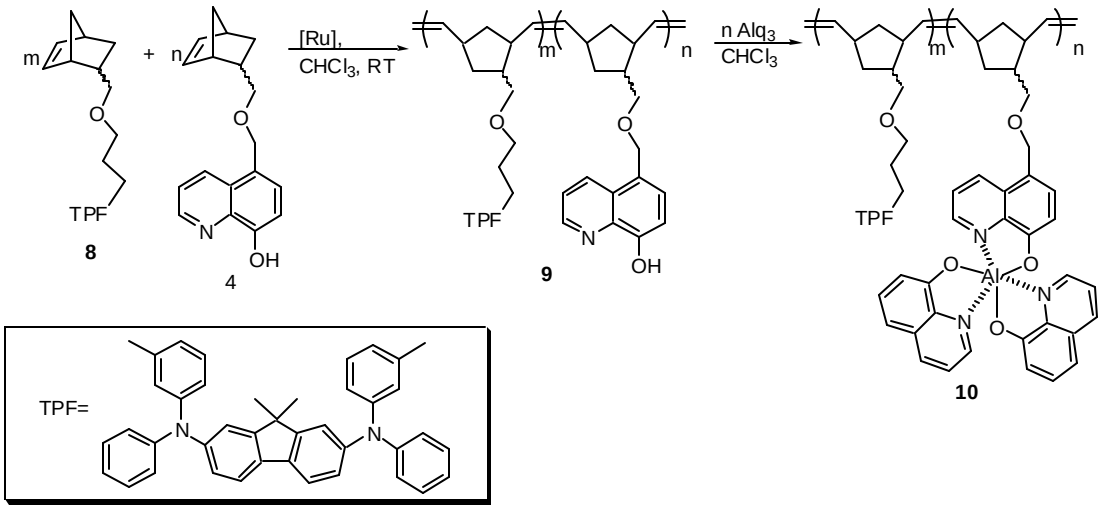

Figure 6.3 Copolymerization scheme of TPF-monomer and Quinoline-monomer and formation of Alq_3-copolymer.

Table 6.1 Characterization data for TPF- and Quinoline-monomers and copolymers.

Compound	UV/Vis $?_{max}$ (nm)	Solution Emission $?_{max}$ (nm)	Thin Film Emission $?_{max}$ (nm)	Mn	Mw	PDI	Tg (°C)	Td (°C)
TPF-Monomer **8**	311, 376	413	---	n/a	n/a	n/a	n/a	n/a
Quinoline-Monomer **4**	318	n/a	n/a	n/a	n/a	n/a	n/a	n/a
1:1 TPF-co-Q polymer **9**	315, 379	422	---	9400	5000	1.8	102	260
1:1 TPF-co-Alq_3 polymer **10**	312, 380	424, 530	521	8800	5700	1.5	---	250

Key: n/a = not applicable --- = not observed

The fluorescence spectra of the copolymers as well as the TPF-monomer are shown in Figure 6.4. When excited at 380 nm, the TPF-monomer, in solution, shows an emission wavelength of 415 nm. When the TPF-co-Alq_3 copolymer was excited in solution, it showed two emission wavelength maxima, one at 422 nm and the other at 530 nm, indicating emission from both the TPF side-chain and the Alq_3 side-chain of the copolymers. However, when the copolymer was casted as a thin film, the only emission detected was from the Alq_3 side-chain, centered at 521 nm. These results clearly indicate that both the TPF- and Alq_3-monomer were incorporated into the copolymer and that only the Alq_3 side-chain is responsible for light emission in the solid-state.

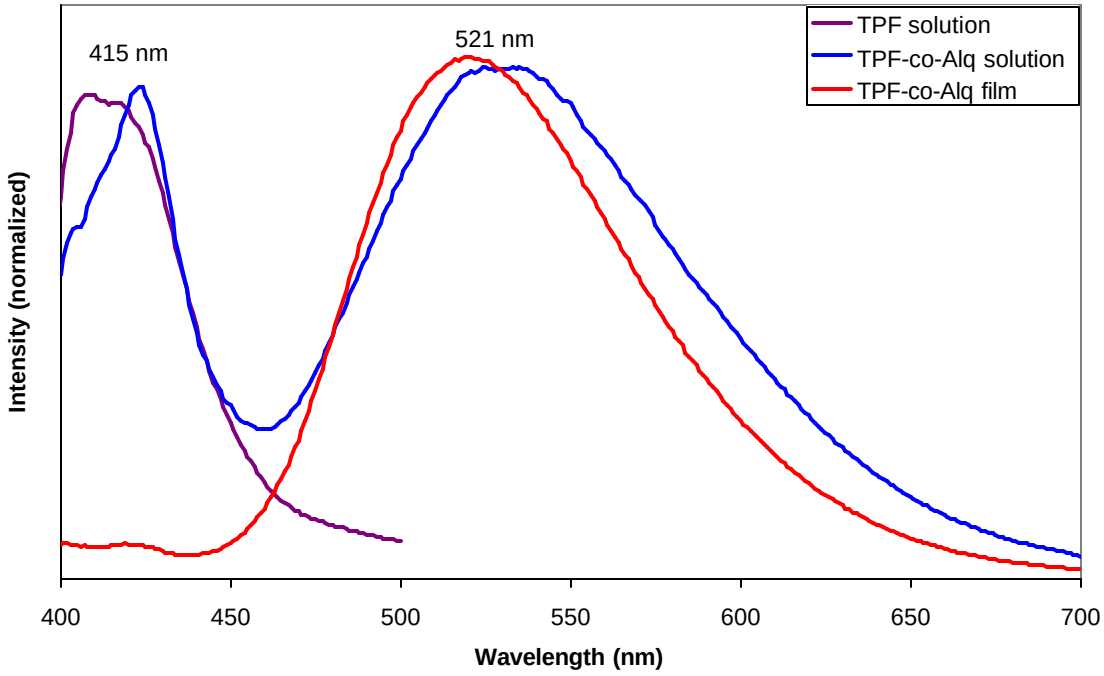

Figure 6.4 Photoluminescence spectra for TPF polymer and TPF-co-Alq_3 copolymer, excited at 380 nm either in chloroform or as a thin film.

The TPF-co-Alq_3 copolymer was then used in the fabrication of an OLED. Three-layer LEDs were prepared using indium tin oxide (ITO) as the anode, TPD-co-Cinn **11** (shown in Figure 6.5) as the hole-transport layer, TPF-co-Alq_3 as the emitting layer, Alq_3 as the electron-transport layer, and Mg:Ag as the cathode. Alq_3 was necessary for device fabrication because the metal cathode would not stick to the TPF-co-Alq_3 copolymer. The TPD-co-Cinn copolymer was spin-coated from toluene onto the ITO coated slide and exposed to UV light (350 nm), allowing for the cinnamate group to undergo [2+2] cycloaddition, shown in Figure 6.5, forming an insoluble cross-linked

HTL **12** with a thickness around 30 nm.[14,21-23] The TPF-co-Alq_3 copolymer was then casted onto the cross-linked HTL from chloroform, forming a 50 nm layer, and a 10 nm layer of Alq_3 was deposited on top, followed by the deposition of the metal cathode.

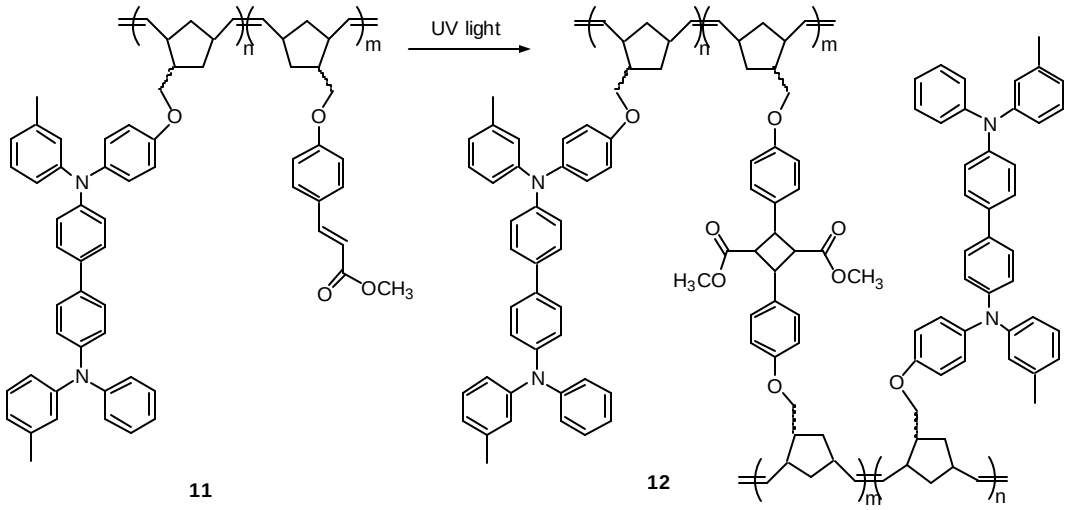

Figure 6.5 Cross-linking scheme of TPD-co-Cinn copolymer.

The electroluminescence of the multi-layer polymeric device is shown in Figure 6.6. The green emission of the polymeric device, centered at 521 nm, is comparable to the emission seen for a similar device fabricated with evaporated Alq_3, indicating that the TPF side-chain of the copolymer does not interfere with the electroluminescence properties of the Alq_3 side-chain. While the emission can be from either the TPF-co-Alq_3 copolymer or the evaporated Alq_3 layer, a current was able to flow through the device,

indicating that the TPF-co-Alq_3 copolymer is capable of charge transport. While a high brightness of 800 cd/m^2 was recorded at 15 V, the device showed external quantum efficiencies of only 0.02%, a magnitude lower than some of the previously published devices using the TPD-co-Cinn cross-linked HTL and Alq_3 as the ETL.[14,15,17,18,22] However in these reports, devices that differ only in a cross-linked HTL compared to a non-cross-linked HTL, showed much lower efficiencies when the HTL was cross-linked compare to those that were not cross-linked.[17] A study into varying the concentration of the Alq_3-monomer in the copolymer, altering the thicknesses of both polymer layers, and improving the electron injection into the device will need to be performed in order to optimize the efficiency of the device. Nevertheless, a working OLED was fabricated using the TPF-co-Alq_3 copolymer, indicating that the polymer backbone does not prohibit electroluminescence.

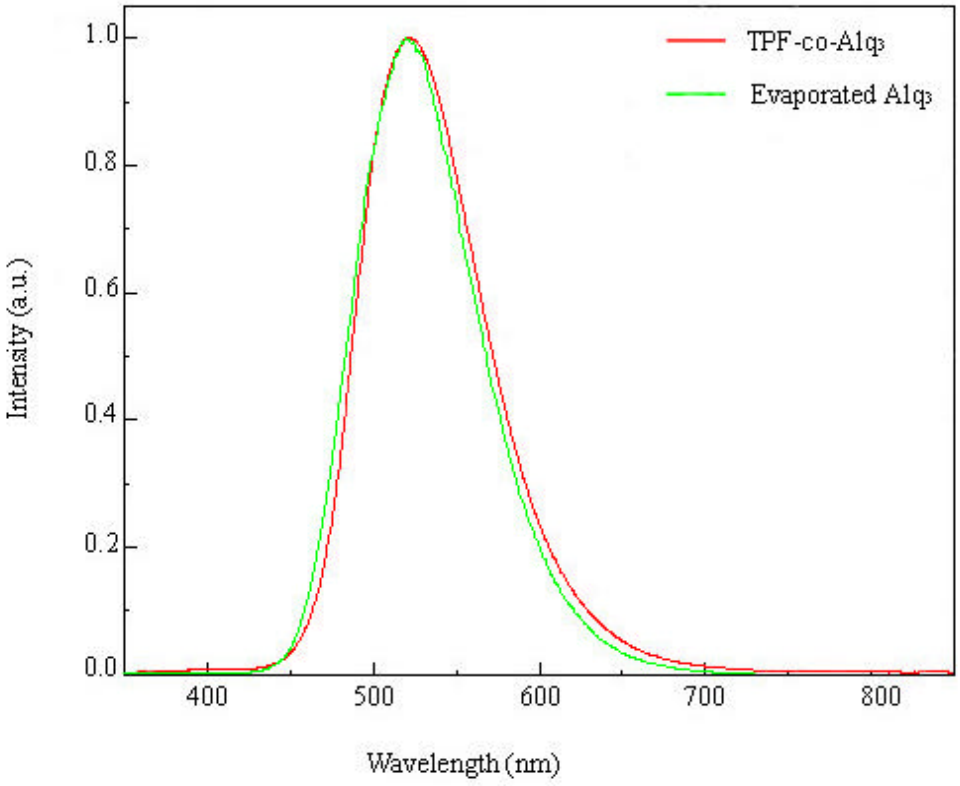

Figure 6.6 Electroluminescence spectra of TPF-co-Alq_3 and evaporated Alq_3.

Conclusion

The synthesis and characterization of a statistical copolymer containing both the hole-transport side-chain TPF and the electron-transport/emitting side-chain Alq_3 was performed. The copolymerization of the 8-hydroxyquinoline monomer with the TPF-monomer, followed by the formation of Alq_3 on the quinoline monomer showed a fast and efficient manner in preparing a copolymer containing both hole- and electron-transport material side-chains. The fluorescence spectrum of the copolymer indicated

that only the Alq_3 side-chain emitted light in the solid-state, again suggesting that the polymer backbone does not interfere with the photoluminescent properties of the Alq_3 side-chain. A device, using the TPF-co-Alq_3 copolymer as the emitting layer, did show bright green emission, although the efficiencies of the device were much lower than other reports using similar materials. This is the first fully characterized working OLED using a polymeric form of Alq_3 as the emitting layer. Future investigations will focus on improving polymeric-Alq_3 for applications in electronic devices.

Experimental

General: All chemicals were purchased from Acros Organics or Aldrich and used without further purification. Flash column chromatography was carried out on silica gel 60, 230-400 mesh (Sorbent Tech.). NMR spectra were recorded on a Varian Mercury 300 spectrometer. Gel permeation chromatography (GPC) analyses were carried out using a Shimadzu instrument and linear mixed bed column packed with 10µ AM Gel with THF as an eluent and a multidiode array UV detector. Differential scanning calorimetry (DSC) was preformed under nitrogen using a Mettler Toledo DSC 822e cooled by liquid nitrogen. The temperature program provided heating and cooling cycles between -20 and 360 °C at 10 °C/min. UV/Visible spectra were obtained on a Perkin-Elmer Lambda 19 UV/VIS/NIR Spectrometer. The fluorescence spectra were obtained on a Spex Fluorolog Spectrofluorimeter. Ellipsometry measurements were taken on a J. A. Woollam Co. Inc. Spectroscopic Ellipsometer, M-2000VI. The TPF-monomer **2** was prepared by Dr. J. D. Cho of the Marder group according to the literature procedure.[16]

Synthesis of 5-(Bicyclo[2.2.1]hept-5-en-2-yl-methoxymethyl)-quinolin-8-ol (1).

The hydroxyquinoline monomer **4** was prepared by stirring chloromethylhydroxyquinoline hydrochloride **2** (2.0 g, 8.7mmol) and sodium bicarbonate (0.8 g, 9.5 mmol) in a large excess of norbornene methanol **3** (10 mL) at 90 °C for 1 hour.[24] The excess alcohol was distilled off and the remaining solid was dissolved in water. The organic material was extracted using CH_2Cl_2, washed with a brine solution, and dried over sodium sulfate. The solvent was removed leaving a greenish-yellow solid, which was purified by column chromatography (silica gel, 4:1 hexanes/ethyl acetate) yielding an off-white solid (1.8 g, 72% yield). ^{1}H NMR (300 MHz, $CDCl_3$) δ 8.81 (1H, dd, *J* = 1.65, 4.39); 8.54 (1H endo, dd, *J* = 1.65, 8.79); 8.53 (1H exo, dd, *J* = 1.65, 8.79); 7.52 (1H, dd, *J* = 4.39, 8.79); 7.43 (1H endo, d, *J* = 7.69); 7.42 (1H exo, d, *J* = 7.69); 7.11 (1H exo, d, *J* = 7.69); 7.10 (1H endo, d, *J* = 7.69); 6.07 (2H exo, m); 6.06 (1H endo, m); 5.71 (1H endo, m); 4.85 (2H endo, dd, *J* = 12.08, 30.12); 4.84 (2H exo, s); 3.56-3.01 (2H, m); 2.86-2.70 (2H, m); 2.36 (0.5H endo, m); 1.82 (1H endo, m); 1.74 (1H exo, m); 1.43 (1H endo, m); 1.29 (3H, m); 1.19 (1H, m); 0.47 (0.5H endo, m). ^{13}C NMR (75 MHz, $CDCl_3$) δ 152.5, 147.8, 138.8, 137.4, 136.8, 133.7, 132.3, 128.7, 127.6, 124.9, 122.0, 108.9, 75.0, 7.38, 71.3, 49.6, 45.3, 44.2, 44.1, 42.5, 41.8, 39.1, 30.1, 29.4, 27.2. Anal. Calcd. for $C_{18}H_{19}O_2N_1$: C, 76.8; H, 6.8; N, 5.0. Found C: 77.0; H: 7.0; N: 4.7.

Copolymerization of Monomers 4 and 8

The quinoline-monomer **4** (0.060g, 0.22 mmol) and the TPF-monomer **8** (0.152 g, 0.22 mmol) were dissolved in 5 mL of chloroform. A chloroform solution of ruthenium catalyst **3** (0.019 g, 0.022 mmol/mL) was added to the monomer solution and stirred for 5 minutes, followed by the addition of ethyl vinyl ether (1 mL). After stirring for an addition 10 minutes, the solution was concentrated down to 1 mL and added drop wise to 100 mL of hexanes. The polymer, which precipitated out of solution, was collected and redissolved in 1 mL of chloroform and precipitated into hexanes. This precipitation procedure was repeated three times. The final product was collected as a brown solid **9**. (0.190 g, 90% Yield). ^{1}H NMR (300 MHz, $CDCl_3$) δ 8.72 (1H, broad); 8.44 (1H, broad; 7.44 (3H, broad); 7.26 (5H, broad); 7.11 (10H, broad); 6.95 (8H, broad); 6.81 (1H, broad); 5.20 (4H, broad); 4.73 (2H, broad); 3.48 (1H, broad); 3.23 (2H, broad); 3.06 (2H, broad); 2.71 (1H, broad); 2.24 (8H, broad); 1.78 (6H, broad); 1.30 (6H, broad); 0.98 (8H, broad). ^{13}C NMR (75 MHz, $CDCl_3$) δ 153.1; 152.4; 148.2; 148.0; 147.7; 146.8; 139.1; 138.7; 135.1; 133.8; 129.8; 128.7; 124.7; 124.0; 123.5; 122.5; 121.9; 121.2; 120.1; 119.3; 109.5; 73.1; 71.7; 50.6; 43.2; 42.8; 41.5; 39.6; 38.0; 37.3; 30.1; 26.8; 25.4; 21.8. Anal. Calcd. for $C_{69}H_{69}O_3N_3$:C, 82.5; H, 6.8; N, 4.3. Found C: 81.8, H: 7.2, N: 4.1.

Formation of Alq_3-copolymer 10.

Prepared Alq_3 (0.046 g, 0.10 mmol) was added to a chloroform solution of the TPF-co-Q polymer **9** (0.10 g). After stirring for 30 minutes, the solution was concentrated down to 1 mL and added drop wise to 100 mL of hexanes. The polymer, which precipitated out of solution, was collected and redissolved in 1 mL of chloroform

and precipitated into hexanes. This precipitation procedure was repeated five times. The final product was collected as a yellow solid **10**. (0.11 g, 85 % Yield). ^{1}H NMR (300 MHz, $CDCl_3$) δ 8.86 (2H, broad); 8.30 (3H, broad; 7.52 (11H, broad); 7.22 (25H, broad); 5.16 (4H, broad); 4.59 (2H broad); 3.17 (4H, broad); 2.18 (8H, broad); 1.71 (9H, broad); 1.25 (12H, broad). ^{13}C NMR (75 MHz, $CDCl_3$) δ 159.0; 158.6; 153.1; 152.4; 148.2; 148.0; 147.7; 146.8; 145.0; 144.6; 142.4; 139.8; 139.5; 139.1; 138.7; 135.1; 133.8; 131.5; 131.0; 129.8; 129.6; 129.4; 128.7; 124.7; 124.0; 123.5; 122.5; 121.9; 121.2; 121.2; 120.1; 119.3; 113.6; 112.9; 112.5; 112.2; 112.0; 109.5; 73.1; 71.7; 50.6; 43.2; 42.8; 41.5; 39.6; 38.0; 37.3; 30.1; 26.8; 25.4; 21.8.

Thin film fabrication and characterization. The polymers were dissolved in chloroform (5mg/mL) and casted onto quartz slides spinning at 1000 rpm for 30 seconds. The films made for the ellipsometry experiment were prepared in a similar manner using gold-coated glass slides (100 nm of Au) instead of quartz slides. The film thicknesses were measured by ellipsometry by collecting data every 5° from 65° to 75° and were fitted using a Cauchy film on gold model.

Device fabrication. Oxygen plasma-treated indium tin oxide (ITO) with a sheet resistance of 20 O/? (Colorado Concept Coatings, L.L.C.) was used as the anode. The copolymer **11** in a toluene solution with a concentration of 10 mg/mL was spin-coated onto the ITO, and then was exposed to 350 nm light from a mercury arc lamp with a 12 mW/cm^2 power density for 10 seconds. The second copolymer **10** was casted from a chloroform solution (5 mg/mL) onto the first cross-linked polymer layer. The electron-

transport layer of Alq_3 was thermally evaporated at a rate of 1 Å/s under a pressure of 1 x 10^{-6} Torr on top of the second copolymer layer. The metal cathode, an alloy of silver and magnesium in a 1:10 ratio, was deposited through a shadow mask to define five devices per substrate with an emissive area of 0.1 cm^2 each.

References

1. Greiner, A. *Polym. Adv. Technol.* **1998**, *9*, 371-389.

2. Friend, R. H.; Gymer, R. W.; Holmes, A. B.; Burroughes, J. H.; Marks, R. N.; Taliani, C.; Bradley, D. D. C.; Santos, D. A. D.; Bredas, J. L.; Logdlund, M.; Salaneck, W. R. *Nature* **1999**, *397*, 121-128.

3, Berggren, M.; Inganas, O.; Gustafsson, G.; Rasmusson, J.; Andersson, M. R.; Hjertberg, T.; Wennerstrom, O. *Nature* **1994**, *372*, 444-446.

4. Schmitz, C.; Posch, P.; Thelakkat, M.; Schmidt, H.-W.; Montali, A.; Feldman, K.; Smith, P.; Weder, C. *Adv. Funct. Mater.* **2001**, *11*, 41-46.

5. Morteani, A.; Dhoot, A. S.; Kim, J.-S.; Silva, C.; Greenham, N. C.; Murphy, C.; Moons, E.; Cina, S.; Burroughes, J. H.; Friend, R. H. *Adv. Mater.* **2003**, *15*, 1708-1712.

6. Jiang, X.; Register, R. A.; Killeen, K. A.; Thompson, M. E.; Pschenitzka, F.; Sturm, J. C. *Chem. Mater.* **2000**, *12*, 2542-2549.

7. Bai, Y.; Chiniwalla, P.; Elce, E.; Bidstrup, S.; Kohl, P. A. *J. Appl. Polym. Sci.* **2004**, *91*, 3031-3039.

8. Bai, Y.; Chiniwalla, P.; Elce, E.; Shick, R. A.; Sperk, J.; Bidstrup, S.; Kohl, P. A. *J. Appl. Polym. Sci.* **2004**, *91*, 3023-3030.

9. Rutenberg, I. M.; Scherman, O. A.; Grubbs, R. H.; Jiang, W.; Garfunkel, E.; Bao, Z. *J. Am. Chem. Soc.* **2004**, *126*, 4062-4063.

10. Abkowitz, M.; Pai, D. M. *Philos. Mag. B* **1986**, *53*, 193-216.

11. Adachi, C.; Tsutsui, T.; Saito, S. *Appl. Phys. Lett.* **1989**, *55*, 1489-1491.

12. Adachi, C.; Tsutsui, T.; Saito, S. *Appl. Phys. Lett.* **1990**, *56*, 799-801.

13. Bolink, H. J.; Arts, C.; Krasnikov, V. V.; Malliaras, G. G.; Hadziioannou, G. *Chem. Mater.* **1997**, *9*, 1407-1413.

14. Bellmann, E.; Shaheen, S.; Thayumanavan, S.; Barlow, S.; Grubbs, R. H.; Marder, S. R.; Kippelen, B.; Peyghambarian, N. *Chem. Mater.* **1998**, *10*, 1668-1676.

15. Hreha, R. D.; George, C. P.; Haldi, A.; Domercq, B.; Malagoli, M.; Barlow, S.; Bredas, J.-L.; Kippelen, B.; Marder, S. R. *Adv. Funct. Mater.* **2003**, *13*, 967-973.

16. Hreha, R. D.; Haldi, A.; Domercq, B.; Barlow, S.; Kippelen, B.; Marder, S. R. *Tetrahedron* **2004**, *60*, 7169-7176.

17. Jabbour, G. E.; Kawabe, Y.; Shaheen, S. E.; Wang, J. F.; Morrell, M. M.; Kippelen, B.; Peyghambarian, N. *Appl. Phys. Lett.* **1997**, *71*, 1762-1764.

18. Maldonado, J.-L.; Bishop, M.; Fuentes-Hernandez, C.; Caron, P.; Domercq, B.; Zhang, Y.-D.; Barlow, S.; Thayumanavan, S.; Malagoli, M.; Bredas, J.-L.; Marder, S. R.; Kippelen, B. *Chem. Mater.* **2003**, *15*, 994-999.

19. Tang, C. W.; VanSlyke, S. A. *Appl. Phys. Lett.* **1987**, *51*, 913-915.

20. Tang, C. W.; VanSlyke, S. A.; Chen, C. H. *J. Appl. Phys.* **1989**, *65*, 3610-3616.

21. Zhang, Y.-D.; Hreha, R. D.; Jabbour, G. E.; Kippelen, B.; Peyghambarian, N.; Marder, S. R. *J. Mater. Chem.* **2002**, *12*, 1703-1708.

22. Domercq, B.; Hreha, R. D.; Zhang, Y.-D.; Larribeau, N.; Haddock, J. N.; Schultz, C.; Marder, S. R.; Kippelen, B. *Chem. Mater.* **2003**, *15*, 1491-1496.

23. Domercq, B.; Hreha, R. D.; Zhang, Y.-D.; Haldi, A.; Barlow, S.; Marder, S. R.; Kippelen, B. *J. Polym. Sci.: Part B: Polym. Phys.* **2003**, *41*, 2726-2732.

24. Burckhalter, J. H.; Leib, R. I. *J. Org. Chem.* **1961**, *26*, 4078-4083.

25. Hopkins, T. A.; Meerholz, K.; Shaheen, S.; Anderson, M. L.; Schmidt, A.; Kippelen, B.; Padias, A. B.; H.K. Hall, J.; Peyghambarian, N.; Armstrong, N. R. *Chem. Mater.* **1996**, *8*, 344-351.

CHAPTER 7

PHOTOLUMINESCENCE AND ELECTROLUMINESCENCE CHARACTERIZATION OFAN EMISSIVE ELECTRON-TRANSPORT COPOLYMER CONTAINING ALQ_3- AND PENTAPHENYLSILACYCLOPENTADIENE-MONOMERS

In the previous chapter, the Alq_3-monomer was copolymerized with the TPF-monomer to form a statistical copolymer capable of both hole- and electron-transport, as well as being an emissive polymer. The TPF-co-Alq_3 copolymer was incorporated into an OLED as the emitting layer. The device emitted bright green light when a potential was applied, however the overall efficiencies of the device were very low. It was rationalized that the low efficiencies were caused by poor charge transport through the copolymer layer. A recent report indicated that the electron injection in OLEDs is inferior to hole injection and is usually the cause of poor efficiencies.[1] In order to improve the electron injection, and at the same time improve the electron mobilities, a compound with a higher electron affinity or lower LUMO was needed.[1,2]

Higher efficiencies were reported for a device containing Alq_3 as the emitting material and a silole derivative (silacyclopentadiene as shown in Figure 7.1) as the electron-transport material, compared to a device using only Alq_3 as both the emitting and electron-transport material.[1] The Alq_3-silole device was three times more efficient

and almost four times brighter than the Alq_3 device.[1] Another silole derivative, copolymerized with thiophene, showed improving conductivity as the silole content of the copolymer increased.[3] Studies into the electronic structure of the silacyclopentadiene were performed in order to determine why this compound improved the properties of the devices to such a large extent.[4,5] It was determined that the molecular orbitals of the silylene and the butadiene come together to form an *s**-*?* * conjugation by the in-phase combination of the *s* * orbital of the silylene and the *?* * orbitals of the butadiene.[4,5] This *s**-*?* * conjugation results in a low-lying LUMO, which in turns gives a high electron affinity.[4] Other group 14 metals, such as germanium and tin, also show this type of conjugation.[5]

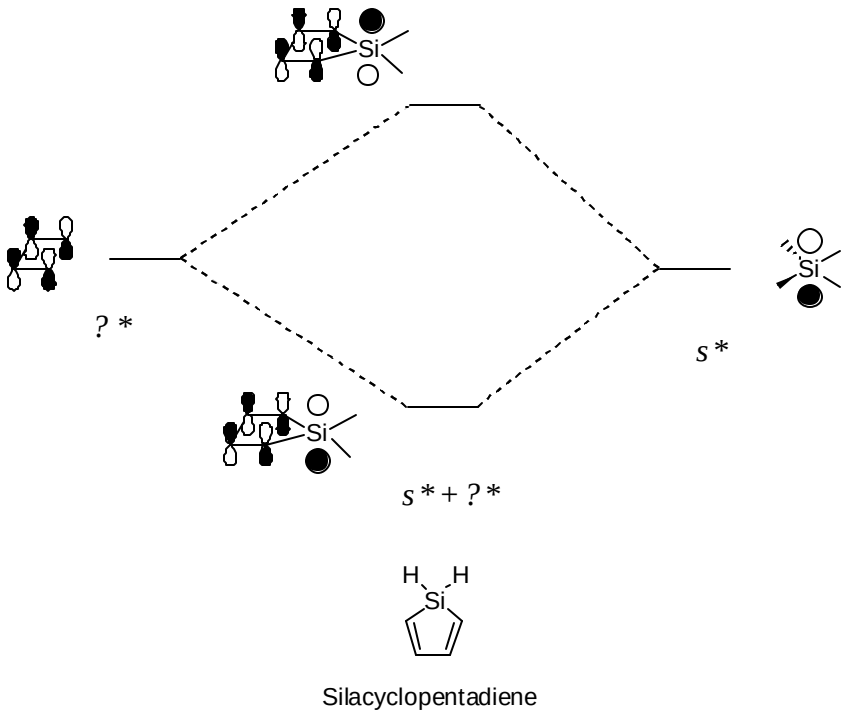

Figure 7.1 Structure of silacyclopentadiene and its LUMO molecular orbitals.

Later studies using a silole derivative found it to have very high electron mobilities, more than two orders of magnitude higher than that of Alq_3.[2] This was a very important finding, considering that the silole derivative was an amorphous solid. Previously, only crystalline material such as pentacene and C_{60} were capable of such high electron mobilities.[2] The silole was also found to have a much lower dipole moment than that of Alq_3.[2] The dipole of the silole was 0.54 Debye, while Alq_3 is 4.1 Debye.[2] The higher the dipole in an electronic material, the more build up of space charge, leading to an increase in operational voltage, which will degrade the device performance.[2] The devices made with some of the silole derivatives showed efficiencies as high as 4.8%, with a brightness of 1400 cd/m^2 at only 6.5 V.[6] However, the silacyclopentadiene does not emit in the solid-state, so these devices are used in conjunction with an emitting material such as Alq_3. A blue-emitting silole (tetraphenylsilole) was prepared, but its efficiencies in a device were much lower (0.65%) compared to that of the non-emitting silole devices.[7] A polysilole compound was also prepared and used as both the electron-transport and emitting layer in an OLED.[8] However, the efficiency from that device was only 0.03%.[8]

From these reports, it is clear that silole compounds can improve both the electron mobility and the efficiency in OLEDs, especially when used with Alq_3 as the emitting material. However, silole compounds, like Alq_3, must also be vacuum deposited. If theses compounds were attached to a polymeric backbone containing an Alq_3-side-chain, the resulting copolymer would not only be solution-processed, but it would also contain the components to make an efficient and highly fluorescent OLED. This chapter will focus on the copolymerization of the Alq_3-monomer with a norbornene monomer

derivative of the silole compound, Ph_5SiCp-monomer, and the photoluminescent and electroluminescent studies of the copolymer.

Results and Discussion

The pentaphenylsilacyclopentadiene-norbornene monomer (Ph_5SiCp-monomer **2**) was prepared for use in electronic devices as an electron-transport material. The properties of the monomer and homopolymer will be discussed elsewhere. A 1:1 molar ratio of the quinoline-monomer **1** and **2** were copolymerized using the 3rd generation Grubbs' ruthenium catalyst **3**. The copolymerization was complete within 1 minute in chloroform at room temperature.

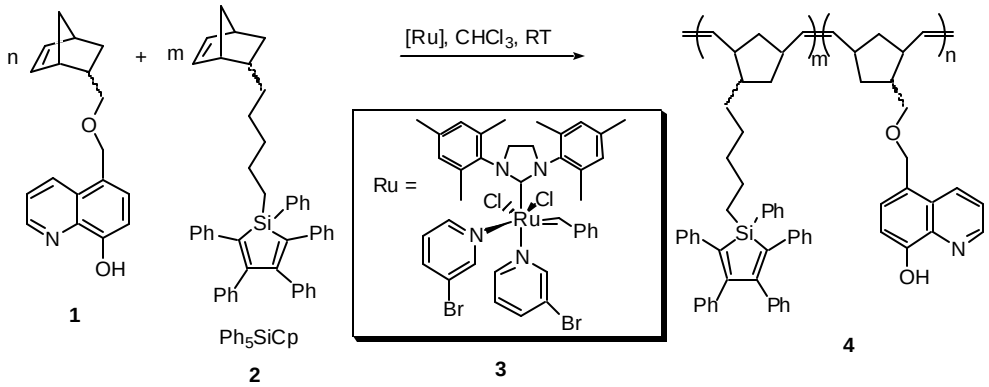

Figure 7.2 Copolymerization of the Ph_5SiCp- and Quinoline-monomers.

After purification of the Si-co-Q **4**, the copolymer was dissolved in chloroform, and freshly prepared Alq_3 was added to the solution.[9] Upon repeated precipitation of the copolymer into hexanes, a pure Si-co-Alq_3 copolymer **5** was isolated. The copolymer was characterized by NMR, GPC, DSC, UV/Vis, and fluorescence spectroscopy, with the results being summarized in Table 7.1. From the table, it is clear that the Alq_3 side-chain plays a major role in the thermal properties of the polymer. The Si-co-Q copolymer shows a glass transition temperature at 84 °C, while the Si-co-Alq_3 copolymer does not display a glass transition temperature. However, both copolymers decompose at approximately the same temperature 240-250 °C (which is approximately the same temperature as the copolymers discussed in the previous chapters).

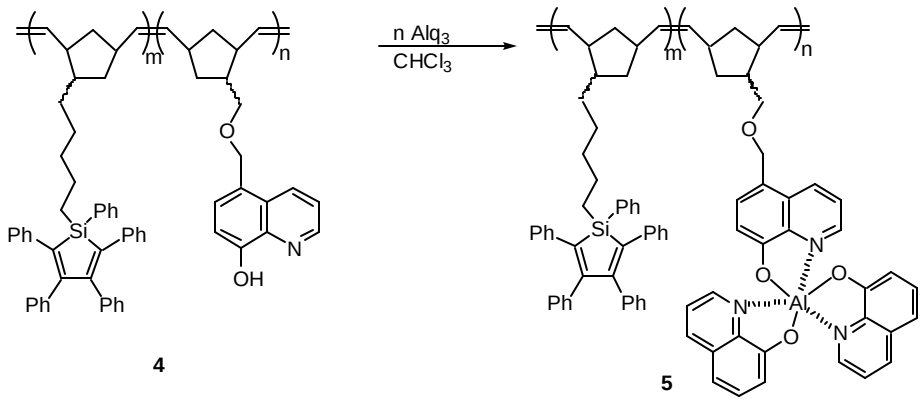

Figure 7.3 Formation of the Si-co-Alq_3-copolymer.

The photoluminescence spectra of the both the Si-co-Q and the Si-co-Alq_3 copolymers as thin films are shown in Figure 7.4. The excitation wavelength for all of the emission spectra collected was 380 nm. While the Ph_5SiCp portion of the Si-co-Q copolymer does produce blue-green emission around 490 nm in the solid state, no evidence of this emission is seen in the Si-co-Alq_3 copolymer. Only the green emission from the Alq_3 side-chain is observed, indicating that any excited electrons formed by the Ph_5SiCp side-chain are transferred to the lower excited energy levels of the Alq_3 side-chain. These results clearly indicate that both the Ph_5SiCp- and Alq_3-monomers were incorporated into the copolymer and that only the Alq_3 side-chain is responsible for light emission.

Table 7.1 Characterization data for Ph_5SiCp- and Quinoline-monomers and copolymers.

Compound	UV/Vis $?_{max}$ (nm)	Solution Emission $?_{max}$ (nm)	Thin Film Emission $?_{max}$ (nm)	Mn	Mw	PDI	Tg (°C)	Td (°C)
Ph_5SiCp – Monomer **2**	335, 352	500	495	n/a	n/a	n/a	n/a	n/a
Quinoline-Monomer **1**	318	n/a	n/a	n/a	n/a	n/a	n/a	n/a
1:1 Si-co-Q polymer **4**	315, 355	507	490	8900	7000	1.3	84	250
1:1 Si-co-Alq_3 polymer **5**	335, 375	526	518	8500	6800	1.3	---	240

Key: n/a = not applicable --- = not observed

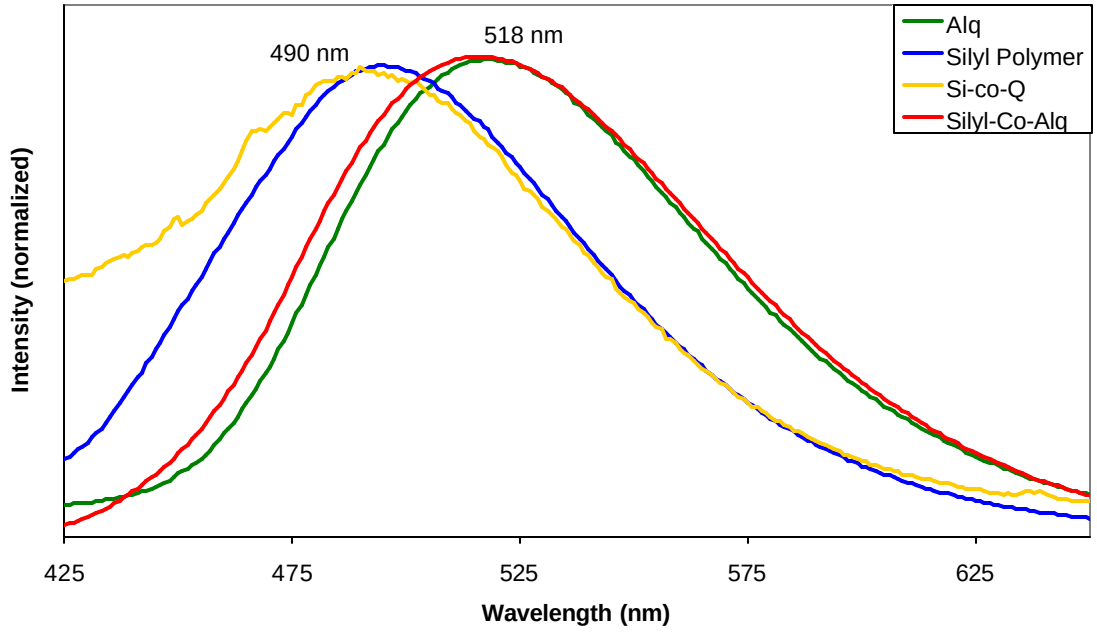

Figure 7.4 Photoluminescence spectra of the Ph_5SiCp-polymer, the Si-co-Q copolymer, and the Si-co-Alq_3copolymer as thin films.

The Si-co-Alq_3 copolymer was then used in the fabrication of an OLED. Three-layer LEDs were prepared using indium tin oxide (ITO) as the anode, TPD-co-Cinn (as discussed in Chapter 6) as the hole-transport layer, Si-co-Alq_3 as the emitting layer, Alq_3 as the electron-transport layer, and Mg:Ag as the cathode. A layer of Alq_3 was necessary for device fabrication because the metal cathode would not stick to the Si-co-Alq_3 copolymer. The TPD-co-Cinn copolymer was spin-coated from toluene onto the ITO coated slide and exposed to UV light (350 nm), allowing for the cinnamate group to undergo a [2+2] cycloaddition, forming an insoluble cross-linked HTL with a thickness around 30 nm. The Si-co-Alq_3 copolymer was then casted onto the cross-linked HTL

from chloroform, forming a 50 nm layer, and a 10 nm layer of Alq_3 was deposited on top, followed by the deposition of the metal cathode.

The electroluminescence of the multi-layer polymeric device is shown in Figure 7.5. The green emission of the Si-co-Alq_3 device, centered at 528 nm, is comparable to the emission seen for a similar device fabricated with evaporated Alq_3 with emission at 521 nm. These results clearly indicate that the emission from the copolymer is due solely from Alq_3 and not the Ph_5SiCp side-chain, and that the Ph_5SiCp side-chain of the copolymer does not interfere with the electroluminescent properties of Alq_3. While the emission can be from either the Si-co-Alq_3 copolymer or the evaporated Alq_3 layer, a current was able to flow through the device, indicating that the Si-co-Alq_3 copolymer is capable of charge transport. Further investigations are underway to determine the efficiencies of the device and if the Ph_5SiCp side-chain improves the electron-transport properties of the copolymer. A study into varying the concentration of the Alq_3-monomer in the copolymer and altering the thicknesses of both polymer layers will need to be performed in order to optimize the efficiency of the device. Nevertheless, a working OLED was fabricated using the Si-co-Alq_3 copolymer, indicating that the polymer backbone does not prohibit electroluminescence.

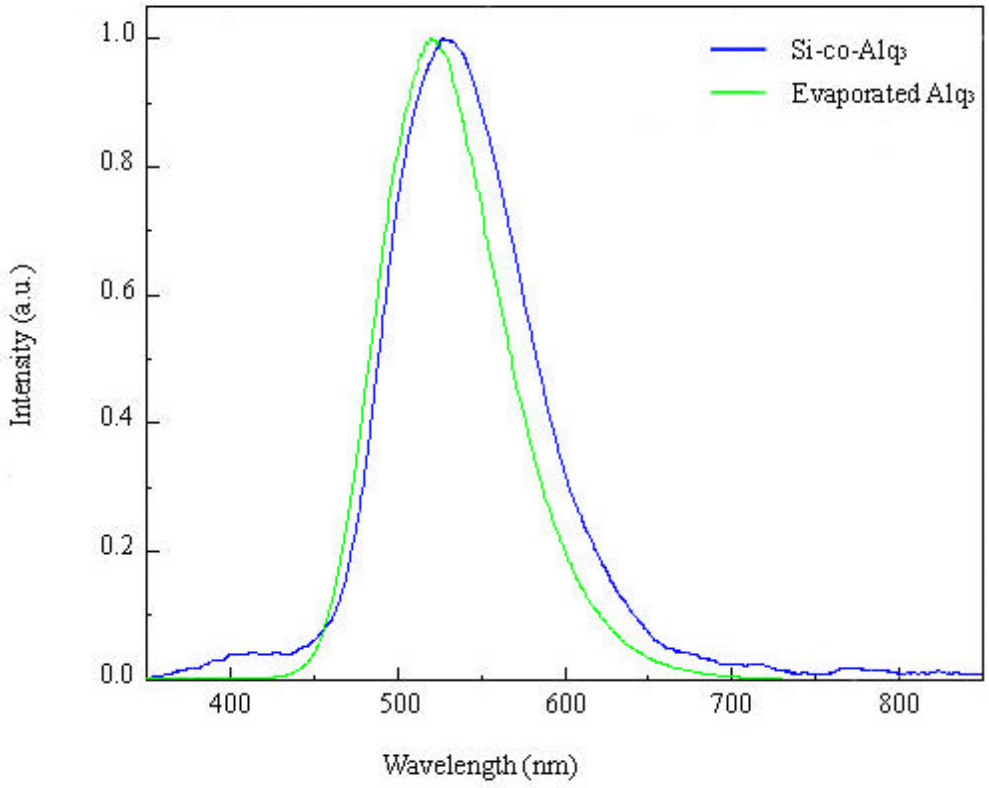

Figure 7.5 Electroluminescence spectra of Si-co-Alq_3 copolymer and evaporated Alq_3.

Conclusions

The synthesis of a statistical copolymer containing the Ph_5SiCp-monomer and the Alq_3-monomer was performed in order to form a copolymer capable of both electron-transport and electroluminescence. The Si-co-Alq_3 copolymer shows bright green photoluminescence both in solution and as a thin film, with no evidence of emission from the Ph_5SiCp portion of the copolymer, indicating that the excited Ph_5SiCp electrons are

transferred to the lower excited energy levels of Alq_3. A multi-layer polymeric device was fabricated, using the Si-co-Alq_3 copolymer as the emitting layer. The electroluminescence from this device again showed only green emission from Alq_3, with no indication of emission from the Ph_5SiCp side-chain. These results demonstrate the potential for multi-layer polymeric electronic devices using Alq_3-copolymers as the emitting layer. Further investigations into improving the charge transport properties and efficiencies of these devices are currently underway.

Experimental

General: All chemicals were purchased from Acros Organics or Aldrich and used without further purification. Flash column chromatography was carried out on silica gel 60, 230-400 mesh (Sorbent Tech.). NMR spectra were recorded on a Varian Mercury 300 spectrometer. Gel permeation chromatography (GPC) analyses were carried out using a Shimadzu instrument and linear mixed bed column packed with 10µ AM Gel with THF as an eluent and a multidiode array UV detector. Differential scanning calorimetry (DSC) was preformed under nitrogen using a Mettler Toledo DSC 822e cooled by liquid nitrogen. The temperature program provided heating and cooling cycles between -20 and 360 °C at 10 °C/min. UV/Visible spectra were obtained on a Perkin-Elmer Lambda 19 UV/VIS/NIR Spectrometer. The fluorescence spectra were obtained on a Spex Fluorolog Spectrofluorimeter. Ellipsometry measurements were taken on a J. A. Woollam Co. Inc. Spectroscopic Ellipsometer, M-2000VI. The synthesis of the

quinoline-monomer **1** was described in the previous chapter. The Ph_5SiCp- monomer **2** was prepared by Dr. Xiaowei Zhan of the Marder group.

Copolymerization of Monomers 1 and 2

The quinoline-monomer **1** (0.020g, 0.070 mmol) and the Ph_5SiCp-monomer **2** (0.044 g, 0.070 mmol) were dissolved in 5 mL of chloroform. A chloroform solution of ruthenium catalyst **3** (0.006 g, 0.007 mmol/mL) was added to the monomer solution and stirred for 5 minutes, followed by the addition of ethyl vinyl ether (1 mL). After stirring for an addition 10 minutes, the solution was concentrated down to 1 mL and added drop wise to 100 mL of hexane. The polymer, which precipitated out of solution, was collected and redissolved in 1 mL of chloroform and precipitated into hexane. This precipitation procedure was repeated three times. The final product was collected as a brown solid **4**. (0.058 g, 90% Yield). ^{1}H NMR (300 MHz, $CDCl_3$) δ 8.72 (1H, broad); 8.46 (1H, broad); 7.63 (2H, broad); 7.34 (5H, broad); 7.00-6.85 (21H, broad); 5.22 (4H, broad); 4.74 (2H, broad); 3.44-3.23 (2H, broad); 2.86-2.21 (4H, broad); 1.85 (4H, broad); 1.53 (3H, broad); 1.18-0.84 (14H, broad). ^{13}C NMR (75 MHz, $CDCl_3$) δ 156.2; 152.4; 147.7; 140.0; 139.8; 139.1; 138.7; 135.0; 133.8; 133.2; 130.1; 129.2; 128.7; 128.4; 128.0; 127.7; 126.5; 125.7; 124.9; 121.9; 109.1; 72.4; 71.3; 43.0; 41.9; 40.3; 38.0; 33.6; 32.2; 28.6; 23.8; 11.1. Anal. Calcd. for $C_{64}H_{63}O_2N_1Si$: C, 83.6; H, 6.9; N, 1.8. Found C: 82.9, H: 7.0, N: 1.8.

Formation of Alq_3-copolymer 5.

Prepared Alq_3 (0.013 g, 0.027 mmol) was added to a chloroform solution of the Si-co-Q polymer **4** (0.025 g). After stirring for 30 minutes, the solution was concentrated down to 1 mL and added drop wise to 100 mL of hexanes. The polymer, which precipitated out of solution, was collected and redissolved in 1 mL of chloroform and precipitated into hexanes. This precipitation procedure was repeated five times. The final product was collected as a yellow solid **5**. (0.030 g, 89 % Yield). ^{1}H NMR (300 MHz, $CDCl_3$) δ 8.86 (2H, broad); 8.30 (3H, broad); 7.60 (4H, broad); 7.52-7.42 (4H, broad); 7.31 (2H, broad); 7.19-7.10 (4H, broad); 6.97-6.83 (23H, broad); 5.18 (4H, broad); 4.65 (2H, broad); 3.46-3.16 (2H, broad); 2.77-1.97 (3H, broad); 1.91-1.50 (8H, broad); 1.18-0.84 (14H, broad). ^{13}C NMR (75 MHz, $CDCl_3$) δ 159.0; 158.6; 156.2; 152.4; 147.7; 145.0; 144.6; 142.4; 140.0; 139.8; 139.5; 139.4; 139.1; 138.7; 135.0; 133.8; 133.2; 131.4; 131.0; 130.1; 129.7; 129.6; 129.2; 128.7; 128.4; 128.0; 127.7; 126.5; 125.7; 124.9; 121.9; 121.2; 113.6; 112.9; 112.5; 112.2; 112.0; 109.1; 72.4; 71.3; 43.0; 41.9; 40.3; 38.0; 33.6; 32.2; 28.6; 23.8; 11.1. Anal. Calcd. for $C_{82}H_{74}O_4N_3SiAl$: C, 79.9; H, 6.0; N, 3.5. Found C: 80.5, H: 5.9, N: 3.4.

Thin film fabrication and characterization. The polymers were dissolved in chloroform (5mg/mL) and casted onto quartz slides spinning at 1000 rpm for 30 seconds. The films made for the ellipsometry experiment were prepared in a similar manner using gold-coated glass slides (100 nm of Au) instead of quartz slides. The film thicknesses were measured by ellipsometry by collecting data every 5° from 65° to 75° and were fitted using a Cauchy film on gold model.

Device fabrication. Oxygen plasma-treated indium tin oxide (ITO) with a sheet resistance of 20 O/? (Colorado Concept Coatings, L.L.C.) was used as the anode. The TPD-co-Cinn copolymer (discussed in Chapter 6) in a toluene solution with a concentration of 10 mg/mL was spin-coated onto the ITO, and then was exposed to 350 nm light from a mercury arc lamp with a 12 mW/cm^2 power density for 10 seconds. The Si-co-Alq_3 copolymer **5** was casted from a chloroform solution (5 mg/mL) onto the first cross-linked polymer layer. The electron-transport layer of Alq_3 was thermally evaporated at a rate of 1 Å/s under a pressure of 1 x 10^{-6} Torr on top of the second copolymer layer. The metal cathode, an alloy of silver and magnesium in a 1:10 ratio, was deposited through a shadow mask to define five devices per substrate with an emissive area of 0.1 cm^2 each.

References

1. Tamao, K.; Uchida, M.; Izumizawa, T.; Furukawa, K.; Yamaguchi, S. *J. Am. Chem. Soc.* **1996**, *118*, 11974-11975.

2. Murata, H.; Malliaras, G. G.; Uchida, M.; Shen, Y.; Kafafi, Z. H. *Chem. Phys. Lett.* **2001**, *339*, 161-166.

3. Tamao, K.; Yamaguchi, S.; Ito, Y.; Matsuzaki, Y.; Yamabe, T.; Fukushima, M.; Mori, S. *Macromolecules* **1995**, *28*, 8668-8675.

4. Yamaguchi, S.; Jin, R.-Z.; Tamao, K. *J. Organometallic Chem.* **1998**, *559*, 73-80.

5. Yamaguchi, S.; Tamao, K. *J. Chem. Soc., Dalton Trans.* **1998**, 3693-3702.

6. Murata, H.; Kafafi, Z. H.; Uchida, M. *Appl. Phys. Lett.* **2002**, *80*, 189-191.

7. Tang, B. Z.; Zhan, X.; Yu, G.; Lee, P. P. S.; Liu, Y.; Zhu, D. *J. Mater. Chem.* **2001**, *11*, 2974-2978.

8. Sohn, H.; Huddleston, R. R.; Powell, D. R.; West, R. *J. Am. Chem. Soc.* **1999**, *121*, 2935-2936.

9. Hopkins, T. A.; Meerholz, K.; Shaheen, S.; Anderson, M. L.; Schmidt, A.; Kippelen, B.; Padias, A. B.; H.K. Hall, J.; Peyghambarian, N.; Armstrong, N. R. *Chem. Mater.* **1996**, *8*, 344-351.

CHAPTER 8

CONCLUSIONS OF THE ALQ_3-FUNCTIONALIZED POLYMERS PROJECT

The objective of this project was to design a polymer, containing functionalized side-chains capable of charge transport and electroluminescence, for potential applications in OLED. The functionalized side-chains were to be well-known compounds that have been previously characterized and tested in devices. The purpose of selecting known compounds as the side-chains is for an easy comparison of the newly designed polymeric materials to the fully tested small molecules. One of the compounds initially chosen was Alq_3, an electron-transport and emitting material currently being used in commercial devices.[1-3] The Alq_3 moiety was attached to a norbornene monomer, which was easily polymerized using ROMP. The final material was a combination of a processable polymer with the emission and charge transport properties of Alq_3. This system was tested and modified in order to determine its applicability as an electron-transport material in OLEDs.

The accomplishments shown in this thesis includes the synthesis of two different monomers, both capable of forming the Alq_3 side-chain; polymerization of these two monomers; and copolymerization of the Alq_3-monomers either with a non-functionalized monomer or a monomer capable of charge transport.[4-6] These compounds demonstrated for the first time that an Alq_3-functionalized monomer can be polymerized using ROMP

and that the Alq_3 functionality does not interfere with the catalytic cycle during the polymerization.[4] The results also show that the polymer backbone did improve the processability of Alq_3, by being able to form uniform thin films, without any indications of phase separation or crystallization, using simple spin-coating procedures.[5] The photoluminescent and electroluminescent results from these polymers are summarized in the following paragraphs.

The photoluminescent studies of the copolymers clearly indicated that the polymer backbone did not interfere with the fluorescent properties of Alq_3, both in solution and in the solid-state.[5,6] The emission wavelength was tuned by altering the percent of the Alq_3-monomer in the copolymers.[5,6] The color of the emission was also changed by adding substituents to the 8-hydroxyquinoline ligands, shifting the wavelength from its usual 525 nm to almost any color in the range from 430 nm to 565 nm.[5,6] Besides ligand substitution, the metal center was also substituted from aluminum to zinc in order to alter the emission wavelength and potentially improve the charge transport of the copolymer.[6]

While copolymerizing the nonylnorbornene monomer with the Alq_3-monomer did show improved processing ability over the Alq_3-homopolymer, the copolymers did not shown any electroluminescence or charge-transport capabilities. To overcome this challenge, the Alq_3-monomer was copolymerized with a hole-transport monomer (TPF) and an electron-transport monomer (Ph_5SiCp). The photoluminescence results from each of these copolymers indicated that only the Alq_3 side-chains were responsible for light emission. Fabrication of OLEDs with these copolymers showed much improvement over the nonylnorbornene copolymers. The devices were able of supporting a current and

electroluminescence was detected from devices containing both the TPF-co-Alq_3 and the Ph_5SiCp-co-Alq_3 copolymers. While much work is needed improving the device fabrication and optimization, these are the first Alq_3-copolymer systems which have been fully characterized and shown to work in OLED devices.

This work has opened up many more opportunities for similar projects. It is easy to imagine this type of system being manipulated to work with other polymers or charge transport side-chains for OLEDs or other electronic devices such as photovoltaic cells. One system has already been reported using Alq_3-acrylate polymers in OLEDs.[7] Besides electronic applications, this system can also be used to make other materials such as tagging species in biological systems. Current work on this system includes polymerizing and characterizing Alq_3-styrene and Alq_3-cyclooctene monomers as well as changing the metal center and ligands to form phosphorescent polymers. Other work will also include synthesizing a water-soluble sugar-based polymer containing Alq_3 side-chains for fluorescent tagging of sugar uptake by proteins. Future ideas for this project will be discussed in the next chapter. Regardless of the outcomes of these projects, the Alq_3-functionalized poly(norbornene) was the first system to incorporate the well-known compound onto a polymer backbone, rendering a solution-processable form of Alq_3 that was used as the emitting material in an OLED.

References

1. Tang, C. W.; VanSlyke, S. A. *Appl. Phys. Lett.* **1987**, *51*, 913-915.

2. Tang, C. W.; VanSlyke, S. A.; Chen, C. H. *J. Appl. Phys.* **1989**, *65*, 3610-3616.

3. Chen, C. H.; Shi, J. *Coor. Chem. Rev.* **1998**, *171*, 161-174.

4. Meyers, A.; Weck, M. *Macromolecules* **2003**, *36*, 1766-1768.

5. Meyers, A.; Weck, M. *Chem. Mater.* **2004**, *16*, 1183-1188.

6. Meyers, A.; South, C.; Weck, M. *Chem. Comm.* **2004**, 1176-1177.

7. Takayama, T.; Kitamura, M.; Kobayashi, Y.; Arakawa, Y.; Kudo, K. *Macromol. Rapid Commun.* **2004**, *25*, 1171-1174.

CHAPTER 9

IDEAS FOR FUTURE WORK CONCERNING ALQ_3-FUNCTIONALIZED POLYMERS

The goal of this thesis was to design and synthesize an Alq_3-functionalized polymer that can be used as the electron-transport and emitting layer in an OLED. As the previous chapters have illustrated, this goal was achieved. The future of this project does look promising; however, the path of the project can move in two different directions. The original project can be broken down into two main parts: the synthesis of an Alq_3-polymer and the design of a polymeric light-emitting diode. The questions that need to be addressed now are 1) Can an Alq_3-polymer have applications other than in OLEDs? and 2) Can an electronic device be made with other metal-containing polymers?

Idea 1

To answer the first question, the role of Alq_3, and other metal-quinolate complexes, in non-electronic applications needs to be addressed. Using 8-hydroxyquinoline as a metal-chelater has been reported since the 1950s.[1-5] In most of these cases, it was used to detect trace amounts of metal in specific media, such as aluminum in steel.[2] It has also been shown to act as an effective ion-exchange resin,

being able to remove copper, nickel, and cobalt from an aqueous solution and then separately releasing each metal based on the pH of the eluant.[5] Traces of copper (0.32 ppm) were also quantitatively removed from a concentrated salt solution (12500 ppm) using the hydroxyquinoline resin.[5] Besides copper, nickel, and cobalt, 8-hydroxyquinoline has been shown to chelate with many other metals, some of which include mercury, lead, tin, cadmium, iron, and uranium.[6] Currently, the removal of these metals from industrial waste water is a major environmental concern.[7] An idea for a future project includes the synthesis of a cross-linked polymer bead with 8-hydroxyquinoline side-chains, shown in Figure 9.1. The bead can then be added to the waste water system before the water is released back into the environment. The hydroxyquinoline side-chains will be able to chelate with any metals in the water, potentially cross-linking with other beads. The beads can then be filtered from the water, leaving behind a metal-free and polymer-free solution.

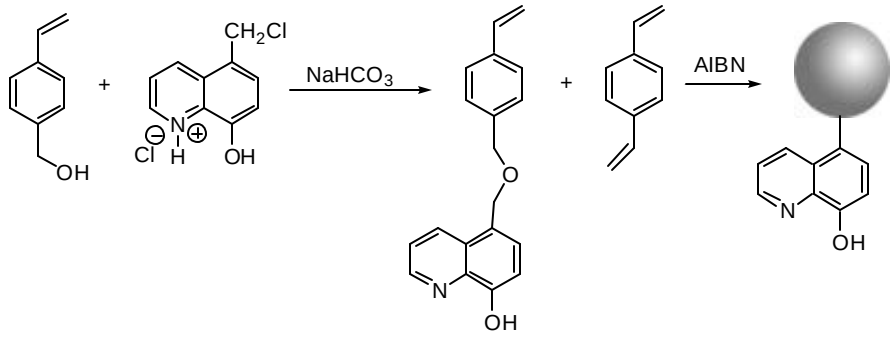

Figure 9.1 Synthetic scheme and polymerization of a polymeric bead with 8-hydroxyquinoline side-chains.

Another group reported the use of quinoline-terminated polymers containing iron as the metal center that connected two polymer ends.[6] The polymer was then used as a slow-release fertilizer.[6] The polymer, shown in Figure 9.2, was mixed into the iron-deficient soil of a chrysanthemum plant.[6] Because of the good reverse ion-exchange properties of the polymer, the iron center was slowly released into the soil.[6] Over time, the yellow plant turned green due to the uptake of iron.

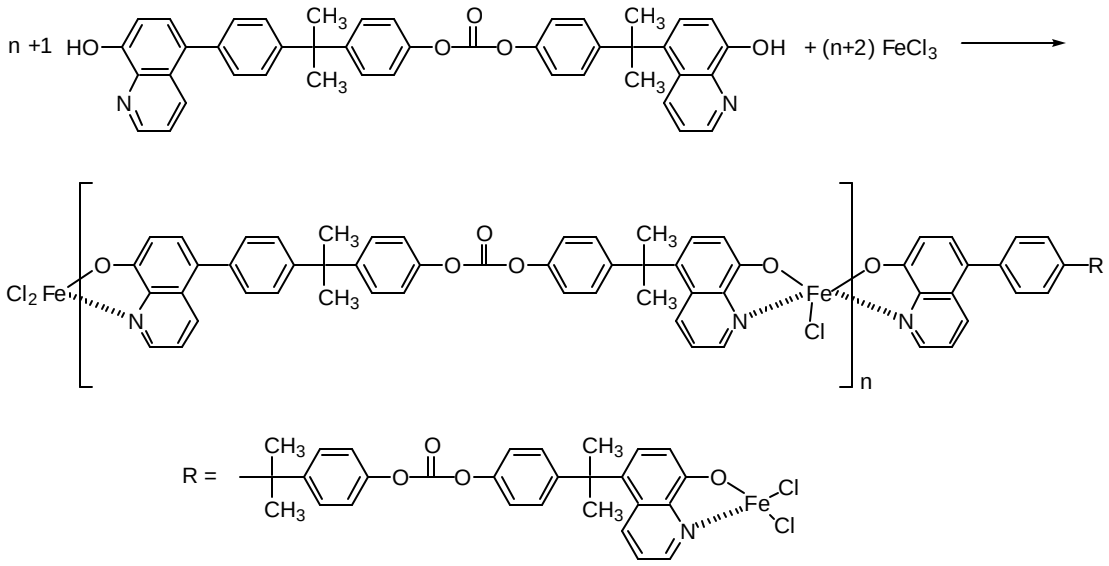

Figure 9.2 Polymerization scheme of end-functionalized hydroxyquinoline polymers.

Another idea for the hydroxyquinoline polymer project would be to design the polymer so that it contains valuable minerals such as iron and that the polymer, such as

poly(styrene), can be processed into the shape of a flower pot. After planting the flower or vegetable into the pot, a slow release of the valuable mineral will benefit the plant, while excess metals in the soil will chelate to the hydroxyquinoline side-chains, providing a healthy environment for the plant. An added benefit would be if a nutrient or fertilizer can be chelated to the metal center before processing.

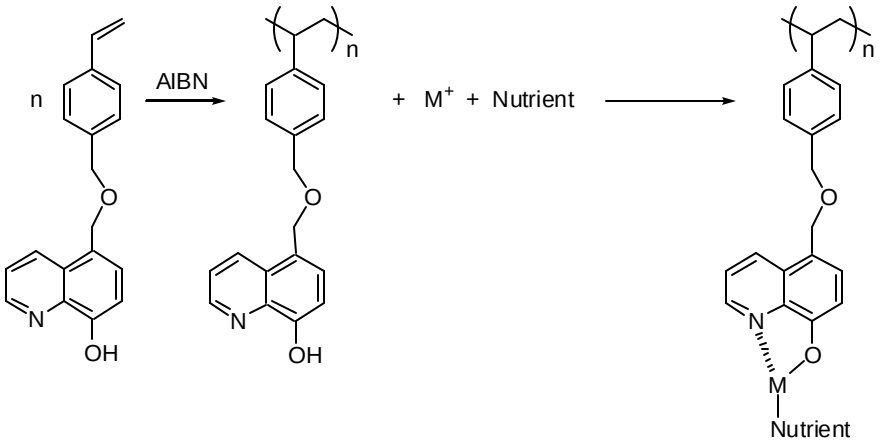

Figure 9.3 Polymerization scheme of metal- and nutrient-containing hydroxyquinoline polymer, capable being processed.

Idea 2

In order to answer the second question, "can an electronic device be made using other metal-containing polymers," the reason why the Alq_3-polymer devices did not show outstanding properties needs to be addressed. The Alq_3-homopolymers were not soluble

by themselves, so a charge transport monomer was copolymerized with the Alq_3-monomer. It was also necessary to have a high percentage of the Alq_3-monomer in the copolymer in order to obtain decent electroluminescence. If a compound can be use in conjunction with a host material capable of charge transport and energy transfer, then only a small amount of the emitting compound would be necessary to obtain a good working device. The proposed idea is to use a lanthanide metal coordinated to the hydroxyquinoline monomer, and then polymerize the monomer with the previously mentioned TPD-monomer in order to obtain an infrared emitting copolymer capable of charge transport.

Lanthanides are an excellent choice for electronic devices because the theoretical quantum efficiencies can be as high as 100%.[8] The energy levels associated with the lanthanide metals align with the triplet energy levels of many ligands.[8-14] Excitation of the ligands, followed by intrasystem crossing from the singlet state of the ligand to the triplet state then leads to energy transfer from the ligand's triplet state to the energy levels associated with the f-orbitals of the lanthanide metal.[8] Radiative relaxation then results in low energy infrared emission (900-1500 nm).[8-18] However, this low energy emission can result in low efficiencies due to non-radiative relaxation, considering that the vibrations of a C-H stretch requires only 0.4 eV where as the emission from the europium ion is around 1.55 eV.[8] Low efficiencies can also be a result from the triplet-triplet annihilation, preventing the energy transfer to the metal ion, or from multiphoton decay as seen with the neodymium ion.[8,11-13,17] Despite these drawbacks, the benefits associated with obtaining an infrared emitting polymer can potentially outweigh the obstacles.

Lanthanide metals have been used with the 8-hydroxyquinoline ligand in previous reports.[8,9,11,15-17] Depending on the metal center, emission can be obtained from 980 nm using ytterbium up to 1500 nm using erbium with lifetimes around 250 μs.[8,9,11,15-17] In the device fabrication, the lanthanide complex is either blended with a known conducting polymer, such as PVK (poly(vinylcarbazole)), or sublimed with another small molecule capable of charge transport, such as TPD (discussed in Chapter 6).[9,10,13-15,17] In either case, only 10-20% of the mixed layer is composed of the lanthanide complex in order to avoid self-quenching.[9,10,13-15,17] For the proposed project, the previously prepared quinoline monomer (Chapter 6) can be added to a solution containing the lanthanide ion (La = Nd, Yb, Er), then two equivalents of 8-hydroxyquinoline can be added in order to form the Laq_3-monomer, shown in Figure 9.4.

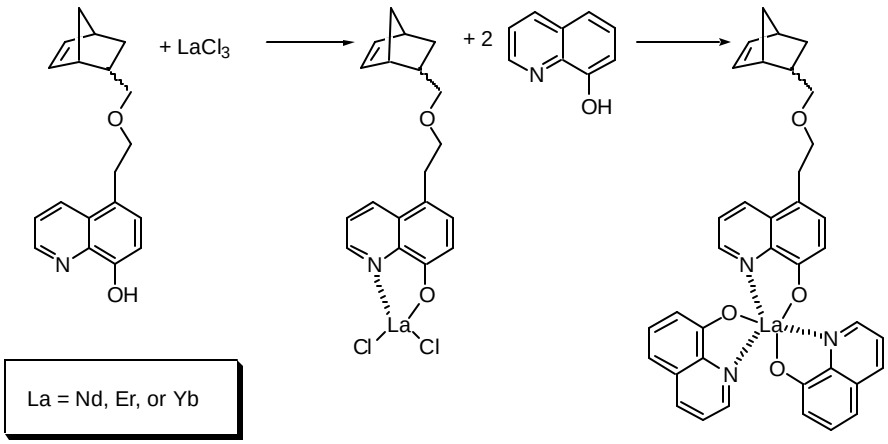

Figure 9.4 Proposed synthetic scheme of the lanthanide-quinoline monomer (Laq_3).

The copolymerization of the monomer with 8-9 equivalents of the TPD-monomer will form a copolymer capable of charge transport as well as infrared emission. Other charge transport monomer can also be used, the TPD-monomer was chosen only as an example. An OLED can then be fabricated in a similar manner as described in Chapter 6 and 7.

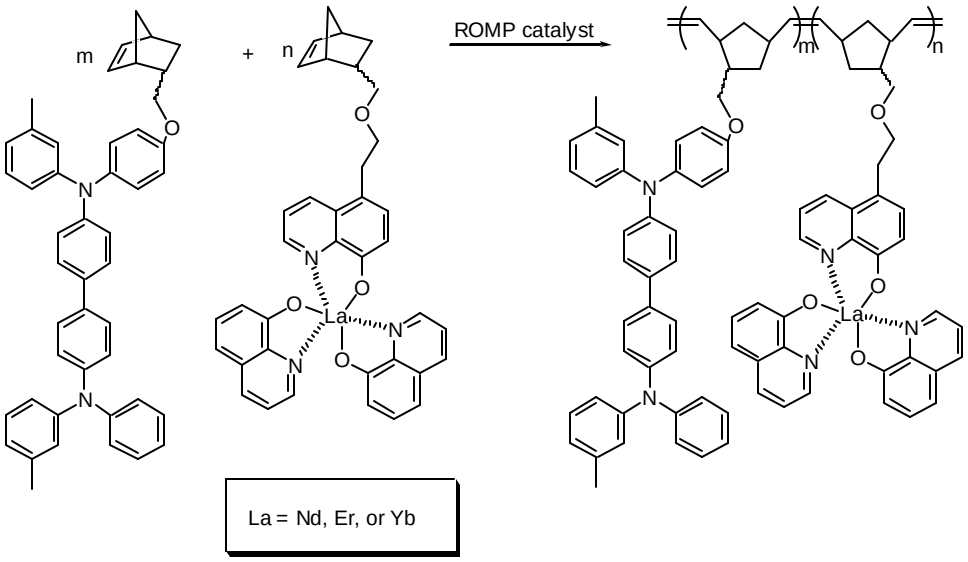

Figure 9.5 Proposed copolymerization scheme of Laq_3-monomer with TPD-monomer.

Conclusions

Based on the results from Chapter 6 and 7, it is unclear whether or not an OLED based on the Alq_3-polymer is possible. Much more work is needed in the optimization of the device. If a good working device is achieved, then developing an infrared emitting polymer could be a valuable tool for military applications. However, if metal-containing hydroxyquinoline polymers cannot be used in electronic devices, then using the polymers in environmental applications can be the new route for this project.

References

1. Goon, E.; Petley, J. E.; McMullen, W. H.; Wiberley, S. E. *Anal. Chem.* **1953**, *25*, 608-610.

2. Wiberley, S. E.; Bassett, L. G. *Anal. Chem.* **1949**, *21*, 609-612.

3. Freeman, D. C.; White, C. E. *J. Am. Chem. Soc.* **1956**, *78*, 2678-2682.

4. Freeman, S. K.; Spoerri, P. E. *J. Org. Chem.* **1951**, *16*, 438-442.

5. Pennington, L. D.; Williams, M. B. *Ind. Eng. Chem.* **1959**, *51*, 759-762.

6. Idel, K.; Freitag, D.; Vernaleken, H. *Makromol. Chem.* **1976**, *177*, 2927-2943.

7. Fernando, Q. *Environ. Health Perspect.* **1995**, *103*, 13-16.

8. Curry, R. J.; Gillin, W. P. *Curr. Opin. Solid State Mater. Sci.* **2001**, *5*, 481-486.

9. Curry, R. J.; Gillin, W. P. *Synth. Met.* **2000**, *111-112*, 35-38.

10. Hong, Z. R.; Liang, C. J.; Li, R. G.; Zhao, D.; Fan, D.; Li, W. L. *Thin Solid Films* **2001**, *391*, 122-125.

11. Iwamuro, M.; Adachi, T.; Wada, Y.; Kitamura, T.; Nakashima, N.; Yanagida, S. *Bull. Chem. Soc. Jpn.* **2000**, *73*, 1359-1363.

12. Kawamura, Y.; Wada, Y.; Yanagida, S. *Jpn. J. Appl. Phys* **2001**, *40*, 350-356.

13. Slooff, L. H.; Polman, A.; Cacialli, F.; Friend, R. H.; Hebbink, G. A.; van Veggel, F. C. J. M.; Reinhoudt, D. N. *Appl. Phys. Lett.* **2001**, *78*, 2122-2124.

14. Sun, R. G.; Wang, Y. Z.; Zheng, Q. B.; Zhang, H. J.; Epstein, A. J. *J. Appl. Phys.* **2000**, *87*, 7589-7591.

15. Curry, R. J.; Gillin, W. P. *Appl. Phys. Lett.* **1999**, *75*, 1380-1381.

16. Gillin, W. P.; Curry, R. J. *Appl. Phys. Lett.* **1999**, *74*, 798-799.

17. Khreis, O. M.; Curry, R. J.; Somerton, M.; Gillin, W. P. *J. Appl. Phys.* **2000**, *88*, 777-780.

18. Pei, J.; Liu, X.-L.; Yu, W.-L.; Lai, Y.-H.; Niu, Y.-H.; Cao, Y. *Macromolecules* **2002**, *35*, 7274-7280.